INFORMATION TO USERS

This manuscript has been reproduced from the microfilm master. UMI films the text directly from the original or copy submitted. Thus, some thesis and dissertation copies are in typewriter face, while others may be from any type of computer printer.

The quality of this reproduction is dependent upon the quality of the copy submitted. Broken or indistinct print, colored or poor quality illustrations and photographs, print bleedthrough, substandard margins, and improper alignment can adversely affect reproduction.

In the unlikely event that the author did not send UMI a complete manuscript and there are missing pages, these will be noted. Also, if unauthorized copyright material had to be removed, a note will indicate the deletion.

Oversize materials (e.g., maps, drawings, charts) are reproduced by sectioning the original, beginning at the upper left-hand corner and continuing from left to right in equal sections with small overlaps.

Photographs included in the original manuscript have been reproduced xerographically in this copy. Higher quality 6" x 9" black and white photographic prints are available for any photographs or illustrations appearing in this copy for an additional charge. Contact UMI directly to order.

ProQuest Information and Learning
300 North Zeeb Road, Ann Arbor, MI 48106-1346 USA
800-521-0600

UMI®

SOLID FREEFORM FABRICATION OF CONTINUOUS FIBER REINFORCED COMPOSITE MATERIALS

ERJIAN MA

A Dissertation

Submitted to

the Graduate Faculty

of Auburn University

in Partial Fulfillment of

the Requirements for

the Degree of

Doctor of Philosophy

Auburn Alabama

August 6, 2001

UMI Number: 3016100

UMI®

Bell & Howell Information and Learning Company
300 North Zeeb Road
P.O. Box 1346
Ann Arbor, MI 48106-1346

SOLID FREEFORM FABRICATION OF CONTINUOUS FIBER REINFORCED COMPOSITE MATERIALS

Except where reference is made to the work of others, the work described in this dissertation is my own or was done in collaboration with my advisory committee

Erjian Ma

Certificate of Approval:

Dan B. Marghitu
Associate Professor
Mechanical Engineering

Bor. Z. Jang, Chairman
Professor
Mechanical Engineering

Sabit Adanur
Professor
Textile Engineering

Stephen L. McFarland
Acting Dean
Graduate School

VITA

Erjian Ma, son of Benli Ma and Yunping Dai, was born on April 12, 1960, in MengCheng County, Anhui Province, P. R. China. He attended Hefei University of Technology, Hefei, P. R. China, where he graduated with a Bachelor of Science degree in Mechanical Science and Engineering in 1982. He then worked for Beijing Research Institute of Mechanical and Electrical Technology, Beijing, P. R. China, for 11 years, with the title of engineer and department director. During this period of time, he attended the graduate school at Harbin Institute of Technology, Harbin, P. R. China, where he received a Master of Science degree in Materials Science and Engineering in 1987. From 1994 to 1996, he was a visiting scholar working at the Materials Research and Education Center at Auburn University, AL. He began to pursue a Doctor of Philosophy degree in Mechanical Engineering at Auburn University in October 1996.

He married his wife, Hong Xu in 1985, and had their daughter Jennifer Ma in Beijing, P. R. China on February 4, 1993 and their son, Jeffrey Ma in Auburn, AL, on September 26, 1996.

DISSERTATION ABSTRACT
SOLID FREEFORM FABRICATION OF CONTINUOUS FIBER REINFORCED COMPOSITE MATERIALS

ERJIAN MA

Doctor of philosophy, August 6, 2001
(M.S. Harbin Institute of Technology, P. R. China, 1987)
(B.S. Hefei University of Technology, P. R. China, 1982)

240 Typed pages

Directed by Bor. Z. Jang

A novel computer-controlled composite layer manufacturing (CLM) process has been proposed and investigated. The CLM process may be considered to be a new development direction in the field of rapid prototyping and manufacturing (RP&M) technology. A traditional RP&M process is capable of producing a concept model or investment-casting pattern point by point and layer by layer by using monolithic materials such as an un-reinforced resin or metal. In contrast, the presently developed CLM process is capable of building a three-dimensional object of a complex shape from a high-strength fiber reinforced composite material.

In the present dissertation study, the technical feasibility of the CLM process has been demonstrated with a CLM machine constructed that is capable of fabricating both thermoplastic and thermosetting resin matrix composites. This automated manufacturing technology could potentially provide (1) a reduction in time from composite part design to production, (2) a cost-effective method of fabricating complex-

shaped composite components, (3) an approach to the fabrication of integrated structures for a reduced number of parts in a system and minimized need for part-to-part joining or welding, and (4) added capabilities for filament-winding.

The dissertation research began with the formulation of new process concepts, continuing with the analysis of part forming strategies, material selection, concept designs for the system, feasibility experiments, detail designs, software and hardware integration, to a final construction of a prototype machine.

Over ten part-forming methods were studied. Several feasibility experiments have been carried out to prove these forming strategies and two main fabrication processes have been selected. They are named Self-Anchoring process and Automatic Extrusion process, respectively. The error sources for the Self-Anchoring Forming Process were analyzed. Based on these results, the requirements of the software development have been established. To find the best parameters for both Self-anchoring and Automatic extrusion Forming Processes, related simulation models have been proposed and evaluated. According to the result of this modeling study, new design plans were conceived and proposed.

Both of the two CLM fabrication methods have been studied experimentally and a system for self-anchoring forming process has been designed and installed. The towpreg, a semi finished material used for the Self-Anchoring process was successfully formed.

To compare the mechanical properties of the parts prepared by the new CLM method and by the conventional composite fabrication methods, three point bending tests were carried. The results indicate that the parts fabricated by CLM have acceptable mechanical properties.

ACKNOWLEDGMENT

I would like to thank my advisor and committee chairman Dr. Bor. Z. Jang for providing knowledge, leadership, advice, and the opportunity to work on this project.

I would like to offer my appreciation to Dr. Dan B. Marghitu and Dr. Sabit Adanur for serving on the advisory committee, support, encouragement and advice for my dissertation and to Dr. G. Mills for reading and correcting my dissertation.

I would like to thank the members of our team, Dr. Leon W. Wu, Professor Jun H. Liu and Jessica Li, for their friendship, encouragements and help.

Manual or journal style used: Polymer

Computer software used: Microsoft Word and Microsoft Excel for Microsoft Office 2000 And AutoCAD 14

TABLE OF CONTENTS

CHAPTER 1 INTRODUCTION

§1-1 FOREWORD

1-1-1 Background

In industry, three basic factors should be considered in developing a new part or structure: cost, quality and time. The quality includes geometry and precision, mechanical properties, convenience for using, safety, durability etc. To obtain a desired geometry, various conventional methods can be employed and they can be classified into several different categories (See Table 1-1).

In response to the different requirements of a part, new fabrication methods are emerging. During the last decade, a new technology has appeared, which is called solid freeform fabrication (SFF), layer manufacturing (LM), or rapid prototyping and manufacturing technology (RP&M or, simply, RP). What is RP? What are the special features of RP? What are their advantages and shortcomings as compared with traditional fabrication technologies? And how does their future hold? All these issues will be briefly introduced in the following.

What is RP? So far, there has been no generally accepted definition of RP. The concept of RP may be considered as a process in which a computer-aided design model of a part can be converted into a physical object through some special materials additive means. A significant difference between the new RP and traditional fabrication

	Typical Method	Features	Application Field
Subtractive Material	Lathe, turning, Planing, Boring,	General Precision	Common Metal Removing
	Electric Spark Machining, Etching Machine,	High Precision, Forming Speed are Low	Mold Manufacture, Special Forming
Additive Material	Welding, Casting	Precision is lower, Mass product	Semi finished Product
	Filament Winding, Injection Molding,	Mass Product	Plastic manufacture
	CVD and PVD,	High Precision and small product	Electric Manufacture
	RPT	Few product	Model Forming, Medical purpose
Deform Material	Forging, Blanking, Stamping	Mass Product	Auto Manufacture
	Plastic Blow	Mass Product	Plastic Manufacture

Table 1-1 Classification of fabrication methods.

techniques are the fact that most of these new techniques build objects by adding material (e.g. layer by layer) instead of removing materials (such as in CNC milling).

What are the features of RP? The new RP methods can be used to build parts or structures with an arbitrarily complex 3D geometry. Some structure simply could not be formed by any other technique except RP (e.g., see Figure 1-1). In a typical rapid prototyping process, a 3-D object is first designed by using a computer-aided design (CAD) approach with a 3-D solid model being created based on the computer data.

Based on a computer-controlled system, the RP process planning begins with transforming a CAD data file into a special interface such as Stereolithography file (STL) to represent the geometry of the object. The STL file is then sliced into layer-wise data to define the outlines or contours of individual cross-sections (A combination of these constituent cross-sections reconstructs a geometric representation of the object). Then, depending upon the specific RP apparatus, this layer file is converted to generate a tool path file, which can be used to control the operations of a forming apparatus to form the desired object layer by layer. Since any complex shape can be sliced into constituent layers or cross-sections, theoretically any object can be made layer by layer. This is why SFF is also commonly referred to as layer manufacturing.

As another feature, a SFF process normally makes use of a generic fabrication machine and does not require the utilization of a part-specific tooling (no mold, die or other shape-forming tool is required). A SFF or RP apparatus requires minimal or no human intervention to operate. The RP technology requires integration of computer software, control, and materials and, in some cases, lasers technologies. The advances in

(a) Snake
Made by Z™ 402
3D Color Printing of Z Corp.

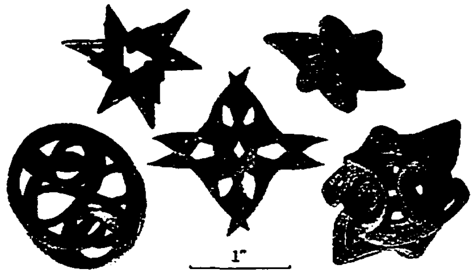

(b) Sculpture Models
Made by Solidscape Modelmaker 2.

(c) Complex aircraft System
Produced by SLS Process DTM Corp.

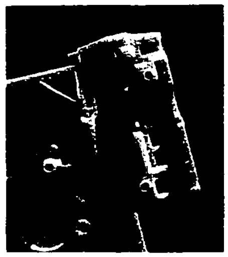

(d) Complex Wax Model
Made by Multi Jet Modeling Process
TNO Industrial Technology.

(e) Sensaos,
An Egyptian Mummy
Made by MJM process
TNO Industrial Technology.

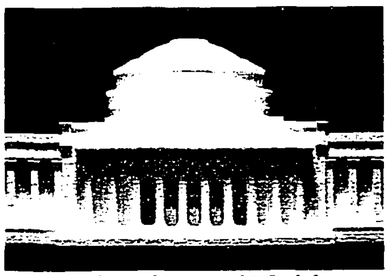

(f) Architectural Model
MIT Three Dimensional
Printing Laboratory

(g) Gearing Assembly
Made by Stratasys
FDM Process
TNO Industrial Technology.

Source: (a) download from http://www.zcorp.com/
(b) Download from http://www.protoshape.com/
(c) Download from http://www.dtm-corp.com/
(d), (e), (g) download from http://www.ind.tno.nl/en/productiondevelopment/

Figure 1-1 The Typical Models And Parts Formed By RPT.

computer science in the last decade have made it possible to develop various RP technologies and have given RP various applications. The following subsections describe these new applications [1].

Advantages and limitations Although RP techniques have only been developed in recent years, the advantages that offer have quickly become obvious. Prototyping is a process of building pre-production models of a product to test various aspects of its design. Usually this process is slow and expensive. The RP technology offers methods that allow a user to quickly produce physical prototypes with the important benefit of reducing the time to market. By use of these methods, prototypes can be built in an automated fashion; the skill of individual craftsmen is needed only at the completion. The resulting design cost will be decreased considerably. Another advantage of the RP technology is the capability of producing complex-shaped objects, especially for cases in which only a small number of parts or structures are needed at a given time, such as for aerospace and medical purposes. Objects can be formed with a comparable precision in a one-step process.

Like any other technology, the RP method has its own limitations. Most RP technologies require the use of specific materials such as photo-curable epoxy, fine powders, thin wire or laminates as well as the need for sophisticated equipment employing different physical principles such as lasing, sintering, etc. These materials could shrink during the curing process, possibly resulting in part distortion. In the meantime, since most of RP processes involve adding materials to form an object with an overhang or other unsupported feature, a support structure is required. This requires a large amount of additional time and skill to clean up the prototypes and waste materials.

1-1-2 Frequently Used SFF Processes

SFF building strategies include photolithography, laser fusion, lamination, extrusion, and ink-jet printing. Listed in the following are most commonly used SFF systems, along with the schematic description of their corresponding operating principles and the range of application.

Stereolithography (SL) One of the earliest developed and most widely used rapid prototyping system [2, 3].

Applications:

1. To fabricate parts used for concept evaluation and for form-fit testing.
2. To fabricate master patterns for processing tools (e.g., in investment casting).
3. To prepare medical models.
4. To prepare electro-forms for Electro Discharge Machining.

Advantages and Disadvantages:

1. Possibility of manufacturing parts, which are impossible to produce conventionally in a single process.

2. Continuous unattended operation, high part resolution and capability of making any geometrical shape with virtually no limitation.

3. Necessity to have support structures.

4. Accuracy is not in the range of mechanical part manufacturing due to materials shrinkage.

5. Application is restricted due to given material properties and the size of model being limited by the chamber dimensions.

6. Labor requirements for post processing, especially cleaning.

Fused Deposition Modeling (FDM) FDM is considered as one of the most promising SFF methods that have great commercial potential [4, 5].

Range of Applications The object formed by FDM is not only used as a model but also used as tooling, such as tooling for investment casting and injection molding. If the object is built from a metal or a thermoplastic material, it can be used as a real part, tooling or for mold repair. Thus far, however, the commercial FDM machines have been limited to the fabrication of models from low melting point polymers.

Laminated Object Manufacturing (LOM)

Range of Applications Considering the specifications of the procedure, the main application of LOM is for conceptual design. LOM can be used for preparation of large bulky models such as sand casting patterns [6-8].

Selective Laser Sintering (SLS)

Range of Applications This method is used for making visual presentation models, functional, tough prototypes and cast metal parts (by use of wax) [9-12].

According to the above analyses, the salient features of SFF may be summarized as follows:

1. Range of applications: the physical prototypes can be rapidly and efficiently produced.

    a. For concept design.

    b. To find design errors.

    c. To check assembly process.

    d. For Metal casting.

    e. For medical purposes.

    f. To produce complex objects, especially for small quantity production at a given time such as aerospace, medical, and die forming.

2. Limitations

    a. Special materials are required for most RP technologies, such as photo-curable epoxy, fine powders, thin wire or laminates.

    b. Most of those materials have some shortcomings: brittleness, low strength, low stiffness, high shrinkage and/or high cost.

    c. Sophisticated equipment is required, such as a laser system.

    d. Support structure is required for some RP processes.

    e. The process speed is lower than that of conventional mass production methods.

1-1-3 Conventional Composite Fabrication Processes

The fabrication technologies for polymer matrix composites are briefly reviewed. First reviewed are selected processing techniques for thermosetting polymer composites, which have dominated the composite material market in the last three decades and this dominating status will continue for at least another decade [13-15].

Thermosetting Resin Matrix Composite:

A. Wet lay-up Method and Prepreg lay-up Method:

In wet lay-up, a fabric or mat is laid into or onto a mold and then catalyzed resin is poured, brushed, or sprayed over the reinforcement. The wet composite layer is rolled by hand or with a proper tool to evenly distribute the resin and to remove air pockets. Another layer of reinforcement is placed on top of this first layer and impregnated with the resin. This procedure is repeated until a desired thickness is reached. The whole part is then cured by temperature and pressure schedule.

In the prepreg lay-up method, a prepreg material is first prepared by impregnating a unidirectional tape or woven fabric with a resin. Layers of prepreg are then cut to desired phases, laid up together, and cured in a mold. This method permits a better control of the resin/fiber ratio, this is simple and can be used to form a structure in which accuracy is not a requirement [16].

B. Vacuum Bagging and Autoclave Curing:

The vacuum bagging process is used predominantly in the aerospace industry where composite part properties rather than high production rate is a priority consideration. The autoclave provides pressure beyond what can be achieved with a vacuum only and therefore imparts greater compression, resulting in reduction of void content. Curing in the autoclave produces a part that is superior to that produced through non-pressure curing in terms of mechanical properties. Autoclave curing requires a heavy capital investment on equipment and the process is slow and tedious [17, 18].

C. Filament winding:

A continuous band or tape of resin-impregnated fibers is wrapped over a mandrel to produce a hollow part. One of the advantages of filament winding is that parts of widely varying size may be produced. Also, non-cylindrical shapes can be made. Panels and fittings for reinforcement can be easily included in the winding process. Low void content and good fiber/resin ratio can be achieved. Parts with high-pressure ratings can be fabricated. But resin viscosity and pot life must be carefully chosen and monitored. Control of key parameters such as fiber tension, fiber wet-out, and resin content is important. Filament winding is not capable of readily making parts with a concave surface or any complex shape [19, 20].

D. Pultrusion:

Pultrusion is a continuous process used to produce fiber-reinforced plastic structures of a constant cross-sectional shape. The process involves feeding collimated bundles of reinforcement fibers through a resin bath, allowing the fiber tows to be impregnated with the matrix resin. The impregnated tows are then driven to go through a preforming die and a final shaping/curing die. The hardened/cured composite is pulled to a cutting device or a winding drum. Pultrusion differs from filament winding in that filament winding places the primary reinforcement in the hoop direction, while Pultrusion has the primary reinforcement in the longitudinal direction [21, 22].

E. Liquid Composite molding (LCM)

LCM includes the resin transfer molding (RTM) and structural reaction injection molding (SRIM).In the RTM process, reinforcement preforms are placed inside a closed and sealed mold and then the resin is injected into the cavity of the mold. SRIM is a very similar process, but usually faster than RTM. In SRIM, mold release and reinforcement sizing are varied to optimize their chemical characteristics for the SRIM chemistry. Once the mold has been closed; the resin is rapidly injected into the mold and reacts quickly to cure fully within a few seconds or minutes. These methods require building a specific mold for each part shape [23-25].

Thermoplastic Matrix Composites:

F. Manufacture of Thermoplastic Prepreg

Mixing a high-performance thermoplastic with continuous fiber tows is a difficult task, mainly because of the high viscosity of a polymer melt, requiring a high shear stress and long residence time to permeate and wet out a fiber bundle. Greatly increasing the melt temperature to lower the resin viscosity is not always possible because decomposition can begin to occur before viscosity reaches a reasonable value. These considerations have made it difficult to fabricate thermoplastic prepreg materials using a conventional hot-melt process.

G. The "FIT" Process.

In this process, fiber tow is spread, passes through a fluidized bed of powder less than *10* microns in size and then is extrusion coated to encapsulate the powder and the tow in a film sheath, forming a "towpreg". The towpreg can later be woven, braided, stitched into a textile structural shape, which is then pressed after powder fusion and allowed to solidify under a desired pressure [26].

H. The Wet Powder Technology.

This process involves dispersing the thermoplastic matrix powders in an aqueous suspension to form slurry, which is used to impregnate the fiber tows. The impregnated tows, again called "towpregs", are dried and wound around a drum. The towpreg can later be woven or braided into a composite shape, which is then pressed after powder fusion and allowed to solidify under a desired pressure [27].

I. The Dry Powder Technology.

The process entails feeding and spreading a fiber tow into a fluidized bed containing moving thermoplastic powder particles. The powder particles are electro-statically charged and the tow is electrically grounded to promote powder pickup. The powders are then partially melted to allow the polymer to glue to the fiber, yet maintaining isolated particles. This process appears to be capable of producing a towpreg rapidly without imposing severe stresses on the fibers or requiring excessively long high-temperature residence times for the polymer [28, 29].

J. Commingled Yarn Technology. The "hybrid yarn" concept represents a major step forward in the developments of thermoplastics composite processing technology. The commingling process requires a texturing procedure to open the reinforcement yarn bundle (for accommodating thermoplastic filaments) without damaging the brittle fibers. This may be difficult to accomplish for a high filament count carbon tow. There is certainly an added cost to produce filaments form matrix polymers. The commingled fibers can later be woven or braided into a composite shape. The thermoplastic filaments are then melted with the whole composite shape being pressed and allowed to solidify under a desired pressure [30, 31].

The shortcomings of the conventional composite fabrication processes are:

1. Part specific tooling is required for most processes.
2. Some processes can only produce semi-finished products, axially symmetric shapes, or structures of a constant cross-section shape.
3. Cannot be used for net-shape fabrication of complex 3D objects.

§1-2 MOTIVATION BEHIND THE DISSERTATION RESEARCH

A 3-D model formed by a RP technology presents a better communication tool than 2-D pictures or a simulated 3-D model on a monitor. The 3-D physical model can be seen and can be touched by the designer for a detailed inspection. With a 3-D physical model at hand, the designer can easily find design errors and eliminate the errors before the part is put on the production line.

The part can be readily re-designed to reach the desired shape. However, a model is an object used for the evaluation of its "form" only (but not "fit" and "function"). The shape cannot be used as a real part or structure. Most materials used in a RP process have the following shortcomings: brittleness, low strength, low stiffness, high shrinkage and/or high cost. In many cases, good strength is needed for a desired object. For example, a human artificial limb should be made with proper mechanical properties and an individual shape. Some parts or structure for aerospace applications need a high strength-to-weight ratio. In some cases, the number of identical parts needed at a time is small. These requirements can be met provided the RP technology is extended for the fabrication of advanced fiber composites.

1-2-1 LM Technology for the Fabrication of Continuous Fiber Composite

The Composite Layer Manufacturing (CLM) takes advantages of the SFF technology (its flexibility in 3D forming) and the superior mechanical properties of composite materials. The primary advantages of CLM are given as follows:

1. As a rapid method of making models of high mechanical integrity:

   Advanced fiber reinforced polymer and metal matrix composites normally have great specific stiffness (modulus-to-density ratio), specific strength (strength-to-density ratio), creep and fatigue resistance, and fracture toughness. A prototype or real part made with an advanced composite will be of superior structural integrity and durability.

2. As a cost-effective way of producing tools:

Composite design approaches have advanced to the status that, by judiciously selecting fibers and their orientations, one can readily produce a composite with a desired Coefficient of Thermal Extension (CTE) e.g. zero CTE. Zero-CTE materials such as INVAR have been shown to meet thermal and durability requirements and are used in current aircraft production programs. INVAR tooling, however, is very expensive and requires a long fabrication lead-time. The presently proposed technology will permit cost-effective, rapid fabrication of durable tools, which themselves are made from continuous fiber composites with thermal characteristics that are compatible with those of the intended composite parts.

3. Potentially a cost-effective composite fabrication method:

Most of the current composites processing techniques are not capable of manufacturing structural parts of a complex geometry. SFF concepts provide effective approaches to the production of complex composite structures without incurring operator interventions or utilizing part-specific tooling (mold or die). Cost-effective processing techniques will significantly broaden the scope of application for composites.

§1-3 LITERATURE SURVEY

1-3-1 History of Commercial RP Systems

1. In 1987, the first commercially available RP system in the world was introduced, which was the precursor to today's popular SLA-250 machine. The SLA-

250 of 3D systems is used for mechanical part design based on the Stereolithography (SL). After that, NTT Data/CMET and Sony/D-MEC SL systems were commercialized in Japan in 1988 and 1989, respectively [32]. Then, Electro Optical Systems (EOS) of Germany sold its first Stereos Stereolithography system in 1990. Cubital introduced Solid Ground Curing (SGC) in 1991, which also works with UV-sensitive liquid polymer. The SGC involves solidifying whole layers at once by flooding UV light through masks created with electrostatic toner on a glass plate. In 1994, Fockele & Schwarze of Germany introduced a stereolithography machine, but on a limited basis.

In 1991, Stratasys invented the Fused Deposition Modeling (FDM) system. In 1994, Model Maker that deposits wax materials with an inkjet print head became available by Sander Prototype. In 1996, Ballistic Particle Manufacturing (BPM) Technology sold its first commercialized Personal Modeler 2100, which deposits high impact polystyrene materials using an inkjet print head [33].

2. In 1991, Helisys introduced Laminated Object Manufacturing (LOM), and in 1994, Kira Corp. of Japan commercialized the first non-stereolithography system called Solid Center that is using paper lamination [34].

3. DTM introduced the Selective Laser Sintering (SLS) system and Teijin Seiki commercialized the technology and named it Soliform Stereolithography System in 1992.

4. In 1993, Massachusetts Institute of Technology (MIT) invented and patented a process, which is named Direct Shell Production Casting (DSPC) for use

in investment casting process though depositing liquid binder onto ceramic powder to form a shell [35, 36]. The same 3-D powder printing technique is now commercialized by Z-Corp. for producing concept models.

1-3-2 Present Profile of RP

1. **Patents:** By the end of October 2000, the US Patent and Trademark Office (USPTO) has proved and issued 666 patents related to RP. Most of the patents (531 items) appeared during 1996 to 2000. After browsing most of the patens, several salient features of these of patents can be found: new processes and material are still the focused points, and most organizations are considering system details to improve existing RP machines.

2. **Open Literature Including Conference and Periodical Paper**: Many home pages, which are related RP can be found through Internet searching using the key words "Rapid Prototyping". A profile of RP developing can be found directly.

    a. Over 2500 Journal articles and conference papers related to RP have been published worldwide.

    b. *Rapid Prototyping Journal* "Keeps you fully informed of the latest developments in rapid prototyping." The journal focuses primarily on rapid product development in a manufacturing environment, but also cover applications within other areas such as medicine and construction. This internationally acclaimed information resource provides truly global perspectives on this dynamic and exciting area.

c. *CAD/CAM Publishing publishes The Rapid Prototyping Report.* The monthly Rapid Prototyping Report is the only independent periodical devoted to rapid prototyping and helps a technology development engineer or manager avoid mistakes by publishing in-depth, objective appraisals of the strengths and weaknesses of each technology.

d. *Rapid News* - time-compression technologies magazine. The magazine discusses the use of time-compression technologies to speed new products to market, with applications-oriented feature articles, news, reviews published by Communications Technologies, Inc.

e. These are many specialized publications.

The status of RP industry has been well summarized by Wohler and associates [37]. The following are the key findings of this report.

3. **RP units sold by US manufacturers**: The Charts 1-1(a) shows the RP system units sold by US manufactures in 1997. Out of 1057 units nearly one-third came from 3D Systems. In 1996, Stratasys units accounted for nearly 41% of the systems sold by US manufactures. 3D System and Stratasys have dominated the market for several years.

4. **Industries Being Served** In the early days of RP, the automotive and aerospace industries dominated the RP market, accounting for about half of the total

market. This is no longer the case as RP has spread into other industries. Charts 1-1 (b) show the industry sectors that are now using RP technology.

5. **How RP Models are Being Used** About 28% of all RP models are being used for fit and function applications, while nearly 36% serve as visual aids for engineering, tooling, requesting quotes, and presenting proposals. Meanwhile, about 25% are being used as patterns for prototype tooling and metal casting. Charts1-1 (c) shows how customers are using RP models.

6. **RP Education**The use of RP at educational institutions started in the late 1980's with a core of about 10 universities worldwide. The number of schools has grown steadily during the 1990s. From 1994 through 1996, the number of universities involved in RP worldwide soared. In 1996, an estimated 225 research institutions, technical colleges, and even a few high schools used RP in some way.

1-3-3 New Developments in RP Technologies

1. **New System** Scientists are always interested in new technology. That is one reason why new technology is appearing one after another. Now several new RP and RT processes are being developed in laboratories around the world. But the challenge still is how to package these technologies into commercially viable products.

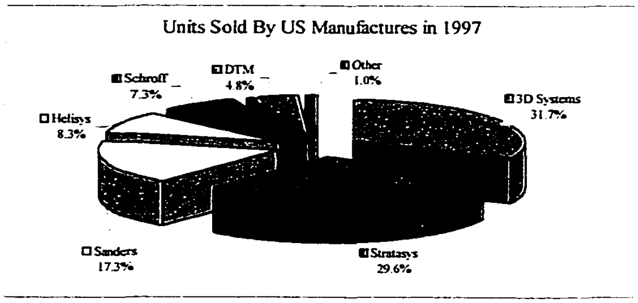

Charts 1-1 (a)

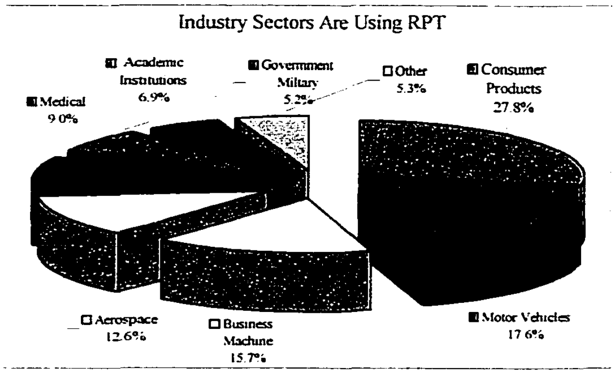

Charts 1-1 (b)

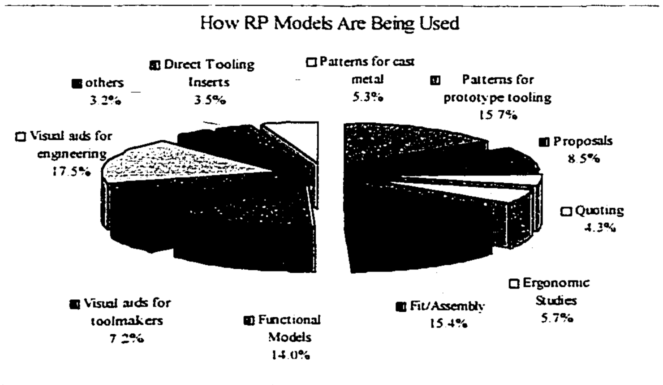

Charts 1-1 (c)

Charts 1-1 Present Profile of RPT (Source: Wohlers Associates, Inc).

a. **LENS at SNL** A new technology named Laser Engineered Net Shaping (LENS) that can make 3D metallic parts or structures directly from CAD solid models has been developed at SNL (Sandia National Laboratories Albuquerque, NM). Metal materials as applied in RPT are a very important research direction and have been achieved by different research organizations [38, 39].

b. **Directed Light Fabrication at LANL** Directed Light Fabrication (DLF) used to form metal components also is being developed at Los Alamos National Laboratory (LANL). The process uses a computer-controlled nozzle system to deposit metal powder into a pool of melted metal created by a focused laser beam. Layer thickness is typically *0.075* to *0.125* mm, which can be built into fully dense, near-net-shape metal components. Similar to LENS and DLF, a system called Laser Generating has been developed by the Fraunhofer Institute for Production Technology (IPT) and the Fraunhofer Institute for Laser Technology (ILT), both are located Aachen, Germany.

c. **Topographic Shell Fabrication (TSF)** The process is developed by Formus (San Jose, CA). The TSF prints shells as large as 3.4×1.8×1.2 meters with silica sand and paraffin wax, and then the shell severs as a temporary form for molding shapes in fiberglass, resin or other materials.

d. **Larger and Faster** LASTFORM (Large Scale Tooling for Rapid Manufacture) has focused on the manufacture of large laminate dies for the aerospace industry. Large RP equipment can form large concept molds; e.g., the car contour. With a large instrument, it is possible to form several molds in one forming operation. Now, some high-speed RP processes can form a part within hours or days instead of days or weeks. Actually, the required mold accuracy requires slicing more logic layers and build more physical layers, thereby extending the forming time. Speed and accuracy still appear to be mutually exclusive for most RP processes [40-44].

2. **New materials** paper is employed in the LOM system and epoxy is employed in the Stereo-lithography system as visual aids only. The parts produced are good enough for prototyping and testing applications. The new materials for RP being developed have the following features:

a. **Modifying the existing RP material** Filler components are added into epoxy to decrease the laser scan time, reduce the shrinkage, and improve mechanical properties.

b. **Function material** Thermoplastic, such as ABS and nylon materials that exhibit good mechanical properties were studied by FDM system users.

c. **Metal** Especially high melting temperature alloys, stainless steel, nickel-based super-alloys such as Incone l625, 690, and 718, H13 tool steel, tungsten, Ti-6Al-4V, Nickel Aluminates, and others have been fabricated with certain systems such as LENS.

d. **Composite material** is another focused material for RP and will be discussed in the next section

e. **Other materials** Scientists at Tsing Hua University (Beijing, China) are investigating the creation of ice models using inkjet printing of water [45].

3. **Software Development** a RP process could not be invented without computer software development. The software, which is used in RP, could be used to convert CAD models into a format that is suitable for controlling the operation of a RP system. The most popular format, used by all commercial RP machines, is the STL (STereoLithography) file developed by 3D Systems. And most CAD software packages can output STL format file now. But the STL files contain flaws and require modifications. New software products and utilities such as Magics can be used to view, measure, slice, and repair STL files.

1-3-4 RP Technology with Composite Materials:

The SFF techniques that potentially can be used to fabricate short fiber- or particulate-reinforced composite parts or their precursor performs include fused deposition modeling (FDM), laminated object manufacturing (LOM) or related lamination-based process, and powder-dispensing techniques. The FDM process operates by employing a heated nozzle to melt and extrude out a material such as nylon, ABS plastic (acrylonitrile-butadiene-styrene) and wax in the form of a rod or filament [46]. The filament or rod is introduced into a channel of a nozzle inside which the rod/filament is driven by a motor and associated rollers to move like a piston. The front end, near a nozzle tip, of this piston is heated to and melted; the rear end or solid portion of this piston pushes the melted portion forward to exit through the nozzle tip. The nozzle is translated under the control of a computer system in accordance with previously sliced CAD data to trace out a 3-D object point by point and layer by layer. In principle, the filament may be composed of a fiber or particulate reinforcement dispersed in a matrix (e.g., a thermoplastic such as nylon). In this case, the resulting object would be a short fiber composite or particulate composite. The FDM method has been hitherto limited to low melting materials such as thermoplastics and wax and has not been practiced for preparation of metallic parts, possibly due to the difficulty in incorporating a high temperature nozzle in the FDM system.

A more recent patent reveals a FDM process for forming 3-D solid objects from a mixture of a particulate composition dispersed in a binder [47]. The method involves additional operations of preparing a mixture of particles and binder and forming the mixture into a filament or rod form. The mixture in this filament or rod form is then introduced into a nozzle with the leading portion of the filament/rod melted and extruded to deposit onto a work surface point by point and layer by layer to form a 3-D shape. The binder in this 3-D shape is later burned off with the remaining particulate composition identified by re-impregnation or high-temperature sintering. A large amount of binder, up to *60-80%* by volume, must be burned off and this represents a significant waste of material and requires a long duration of time to accomplish.

Other melt extrusion-type processes include those disclosed in Valavaara [48-49]. These melt extrusion based deposition systems, if adapted for forming short fiber or particulate composite object, would suffer from the same shortcomings as in FDM. Furthermore, the incorporation of *20 - 40%* short fibers or particulate in a matrix melt would further increase the viscosity of the material in a flow channel, making it more difficult to operate the FDM or related extrusion-based process.

In a series of U.S. patents [e.g., 50], Sachs, et al. disclosed a 3-D powder printing technique that involves using an ink jet to spray a computer-defined pattern of liquid binder onto a layer of uniform-composition powder. The binder serves to bond together those powder particles on those areas defined by this pattern. Those powder particles in the unwanted regions remain loose or separated from one another and are removed at the end of the build process. Another layer of powder is spread over the preceding one, and the process is repeated. The "green" part made-up of those bonded powder particles is separated from the loose powder when the process is completed. This procedure is followed by binder removal and metal melt impregnation or sintering. This technique is limited to one type of powder particles in one layer and is useful for fabricating uniform-composition materials only. The technique does not lend itself for varying the powder composition from point to point for the preparation of heterogeneous materials.

This same drawback is true of the selected laser sintering or SLS technique [51] that involves spreading a full-layer of powder particles and uses a computer-controlled, high-power laser to partially melt these particles at desired spots. Commonly used powders include thermoplastic particles or thermoplastic-coated metal and ceramic particles. The procedures are repeated for subsequent layers, one layer at a time, according to the CAD data of the sliced-part geometry. The loose powder particles in each layer are allowed to stay as part of a support structure. The sintering process does not always fully melt the powder, but allows molten material to bridge between particles. Commercially available systems based on SLS are known to have several drawbacks. One problem is the long time required to heat up and cool down the material chamber after building. In addition, the process has not been successfully applied to fabrication of fiber composite parts.

Most of other prior-art layer manufacturing techniques also have been largely limited to producing parts with homogeneous material compositions. Furthermore, due to the specific solidification mechanisms employed, many other LM techniques are limited to producing parts from specific polymers. For instance, Stereo Lithography and Solid Ground Curing (SGC) rely on ultraviolet (UV) light induced curing of photo-curable polymers such as acrylate and epoxy resins. Additionally, most of the current RP systems are not effective in adding fibers into a RP material or varying the fiber type of a composite object from layer to layer and from spot to spot.

Modified laminated object manufacturing (LOM) has been used to prepare polymer matrix and ceramic matrix composites [52]. The process involves, for instance, feeding, laminating and cutting thin sheets of prepregs (pre-impregnated fiber perform) in a layer-by-layer fashion according to computer-sliced layer data representing cross sectional layers of a 3-D object. The process cycle typically consists of laminating a single sheet of prepreg to an existing stack, laser cutting the perimeter of the part cross section, and laser-dicing or "cubing" the waste material. After all layers have been completed, the part block is removed from the platform, and the excess material is removed to reveal the 3-D object. This process results in large quantities of expensive prepreg materials being wasted.

§1-4 CHALLENGES FOR THE FUTURE

1. **Cost Saving** Current RP system price is very high, from *$50,000* to *200,000* per unit. Many agree that RP must cost less before it will penetrate manufacturing companies worldwide.

2. **Faster, Larger, and Stronger for industries**

   a. Some RP processes are extremely slow to build a component. Days even weeks may be needed. To reduce the forming cycle time is a challenge for each RP process. Desired forming cycle time is within one day or hours.

   b. RP capability or fabrication scale is limited by the size of the forming chamber, working raged of a 3D- motion device, or dimensions of the platform. Large-Scale Model, which are used for automotive industry is another developing direction.

   c. The shape stability and mechanical properties of the RP formed components should be considered in next development step.

3. **Smaller and Cheaper for Family** Desktop RP system and price within thousands is desired for children to practice their design intelligence and everybody can create their own 3D articles at home.

4. **New Applications** Most application of RP technology is practiced on model making used for concept design, error checking, assembly testing and so on. RP technology could be expected to offer advantages in the following fields:

a. **Relief Map** The received data from a satellite can be converted to a format recognizable and realizable with a RP system. A 3D map could be made within hours or less. The relief map could be used for military purposes or in emergency situations.

b. **Medical.** "RP for medical applications is a sleeping giant". In fact, in medical purpose, RP can show its fabulous advantages: process object rapidly and individually.

c. **Metal Casting and Mold Repair**: RP with metallic materials is a large field for RP application. Die-casting had remained the greatest focus in the last few years and probably has the most potential.

5. **New Software Development** Most commercialized software is depending on a specific process. A new process requires new software to match it. For example, CLM requires its own software to control the towpreg deposition.

The current CAD tool can create a 3D machine or structure with different colored components, but could not create arbitrary colors within a component or a structure, nor output a file with a color symbol. Once the problem is solved, RP will be colorful and more useful. Initial success in this aspect has been achieved recently by Z-Corp.

§1-5 RESEARCH OBJECTIVES

The proposed process included impregnating a fiber tow with a matrix material in a liquid state (e.g., melt) and laying up the impregnated tow (towpreg) point-by-point and layer-by-layer according to a computer-aided design file. The main objectives of this dissertation research are:

1. Identification of the necessary operations of fiber tow impregnation, movement and deposition that can be integrated for manufacturing continuous fiber reinforced composite parts of high structural integrity and dimensional accuracy.
2. Development of a simple prototype apparatus to demonstrate the technical feasibility of the presently proposed approach and to evaluate its strengths and limitations.
3. Process simulation and analysis:
   - (A) Simulation of the molten materials flowing inside a nozzle to develop ability for predicting the best process parameters.
   - (B) Analysis of the effect of the towpreg lay-up sequence and fiber orientation on the mechanical properties of a composite.

CHAPTER 2 CONCEPT DESIGN AND ANALYSIS FOR COMPOSITE LAYER MANUFACTURING (CLM)

§2-1 INTRODUCTION

The motivations behind the proposed research have been indicated in the previous chapter. The advantages and features of Composite Layer Manufacture (CLM) and its future development have also been briefly cited. Discussions in this chapter will be focused on how to achieve the proposed research objectives to find the best way to realize the designed plan, and to demonstrate the feasibility of all the concept designs.

To develop a new product technology or a new process, a proper procedure and scientifically sound experimental method of would greatly reduce the effort. For a specific technology, to meet the requirements of the market, more attention should be paid to three basic aspects: cost, quality and time.

The tasks of the present dissertation research project were to develop a new RPT process and a prototype machine using both layer manufacturing and composite fabrication concepts. The new technology and its relation with both RPT and composite fabrication are discussed in this chapter.

§2-2 DEVELOPMENT METHODOLOGIES

2-2-1 Developing a New Technology

A flow chart for developing a new process is shown in Figure 2-1. RPT is an interdisciplinary subject that includes machinery, mechanics, automatic control, computer, optics, materials science, etc. It is necessary to cooperate within a development team and to divide the whole development project into several periods. Each period has its specific goals and tasks [53].

a. Information collection: The advantages and features of the current RPT and various composite fabrication technologies have been summarized in Chapter 1, which provided the foundation of concept design for the present project.

b. Concept design: All collected valuable information is taken into consideration for concept design. In §2-6, there is an introduction of several concept designs based on this principle.

c. Feasibility test: After a concept design is drafted, it is time to do the feasibility test. Several feasibility-testing experiments are necessary to evaluate all parameters possibilities.

2-2-2 Feasibility Experiment

The feasibility experiment is simple and easy to do. It needs just a short period of time and a low cost. Sometimes, an existing equipment can be used to get a judgment

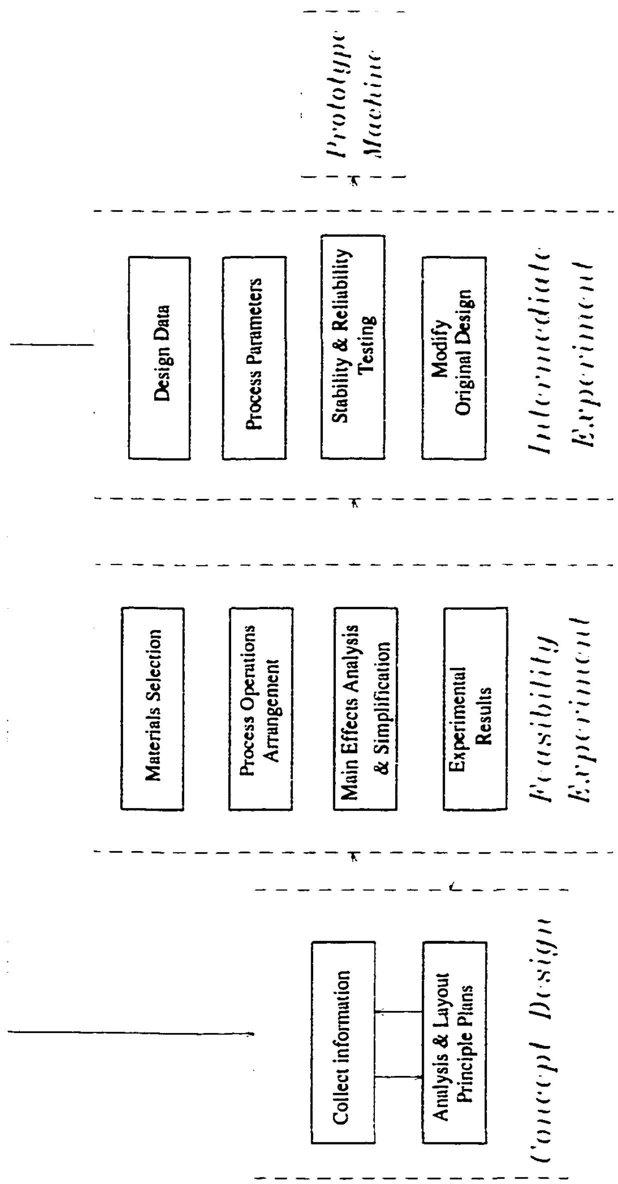

Figure 2-1 Flow chart for a new process development.

result (YES or NO) to serve as a guide for following the experiment. A feasibility experiment can be done using the most important control parameters that simulate the key behavior in a real situation. Commonly, the positive conclusions can be published, but negative conclusions cannot be published, there are positive results if some parameters or conditions have been changed. Anyway, the feasibility experiment can be taken as a positive result at once, and then the experiment can be varied or expanded basically around this design.

The feasibility experiment is a single target experiment with less parameters. The cross-effects are neglected, and care should be taken to interpret the experiment results. Additional intermediate experiments may be needed to verify important conclusions.

To grasp the essence of an issue, the feasibility experiment should be properly done. Throughout the feasibility experiment, modification or optimization of the original plan, through the intermediate experiments, must be constantly executed.

The feasibility of a design can be double checked by means of intermediate experimental verification that is done with various overlay-effort influences. In fact, some parameters and conditions cannot be simulated, nor demonstrated during the feasibility experiment period. Therefore, the true result is confirmed by the intermediate experiment only. So, the intermediate experiments bridges the result of the feasibility experiment to the machine prototype. The optimal design parameters could be found via the intermediate experiment, which will be the foundation of subsequent designs of the prototype machine. Sometimes, when a series of intermediate experiments have been done, the new prototype of the machine will appear.

2-2-3 Intermediate Experiment

During the intermediate experiment, the various process parameters could be determined accurately. The impossible plan could not be seen through, no matter how the experimental parameters changed. In case of the feasible plan, if the designed parameter is not in a right range, an error-judgment also could appear and result in the good technology plan could be abandoned. If the parameter could be controlled exactly, we should consider all possibility of cross-influence during the intermediate experiment. The impossible plans that were shown as "possible" in the original feasibility experiment could be found and thrown-out during this period.

Another important purpose of the intermediate experiment is to check the stability and reliability of a technology. Some parameters such as a stable extruding speed, or an equivalent temperature can only be stabilized when the system was run a period of time. Some problems could not be appeared throughout a short period of time, such as a roll up error, etc. The stability study results can be seen in two aspects: the best technology parameter and whether a plan could be done in a right principle or not. For example, if some RPT machine, such as BPM (Ballistic Particle Manufacturing) is being run for a long time, the polymer that remains inside of the nozzle or transferring hose could age and form scraps that block the hole of the nozzle or the hose. The disadvantage of the design concerning the transportation of materials would be exposed at a longer time.

All the unstable influences must be eliminated at this intermediate experiment period, and then the subsequent development work will be continued. In fact, all kinds of successful developments including both new products and new technology during the time of development could not be seen. But we can only see the success side and cannot see what is behind the success. Why is it successful? How could it be successful? What kind of failure occurred? Only those engineers who are following the basic rule of developmental procedure can do the development. Certainly the new technology that includes new processes and new product development is the process of creating. This kind of creation is not only shown in the result, but also in procedure. The result is to create new products or new technologies, but the market must check them. The development process creates new products and obeys all the developing rules. Only the procedure that is done step by step carefully, will avoid failure.

§2-3 OBJECT FORMING THEORY FOR CLM

For a RP Technology, the different additive methods must be employed for different forming strategies using different materials.

2-3-1 General RPT Depositing Method

Look at Stereolithography (SL): A piece of sweeper that is dipped with epoxy sweeps and coats a thin layer of epoxy upon the object to add a new layer. Another material additive method for Stereolithography is implemented by moving the object elevator downward one layer of thickness each time. Then the epoxy overflows above the top layer, which has been built to add a new raw material layer that is waiting to be scanned and solidified. To build a layer, In the LOM system, the collector roller feeds a sheet of paper onto a platform. Then, the laser beam cuts the corresponding cross-section contours. In the SLS technology, a layer of very fine powder particles is spread on top of the previous layer through a powder-leveling roller. Then the powders are laser-fused at selected contour locations to allow these powders to be bonded together and adhere to the previous layer contour.

FDM, BPM and 3D Print Technology are among the earliest developed and most widely used rapid prototyping system of delivering materials by similar means. This is accomplished by transferring material to the object through a depositing hand commonly called a nozzle. Inside the nozzle, the material state has been changed to a melt or plasters state, and then is squeezed out under the effect of a continuous pressure or pulse pressure.

The common characteristic of the technologies SL, LOM and SLS is that the unit adds materials layer by layer to build an object. For instance, in technologies of FDM, BPM and SLS etc, the method of adding material is particle by particle, line by line and layer by layer, respectively. Because of a laser's very high focusing ability, the heat influence area is small and the thickness of paper is very thin, so the staircase effect is small in SL, LOM, and SLS technologies, leading to a good forming precision. But in FDM, the material being added is something like grains or beads of liquid or plaster passing through the nozzle orifice for deposition. The forming precision is related to the nozzle's orifice directly and the staircase effect in FDM can be observed clearly.

2-3-2 A Concept of Active Material Supplying and Passive Material Supplying

Because CLM is similar to the process of FDM, the characteristics of the material-adding method for the FDM technology are analyzed and summarized in the following:

1. The material is affected by the pressure inside the nozzle that pushes the fluent material out of the orifice and propels the dispensed material toward the object with a certain speed. This way of adding materials to an object being built is called Active Material Supplying. So far, in all the RPT, the material-adding method can be generally regarded as the Active Material Supplying. In the CLM, another material-adding concept is introduced and is called Passive Material Supplying. The detail information and advantages about the Passive Material Supplying will be discussed later.

2. Due to the viscoelastic nature of a polymer melt and the fluctuation of pressure in the nozzle, especially at the time of starting and stopping, the deposition speed may vary with time and a change in the nozzle pressure may cause a delayed variation in the deposition speed.

3. The forming quality of a previous layer dose not influence the forming of the current layer, in the case of active material supplying such as in FDM. However in the case of passive material supplying, the quality of a previous layer has a profound effect on the forming quality of the current layer.

The unique characteristics of the CLM forming process are listed as follows:

1. It is difficult and also unnecessary to form any complicated-shaped parts by only one continuous line of composite material, which is called towpreg. A moving nozzle or depositing head, upon completion of an area of a layer, has to move to another area or another layer, after the nozzle is relocated to another area, the

towpreg that still links the nozzle and the object should be cut off to free the nozzle. If a machine for CLM process is to be designed properly, the cutting function should be considered and this function need to be reliable and durable.

2. It may be necessary to build a support structure for such features as overhangs and isolated islands in a layer. Another nozzle for forming the support structure is necessary. Obviously, if the support structure is formed by the same nozzle and material, the supports structure could be hard to remove after the part was finished. CLM process has another advantage to be mentioned here. In some cases, CLM could use a simplified support structure. For example, a structure of a part is shown in Figure 2-2. When the area included BCEF is to be formed using the FDM technology, the support structure must be formed in the first layer or BC layer before a subsequent layer could be continued. But the support structure is not needed in this situation if the CLM is employed because when BC layer is being formed, each line is arranged in order A→B→C→D, the towpreg between B and C acts like the bridge that supports the subsequent layers between the BCEF.

3. Because the towpreg that links the nozzle and the object has a high tensile strength, it is possible to use Passive Material Supplying. The definition of Passive Material Supplying is that, when the object is moved relative to the nozzle during the forming process, the towpreg is pulled out by the object instead of being pushed out by nozzle pressure. In the nozzle, the forming material is passively moved out by the object's pulling force and not squeezed out actively by its pressure. In the composite forming fabrication, the Filament Winding Process could be considered as a Passive Material Supplying.

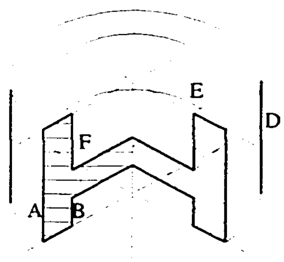

Fig. 2-2A a part is shown with 3-D Model.

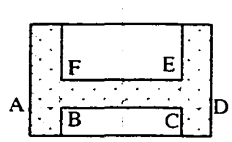

Fig. 2-2B The Cross Section of the Part.

Fig. 2-2 Support structure can be simplified.

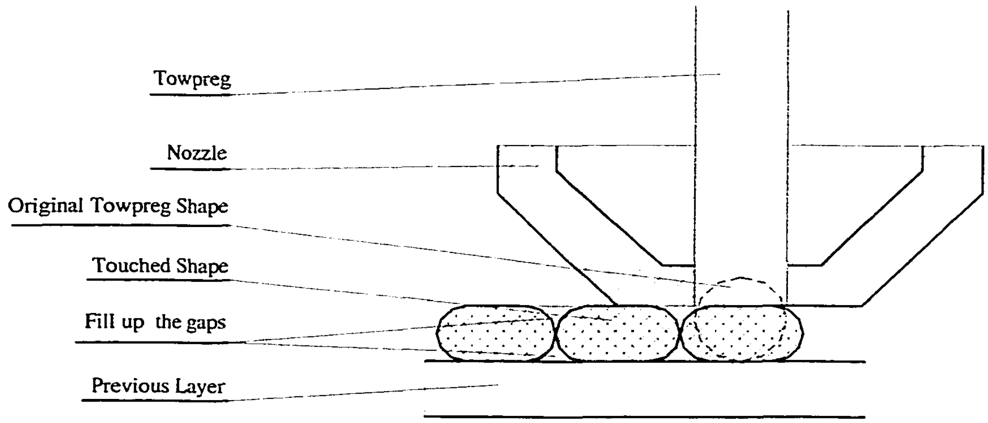

Fig 2-3 Materials distribution.

the towpreg shape has been changed during the deposition process.

4. Because a towpreg has very a high tensile strength, at the beginning of depositing, and especially at the end of the forming process, the deposition process could be easy to control. So the part's precision should be relatively high.

5. With the increase of the fiber volume fraction in towpreg, the effect of adhesion between lines, and layers could become weak. Thus, the volume fraction of fiber is limited in the towpreg.

6. In order to increase the compactness of the composite part and to get proper mechanical properties, it is necessary to keep a proper pressure to the towpreg while being deposited. The bottom surface of the nozzle may be used to push down the deposited towpreg. The distance between the bottom of the nozzle and the surface of the previous layer may be chosen to be slightly less than the diameter of towpreg. The relative position of the nozzle and the object is shown in Figure 2-3. The cross-section shape of a towpreg and the orifice of nozzle are not the same. Because a shape of the cross-section is different in the same forming layer, the boundary condition for deposition is different. Defects could appear such as areas with excessive or deficient resin.

§2-4 EFFECTS OF MATRIX AND FIBER IN THE CLM PROCESS

The RP material used for a model could be selected from wood, wax, gypsum, glass, and even wheat powder or chocolate. But the resulting object may be relatively weak and brittle. If the CLM technology is used to form a model or a real component, the proper material for both matrix and reinforcement fiber should be chosen rationally. The combination of matrix and fiber is illustrated in Figure 2-4.

There are discussions about how to choose matrix and fiber for advanced composite materials in many textbooks, but the matrix and reinforcement fiber in the CLM have to meet certain requirements.

2-4-1 Selecting the Matrix Materials:

Generally if the physical plate of any material can be changed to become a liquid, this material could be applied as a matrix material for RPT. During a common composite forming process, matrix is used as the forming carrier, which solidifies to form the shape of the composite. The fiber is used to improve the mechanical properties of the whole composite. A matrix for the CLM process must meet the following requirements:

1. The phase change speed must be sufficiently high, no matter what kind of energy is applied; the matrix can receive the energy quickly and can cause it to change its physical state as soon as possible. For example, photo curable epoxy, a common RP materials, must be capable of solidifying immediately when it is exposed to a UV beam. The RP forming process is based on adding the materials line by line and layer by layer to build an object. Increasing the phase change the speed decreases the forming time for each line and layer, leading to a reduction in the total forming time.

2. The price of a matrix material should be reasonable especially in forming a large number of parts or a large size structure.

3. The matrix and reinforcing fiber should have high affinity, particularly when

fiber impregnation and towpreg deposition are done at the same time. The matrix is required to impregnate the fiber tow immediately.

2-4-2 Accelerating the Phase Change Procedure

The phase change speed is very important for RPT processes. How to change the phase and increase the phase change speed are challenges and fundamental questions for the RPT developer. If a phase changing method is found, a new RPT is invented.

In the earliest developed SL system a laser system and photosensitive epoxy were applied. The laser beam spot can be focused to become very small, and the energy can be concentrated upon a small area to solidify the thermosetting material in a twinkling. The combination of laser beam and laser sensitive epoxy is an ideal material for RPT, but the price of UV-curable epoxy is very high. And the laser generating and control system is complicated and has a high price. Therefore, other curing mechanisms are needed. The following methods or ideas were proposed and studied for thermosetting resin materials during the period of this dissertation:

Keep the resin in the B-Stage: fiber tow is impregnated with a thermosetting material to form the towpreg, then the towpreg is treated and kept in the B-stage. Towpreg, a Semi-finished product of composite materials in the B-stage could remain inactive for a long time at low temperatures. When needed to do a forming process, a towpreg is heated or is exposed to energy by other means during the depositing movement and is quickly solidified and allowed to adhere to the previous layer. All the deposition and adhering procedures for a towpreg segment could be finished in a short

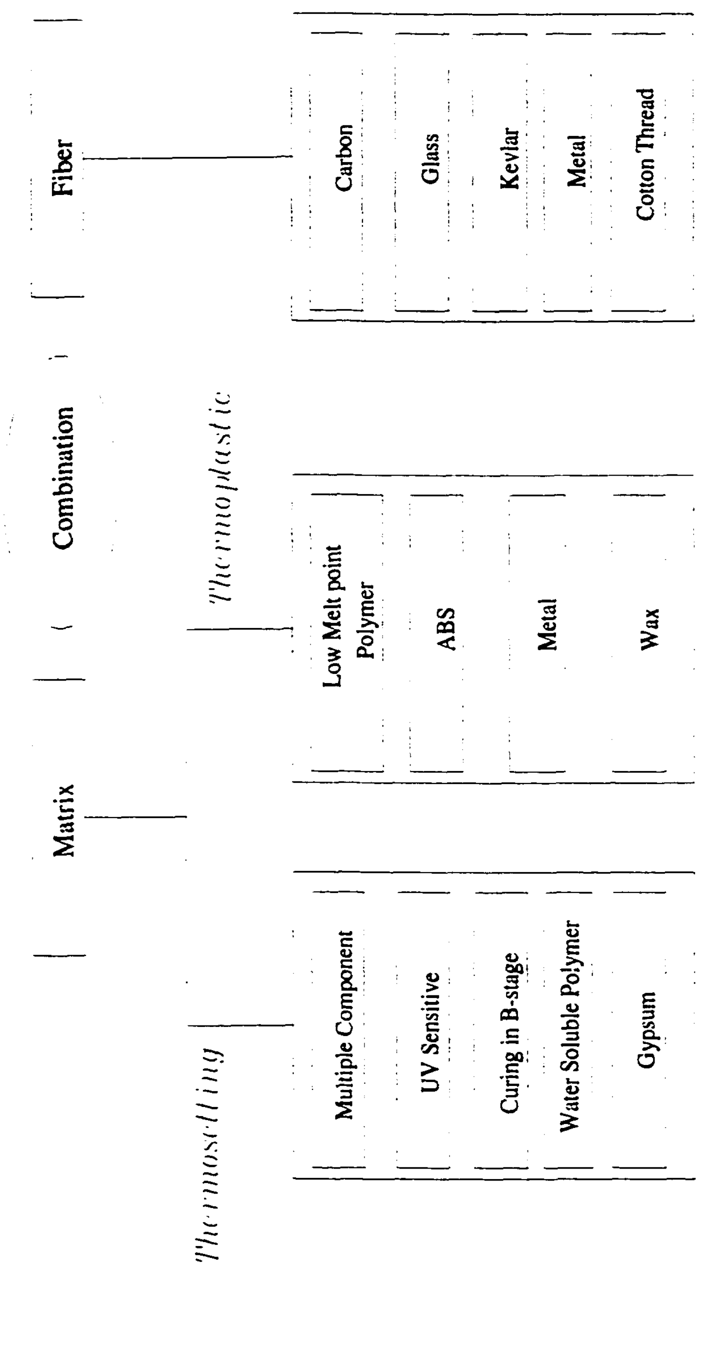

FIG. 2-4 Materials selecting for the CLM process.

time (*0.01-0.1* Second). This method is proposed for common thermosetting materials used in the CLM process.

During the deposition procedure, a curing agent and other ingredients are added into the matrix material with a catalyst and/or photo-initiator to cure and solidify the material resin. Such a chemical method is applied to increase phase change speed as illustrated in Figure 2-5.

Electromagnetic and mechanical methods: the methods are considered to use based on some materials, which are called Electro-Rheological Fluid materials. The ER fluid can exhibit a phase change by applying or removing an electromagnetic field. When an electromagnetic field is applied to the forming platform, an electromagnetic field sensitive material can be mixed into the matrix and deposited upon the platform; the matrix could be solidified immediately. Also a common thermosetting material can be mixed into this matrix. When the whole object is completed, it can be heated in an oven to finalized the object shape with the electromagnetic field being maintained until the thermosetting material is completely cured.

Some materials called shear-thickening or dilatant fluids have been considered as the materials for RPT. The state of stress that is exerted on these materials is controlled to change their phases. This is called the Mechanical Method for RPT. If this kind of material is stirred violently inducing fast solidification, and deposited layer by layer at the nozzle orifice or at the depositing area, the materials could be applied in RPT. But to achieve the proposed mechanism is still a challenge.

All the methods mentioned above have been employed in feasibility experiments except for the electromagnetic and the Mechanical Methods.

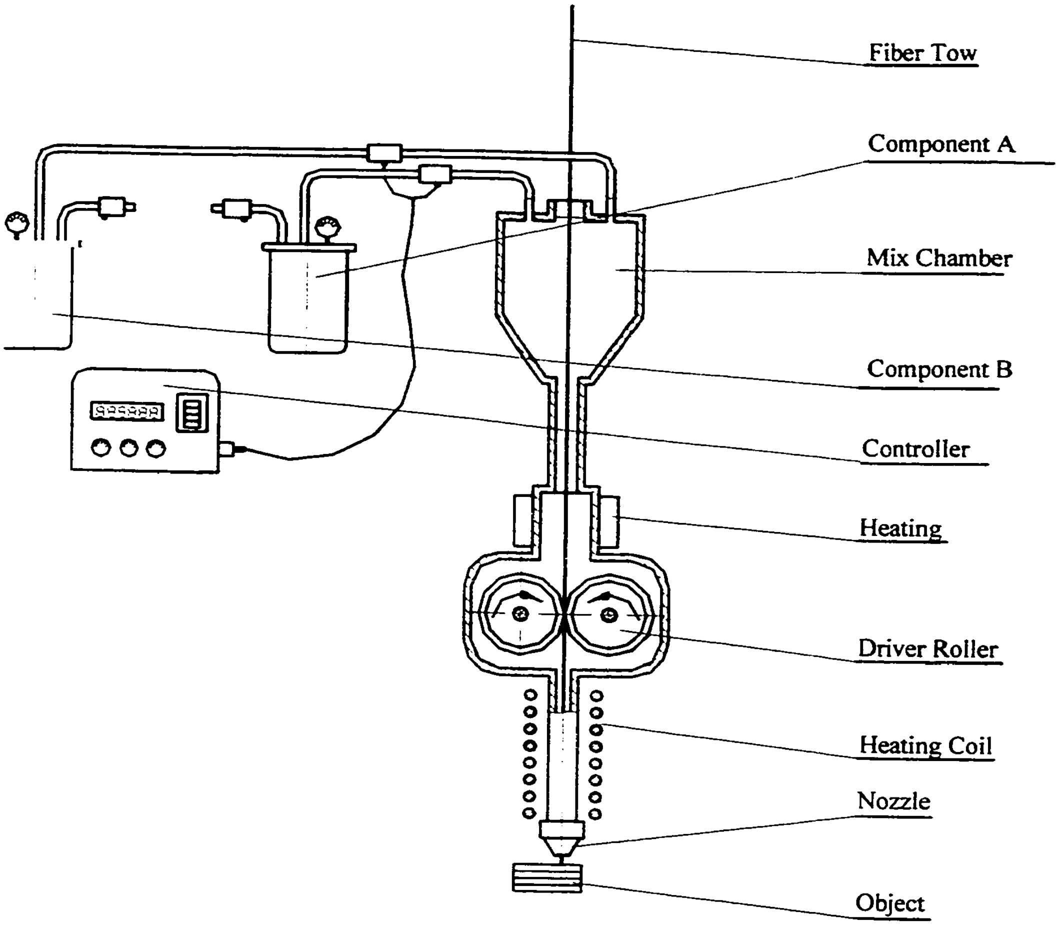

Fig. 2-5 Multi - components matrix composite.

As for thermoplastic materials, in order to increase the phase change speed or solidification speed, the temperature of the nozzle should not be too high; but should be high enough to insure the deposited current layer adheres to a previous layer. The temperature of the nozzle orifice is only 1° C higher than the melting point of the thermoplastic material in the FDM process. The environment temperature near the forming zone could not be too high. Setting the temperature of the forming chamber is another big issue and will be discussed in later chapters.

Speeding up the phase change will reduce the total part or model building time. When a typical thermosetting epoxy material with very low viscosity μ is deposited upon an object, the thermosetting material may not be able to maintain its own shape at the moment and it may flow around arbitrarily, preventing the deposition process from being continued. Hence another basic requirement for matrix materials and deposition processes is that the material fluid should maintain a geometric shape when the matrix is carried to a forming platform.

The phase change speed is acceptable and is relatively easy to control for the thermoplastic materials. For example, they are used in FDM, 3D Print and other RPT.

2-4-3 Effects of Fibers and the Selection of Fibers for CLM

In a composite, if the fiber volume percentage is 50%, the fiber will share over 90% of the force that is loaded on the composite. The mechanical effect of the fiber can be clearly during the composite application. However during the composite forming period, the fiber dose not undergo a phase change. So the fiber properties may not appear to be important for composite forming except for the Filament Winding process and CLM. Effects of the fiber and how to choose the fiber are described as follows:

1. If a fiber reinforcement effect is to be expected, the high physical and mechanical properties of the fiber must be considered.

2. The fiber should have high affinity with the matrix material so that the fiber tow could be impregnated immediately and wetted completely. The fiber must be flexible and pliable so that the towpreg can be formed with small angles when the matrix is in a fluid state.

3. The towpreg must be readily cut off where necessary. This is a required function of the CLM technology.

4. In some RPT processes, which use a UV curable epoxy, some fiber like cotton thread may be pre-mixed with the epoxy during the forming process in order to save the expensive photosensitive epoxy. The fiber is not only the forming process carrier but is also the filler material that is required to be inexpensive, soft, and has good affinity with the epoxy.

§2-5 FORMING STRATEGY AND CONCEPT DESIGN FOR CLM

The strategy for selecting the matrix and fiber for CLM has been analyzed. The selection of the component materials in a composite related to the forming strategy. The concept design and feasibility experiment should be done after conducting enough literature review and analyses. During the course of the present study, these two tasks were done alternately. By carrying out the feasibility study, features and limitation of CLM could be identified, clearly understood and then a new concept design could be performed.

In the discussion of forming a strategy design, two widely used plastic materials have been considered as the matrix materials, which are thermosetting and thermoplastic. Different kinds of materials could have different forming strategies. Even the same kinds of matrix materials could have different forming principles. There also have been a forming design to fit for two kinds of materials.

2-5-1 Concept Design for Thermosetting Matrix Materials

A thermosetting epoxy material was used for the feasibility experiment first. This feasibility experiment is illustrated in Figure 2-6, and more details about it will be explained in the next paragraph and in Chapter 5. Generally, the epoxy curing time takes several minutes or even several hours, which is far different from the requirement of PT. In RPT, the ideal solidification time or phase change time should be within one second, or even one-tenth of a second. Therefore, there are two forming strategies to follow for CLM that involves curing of a thermosetting resin. First, the towpreg could be prepared and kept in the B-stage [54, 55] as a semi-finished product to be used in the depositing procedure. These procedures are depicted in Figure 2-7. The towpreg in the B-State retains a certain cross-section shape, and also has the necessary tackiness. The towpreg is feed into a heated nozzle in which the resin is made to become fluent and chemically re-activated. The towpreg is pulled out of the nozzle orifice for deposition

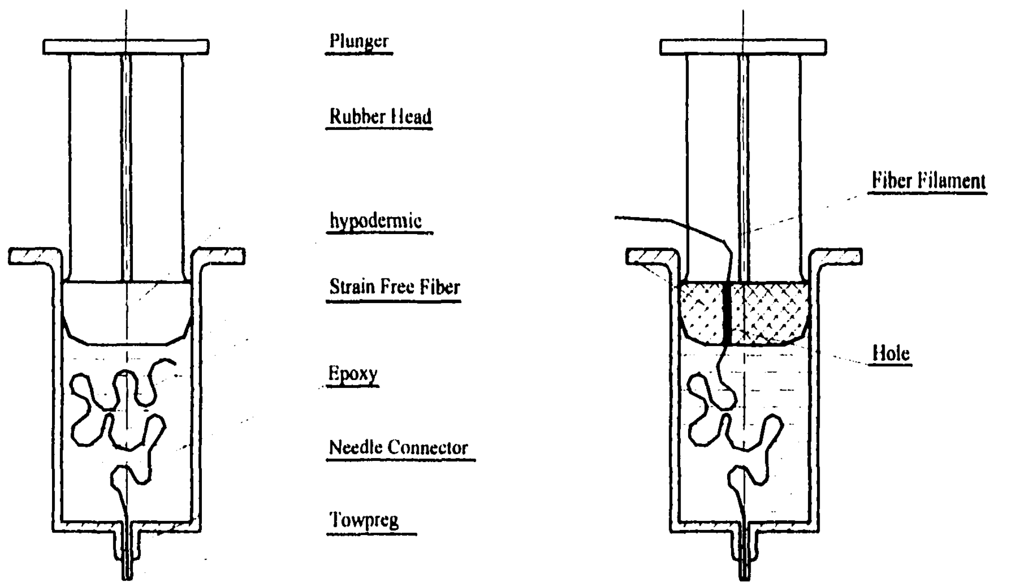

Fig. 2-6 A
A segment of fiber tow was placed inside a hypodermic in where it was pilled out along with epoxy resin.

Fig. 2-6 B
one end of a segment of fiber tow was placed outside the hypodermic, another end was positioned inside the syringe through the rubber head.

Fig. 2-6 A feasibility experiment.

onto a platform or a previous layer. As soon as a segment of towpreg is deposited, the resin in this segment is solidified.

Another method for forming thermosetting materials, mentioned previously, is shown in Figure 2-5. This is called a one-step method because the impregnation and deposition are done at the same time. But the method shown in Figure 2-7 is called a two-step method with this definition.

As shown in the Figure 2-5, the component A is a thermosetting material, and component B is a curing agent. First component A and component B are mixed together and the mixture is used to impregnate the fiber tow to make a towpreg. Then the towpreg is pushed or pulled out of the nozzle and deposited on the top layer of an object by some means. On the current forming layer, the deposited towpreg is heated or treated in way so as to solidify and adhere it to the previous layer.

2-5-2 Concept Design for Thermoplastic Matrix Materials

Up to now, most research and development work done for CLM are based on the thermoplastic matrix. Actually, no matter what matrix material is used, a problem exists with material delivery. The concepts of Active Material Supplying and Passive Material Supplying have discussed in §2-3. The features, principle and concept design of each material supply method will be studied in more detail in this section.

The Active Material Supplying method has been applied in many RPT processes such as FDM. Before several Active Material Supplying methods are introduced, a

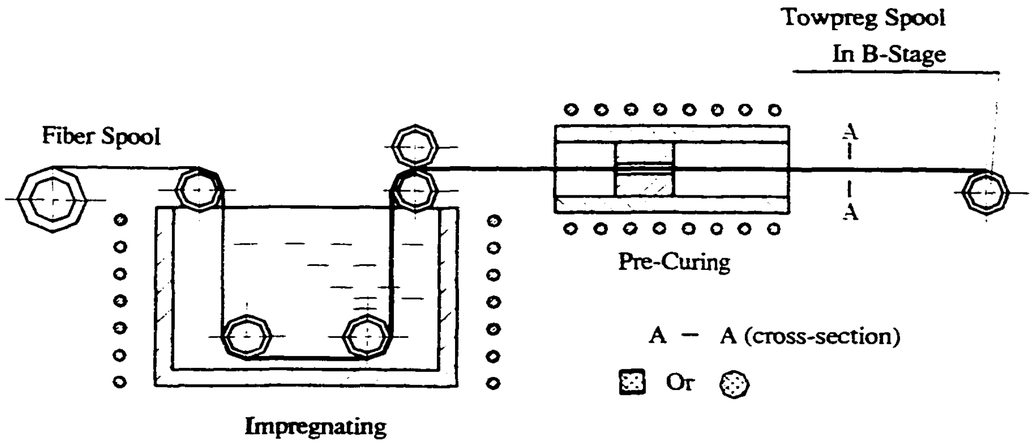

Fig. 2-7A
The step 1: The towpreg is made and kept on B-stage.

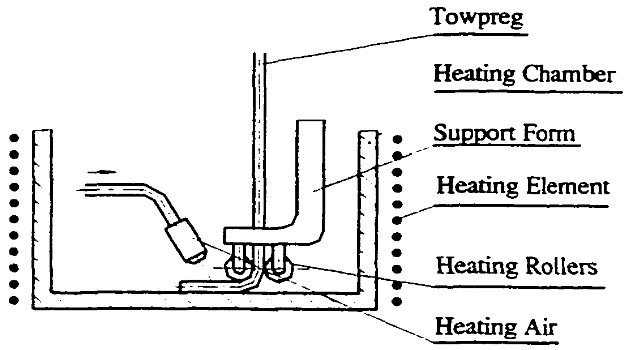

Fig. 2-7B
Step 2: the towpreg is deposited.

Fig. 2-7 CLM using thermosetting materials, a two-step forming method.

feasibility experiment could be used to understand the requirements for the realization of these methods.

The feasibility experiment is shown in Figure 2-6. For the experiment, a piece of fiber tow is put in a hypodermic syringe and one end of the fiber tow is placed outside of the needle connector. Another end of the fiber tow is placed inside of the hypodermic syringe unrestrained. Then the epoxy fluid is filled in the syringe, allowing the thermosetting matrix resin to impregnate the fiber tow. During the experiment, a plunger is pushed forward to extrude out the epoxy. The following phenomena has been observed: with the plunger being pushed forward, the downward flow of the polymer fluid helps to drive the impregnated fiber tow out of the needle connector. From this experiment, one can conclude that:

1. The impregnation and deposition procedures could be done in one step.
2. Active Material Supplying could also be realized with composite materials.

In order to simplify this experiment, the thermosetting epoxy was used as the matrix material at room temperature. But the melted thermoplastic material is expected to work in the same fashion. From the experiment, the design requirements for the CLM process are recognized as the follows:

1. An adjustable pressure vessel is needed in this process and the pressure can be kept at a constant value. An impregnated fiber tow with a matrix, called towpreg, can be pushed out smoothly under the pressure.
2. The fiber tow can be introduced continuously to the vessel to form

the towpreg.

3. If a fiber tow is supplied through a hole in the vessel, the hole is sealed using a one-directional seal mechanism like a check-valve. It could let the fiber tow come into the vessel but avoid the pressured resin to flow backward.

To meet the above requirements, the following designs were given for consideration and discussion in the early stage:

A design is shown in Figure 2-8. Thermosetting or melted thermoplastic matrix is poured into the vessel by a gear pump or an extruder machine to create a pressure field. Under this pressure the matrix polymer could flow out through the nozzle's orifice. The impregnated fiber tow could be brought out by the effect of a shear stress. There is a cone-shape sealing washer at the fiber tow entrance made from a rubber like material that is elastic and can withstand a temperature higher than the melting point of the thermoplastic. The fiber tow can be pulled in through the designed sealing washer only, but the matrix could go up through the washer.

Friction exists between the fiber tow and the rubber washer. The fiber tow is pulled in and pushed out through the vessel only by the shear stress that might not able to surpass the friction. To insure that the fiber tow can be pulled in the vessel smoothly, a couple of rollers are provided, which are controlled by a motor to drive the fiber tow into the vessel. Between the rollers and the nozzle, a segment of towpreg is tensile free and can be pushed out only by the vessel pressure.

This design appeared questionable after it was studied in detail. The sealing washer was not reliable in order to seal the high-pressured resin from going up, and the sealing washer might scratch the filaments of the Kevlar fiber tow. The design is perhaps

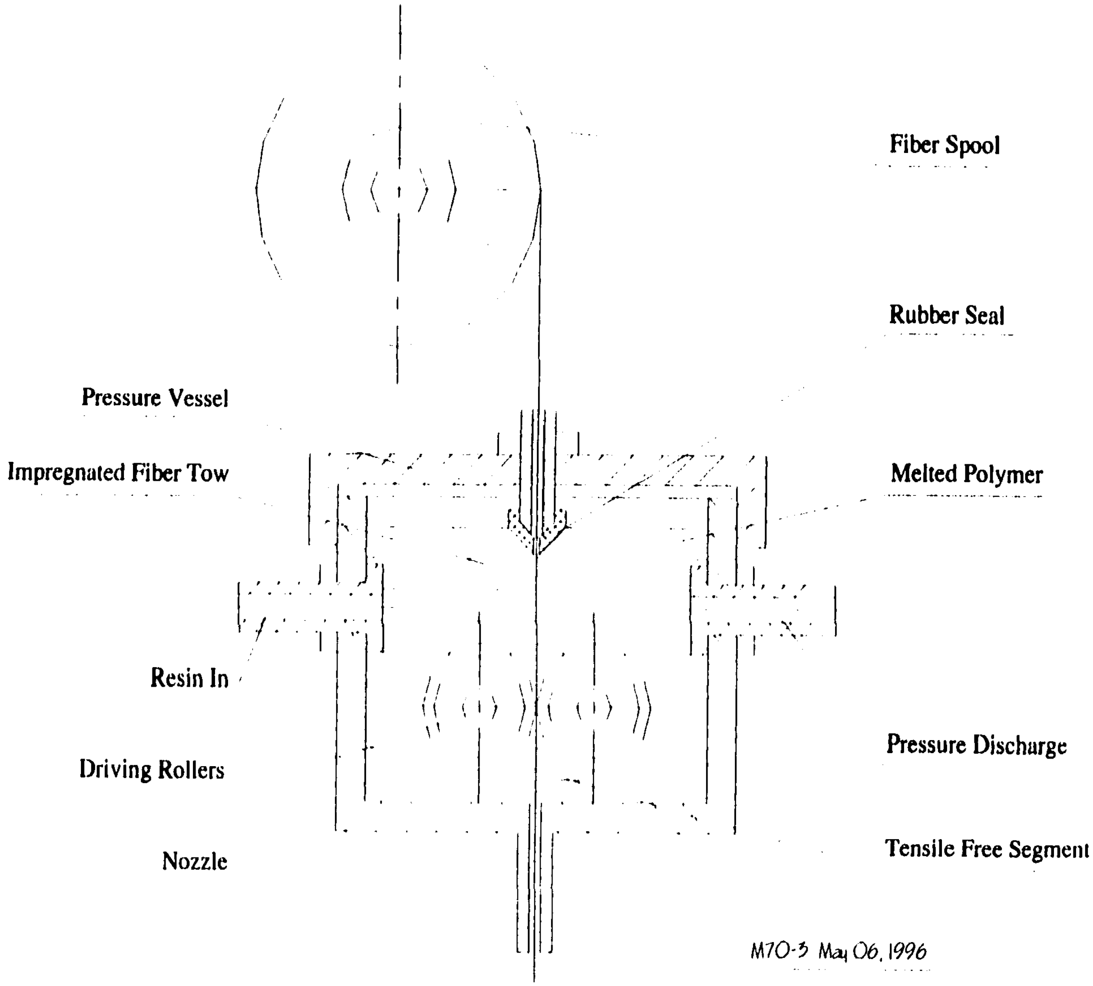

Fig. 2-8 The towpreg was pushed out by resin shear stress.

only suitable for glass fiber or for fibers not sensitive to friction.

Improved designs based on these concepts are pictured in Figure 2-9. The fiber spool is put into the vessel directly, so the sealing washer is no longer needed. Such a design is shown in Figure 2-9A, and it looks very simple. However, the fiber spool is soaked in resin. If the materials are not exhausted in one time, perhaps it could not be reused for a next forming process. Therefore the remaining fiber would be wasted.

To solve the problem, another design is shown in Figure 2-9 B. the matrix resin is filled to half volume of the vessel only; the fiber spool is positioned in the upper part of the container. The resin fluid level is monitored and is controlled at a certain level in order not to reach the fiber spool. So, the fiber spool is kept dry. Either by pumping in resin or pumping in air, a certain pressure inside the vessel could be built.

The shortcoming of this design is that the pressure of air cannot be kept at an exact value, especially at the beginning or stopping of deposition, because the air volume can change too much under pressure. In order to solve the problem, several designs were considered at the earliest research stage.

One of the designs is schematically shown in Figure 2-10. In this principle design, there are series of clips that keep the fiber tow held steadily and these clips are adjusted on circulating conveyer belt. They are being opened when they do not touch the fiber tow; they are brought through a parallel channel that continuously carries the fiber tow downward because the channel changes from wide to narrow and then wide again. Each of the clips hold the fiber tight in the narrow segment, and the fiber tow is pulled down.

Another design idea is shown in Figure 2-11. The principle is that a motor through a connector drives the bevel gear and then an impeller is driven to turn it. One or more

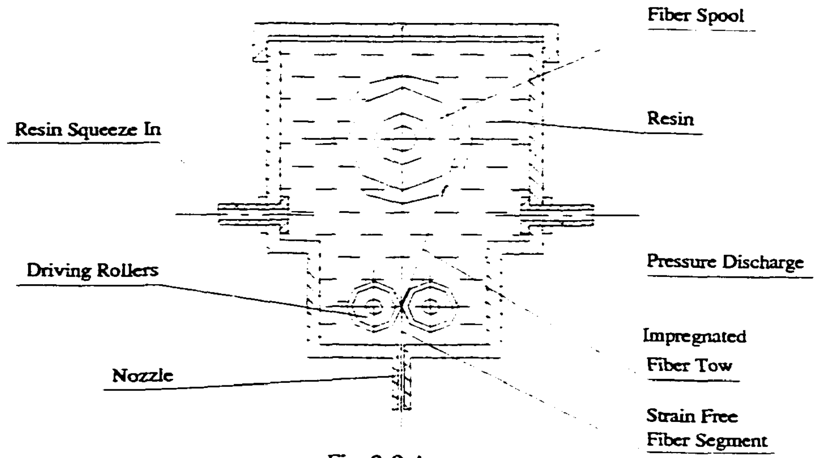

Fig. 2-9 A

Fiber spool is placed inside the vessel and soaked in resin.

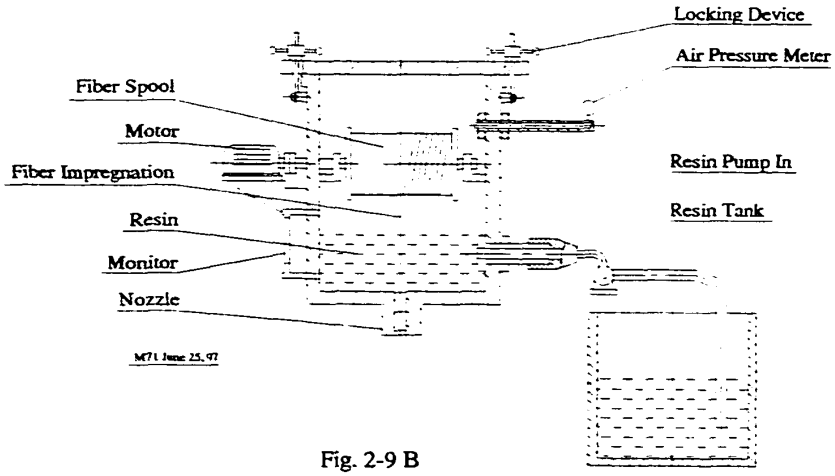

Fig. 2-9 B

Fiber spool is positioned in the upper part of the container.

Fig.2-9 Fiber spool is positioned inside the pressured vessel.

helix blades are fitted on the impeller. When the helix blades are rotated in the vessel, a downward directional field of resin fluid flow is created. The resin fluid impregnates the fiber tow and drives it out through a nozzle. There is a hole on the center axis of the impeller. The fiber tow can be pulled through it to the vessel, but the matrix resin cannot go up through the hole because the resin flows downward. Therefore any a seal washer is not necessary. In the mechanism, the pump or extruder provide only a melted polymer and could not provide pressure to the vessel.

A different design is illustrated in Figure 2-12. The main idea is that the fiber tow is impregnated and driven down by a high-speed resin stream. In this design, an annular pipe replaces the nozzle. A ring slit is cut off from the lower side of the annular pipe. When the annular pipe is injected with matrix resin, a resin stream could be directed through the slit to the fiber tow at an angle to push down and impregnate the fiber tow. The scattered surplus matrix resin is reflected by the fiber tow and collected by a tray. If a photo curable resin is employed for this design, a laser beam should be focused on a point, this point is where the resin stream hits the fiber tow. Around the laser beam focused area, the towpreg is pre-solidified and is deposited on a desired place.

The designs introduced above are used to illustrate how to solve the problem of depositing and impregnating in one step, and how the fiber tow could be added and pushed upon at a desired point. If CLM process is separated into two steps, the design of each process step should be simple. A two-step method for the thermosetting matrix has been introduced in the previous section. In fact, the CLM with the thermoplastic matrix can be separated into two steps too. Figure 2-13 also illustrates the CLM process done in two steps. First, in the fiber tow is impregnated and becomes a towpreg. The second step

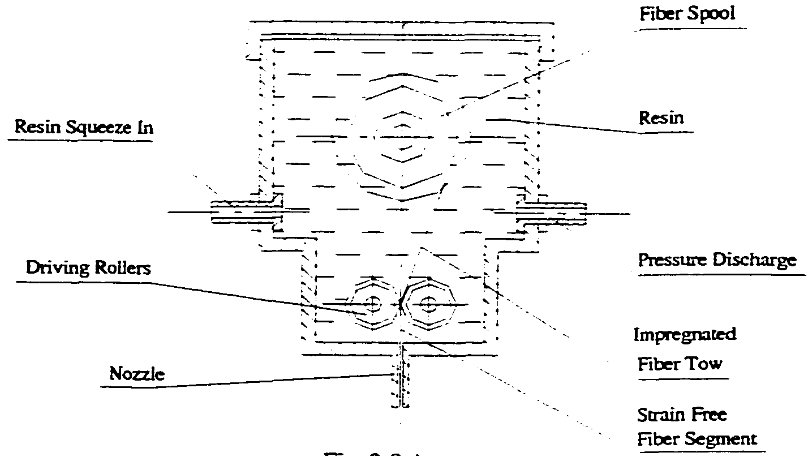

Fig. 2-9 A

Fiber spool is placed inside the vessel and soaked in resin.

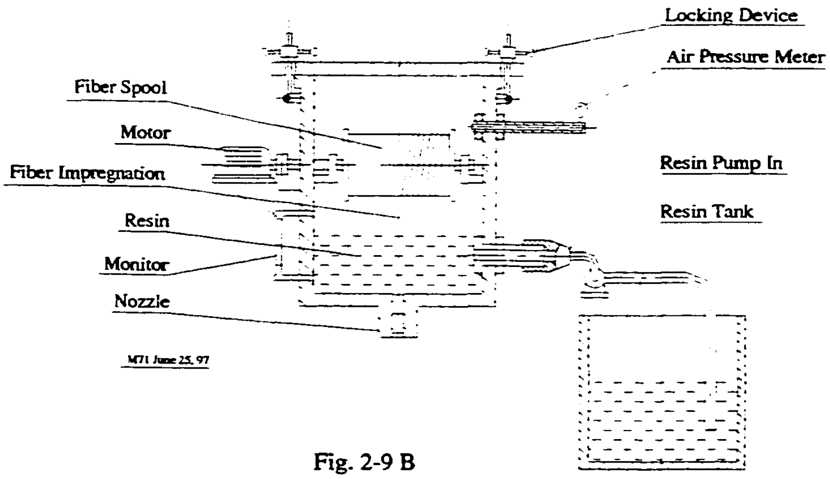

Fig. 2-9 B

Fiber spool is positioned in the upper part of the container.

Fig.2-9 Fiber spool is positioned inside the pressured vessel.

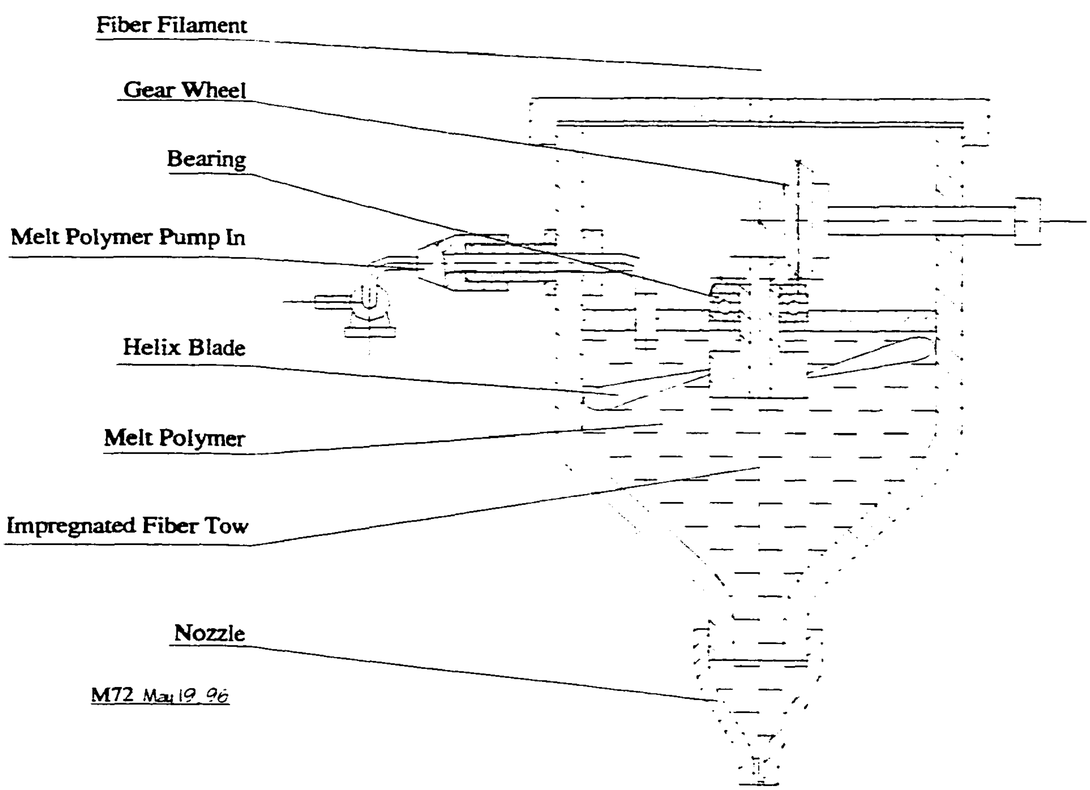

Fig 2-11 When the helix blades are rptated in the vessel, a downward directional velocity field of the resin fluid flow is created. The resin fluid impregnates the fiber tow and drives it out through a nozzle.

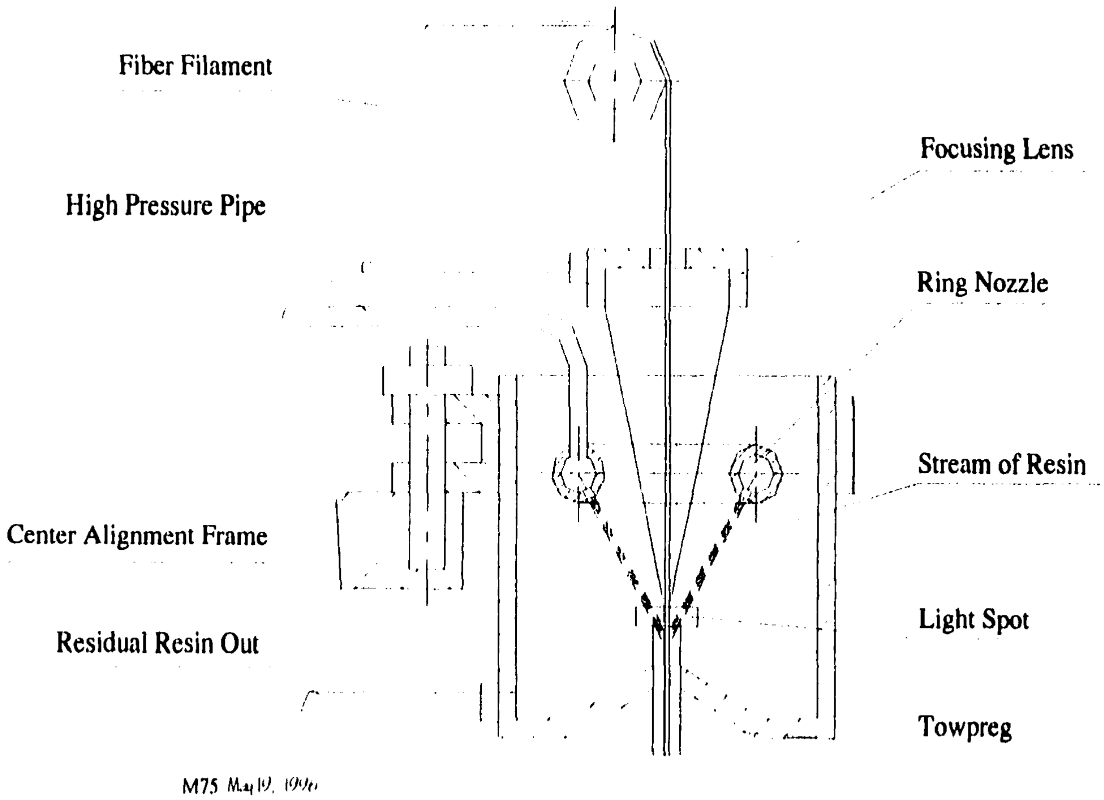

Fig. 2-12 the fiber tow is impregnated and driven down by a high-speed resin stream.

the solidified towpreg is employed as a raw material for deposition. In the schematic design, the main process can be seen. When the fiber tow is passed through the melted thermoplastic material bath, it could be impregnated fully and becomes a towpreg. Then it is cooled to solidify. In Figure 2-13, the solidification of the thermoplastic matrix is done by cool air. But solidification should be faster if water is used as a coolant.

After solidification, a towpreg is like a wire with certain rigidity and can be controlled by a couple of rollers to drive forward and backward reliantly. The depositing process is similar to the FDM process, but the towpreg cutting off function should be considered.

Two methods similar to FDM are designed and pictured in Figure 2-14. A towpreg is delivered to the heating nozzle by a couple of driving rollers and squeezed out of the nozzle. Before the towpreg is driven into the nozzle, it has enough rigidity to perform like a piston. When the towpreg is driven into the nozzle with a temperature gradient, the resin in the towpreg is changed from a solid to a soft and melted substance. The solid towpreg, the piston, is driven by the roller downward to push the melted towpreg out of the nozzle.

An improved design is shown in Figure 2-14B. A cooling water sleeve is installed at the nozzle's entrance. The nozzle's entrance is expected to keep a certain temperature, and the towpreg is ensured to have the piston effect in this design.

The RPT with a metal matrix composite material is expected to work on a similar forming principle. A concept design for the metal matrix composite with RPT process is given in Figure 2-15. The composite contains aluminum as the matrix and continuous carbon fibers as the reinforcement material. As the picture shows, the aluminum metal

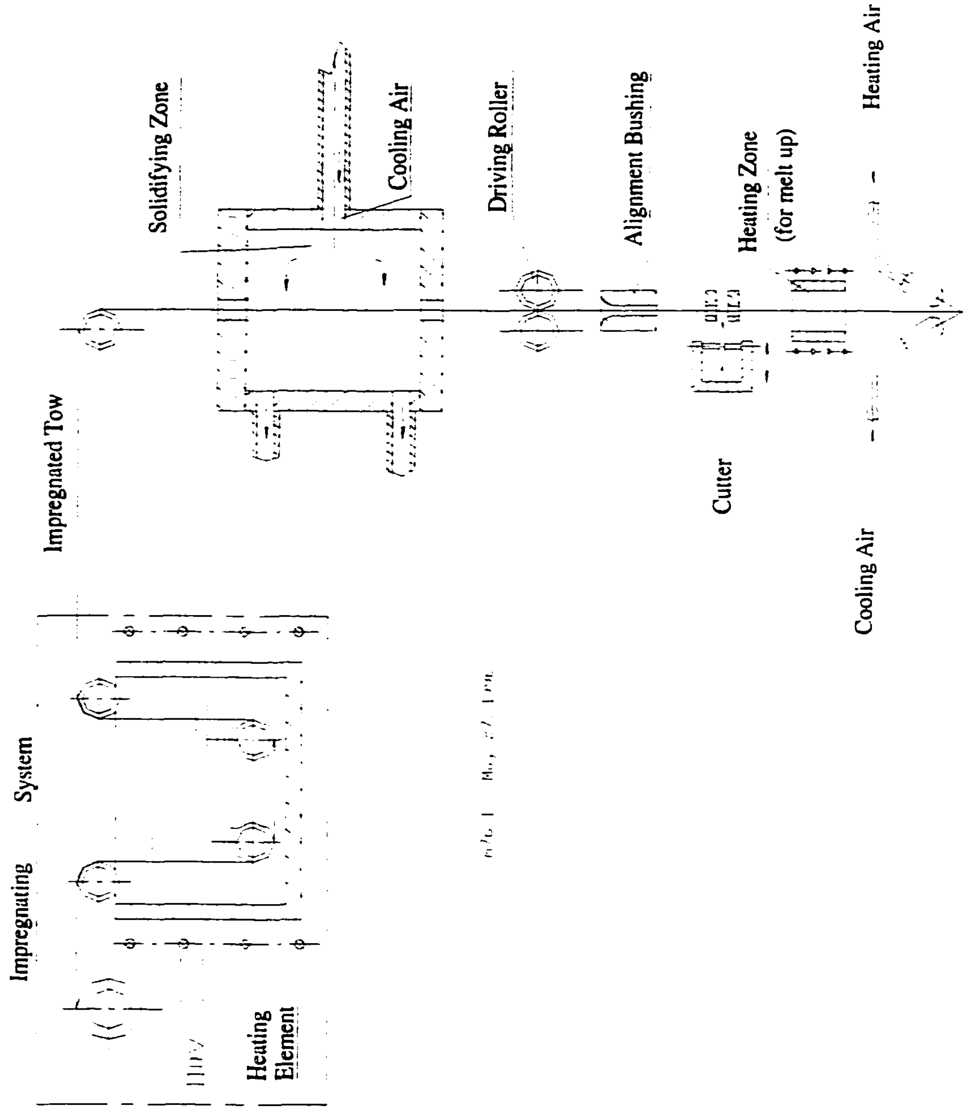

Fig. 2-13 a two-step method for thermoplastic matrix.

stick is driven by a couple of controlling rollers, and there is a hole in the middle of the aluminum stick. Carbon fiber can leave through the hole smoothly. Before the stick is melted, it is a solid and can be used as a piston to push the front part (melted aluminum) and fiber tow together to flow out the nozzle. The entrance diameter of the nozzle is 3 or more times larger than the exit. The solid stick has an enough rigidity to push the melted aluminum. In order to ensure a proper volume fraction of fiber, when the fiber passes through the hole of metal stick center, its speed could be much higher than the stick's forward speed to add into the front melted zone, the molten bath. This is a concept design without much calculation and feasibility test. One of the questions is that the distorted metal could stick as the fiber tow passes through the hole in the soft zone. Even if the principle of the design is correct, the parameters and geometric shape of the nozzle should be studied carefully.

It may be noted that plastic welding can be seen as a RPT process. According to the concept, a deposition method like plastic welding is pictured in Figure 2-16 [56, 57]. If a towpreg made of a thermoplastic material matrix has enough rigidity and can be controlled forward or backward by a device, it can be used as a welding rod to build an object. But in general, the welding rod is thick, and the precision of the welding seam is lower than the requirement for a RPT. It is possible to use the towpreg as the welding rod to build a larger structure or component because the thick towpreg is relatively thin in the larger part. On the other hand, if the towpreg is used as the welding rod in a real plastic welding process, the mechanical properties of the welding seam should be high because the fiber can reinforce the welding seam. The concept designs are shown in from Figure 2-7 to Figure 2-16 and are briefly analyzed above, whatever the materials, all the designs

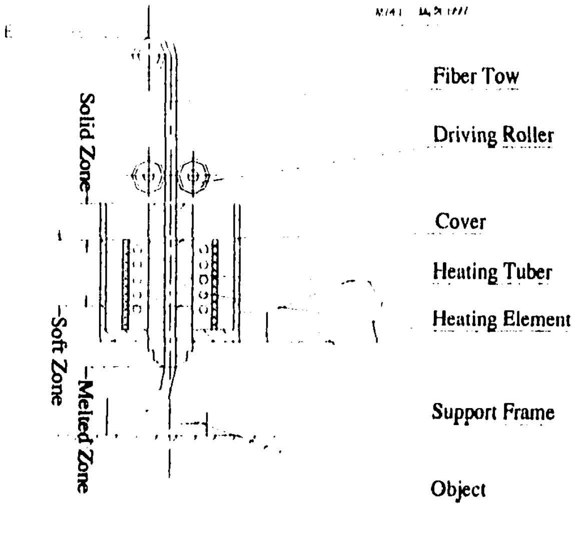

Fig. 2-14A
a towpreg is delivered to the heating nozzle by a couple of rollers and squeezed out of the nozzle by the piston effect.

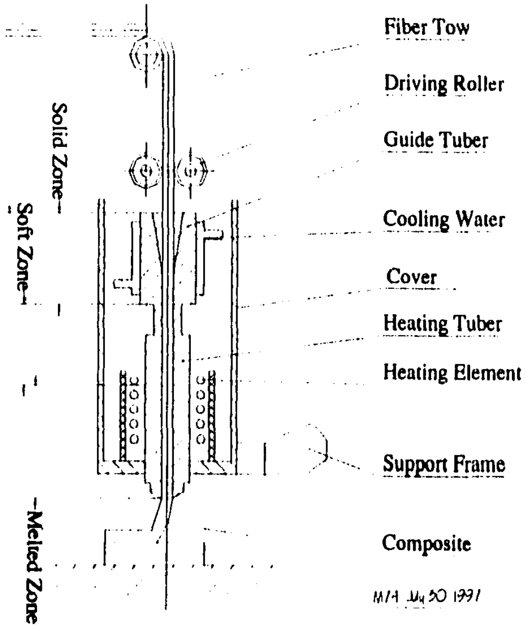

Fig. 2-14B
a cooling water sleeve is installed at the nozzle's entrance to keep a certain temperature.

Fig. 2-14 the piston effect deposition

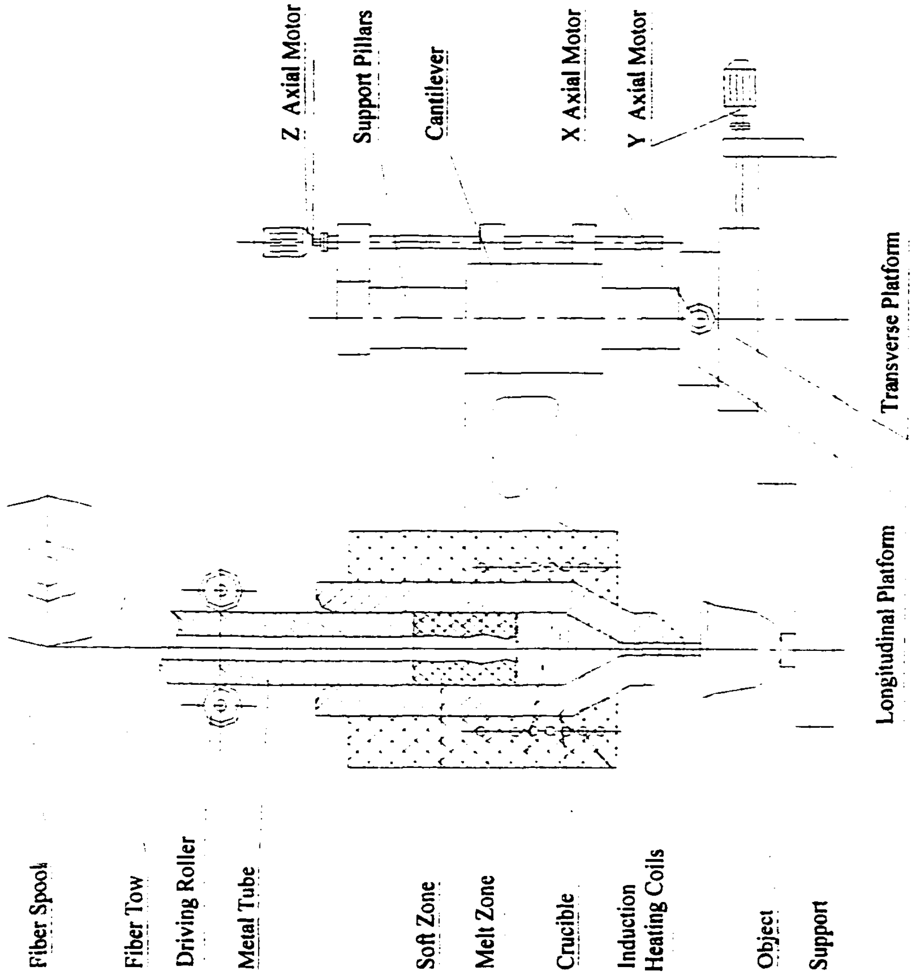

Fig. 2-15 CLM with metal matrix composite is deposited by the piston effect.

can be classified into the Active Material Supplying method.

There is another materials delivery method, Passive Material Supplying. An example that works on this principle is the Filament Winding process. In Figure 2-17, a Filament Winding Machine is shown schematically. When the mandrel is rotated, the filament or fiber is pulled from a carriage and welded on the mandrel layer by layer. The filament path and winding style for each layer can be designed and led by the moving carriage and mandrel rotation. The process is used to form an axisymmetric part or uniform cross-section part only. But from this process, a new material-delivering concept for RPT, the Passive Material Supplying method, can be evaluated and used in the CLM process.

The advantages and shortcomings of the Active and Passive Material Supplying are compared and summarized as follows:

1. Active Material Supplying:

a. The deposition speed would not be limited by the quality of deposition. If the deposited material can be solidified immediately, the depositing speed would only be limited by the speed of a motion device.

b. An error or a mistake in the previous layer does not interrupt the forming process of the current layer.

c. The support structure can be simplified in some situations, which are analyzed in §2-3.

d. The depositing process can be resumed and restarted on demand at once.

e. The machinery and controlling system for this method are

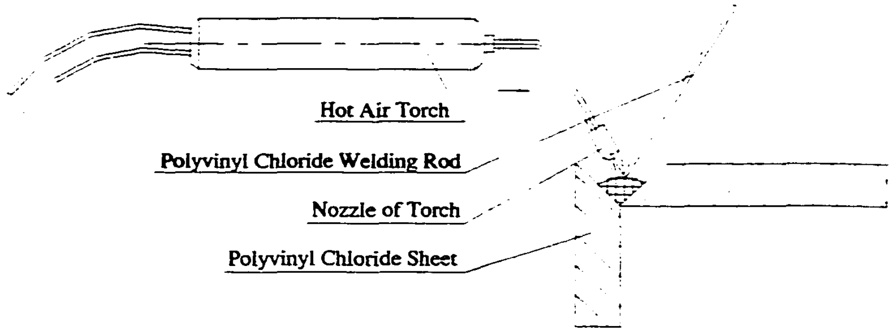

Fig. 2-16 a depositing principle like the plastic welding.

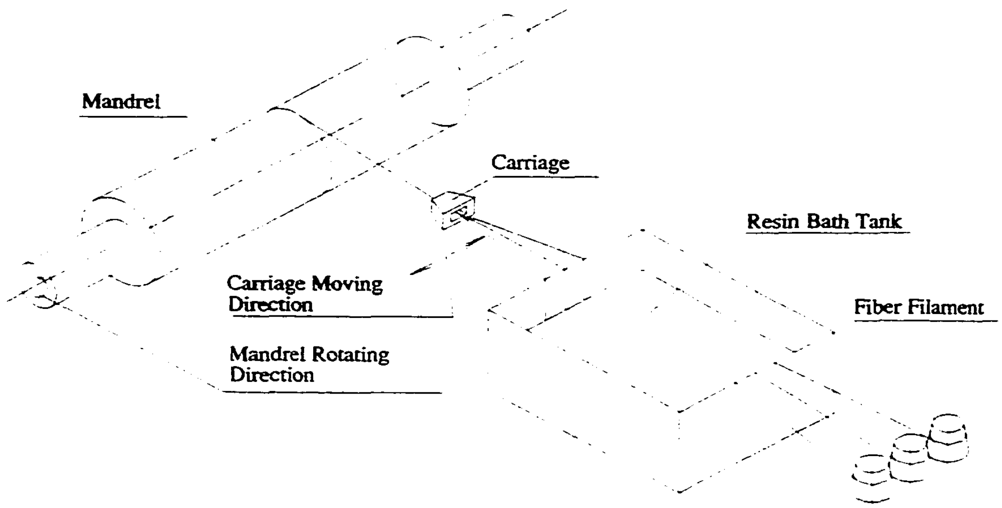

Fig. 2-17 a CLM deposition principle like the filament winding machine.

relatively complex.

2. Passive Material Supplying:

a. The machinery and controlling system for this method are relatively simple.

b. The depositing speed depends on whether or not the towpreg is anchored to the previous layer. The deposition process could be interrupted by a mistake in the previous layer.

c. The method of restarting should be considered.

Two concept designs are described for the Active Material Supplying and Passive Material Supplying methods, respectively. The dissertation research was centered on these two methods.

A two-step, Passive Material Supplying method and for thermoplastic matrix composites is shown in Figure 2-18, but the method of making the towpreg is not shown in these pictures. The towpreg is driven to pass a heating pipe by a couple of driving rollers, and then is heated by the radiation of the heating pipe to a molten state (See Figure 2-18A). Another couple of rollers called a depositing roller is positioned near the bottom of the heating pipe to pull the molten towpreg downward and to help the towpreg roll to a desired location. Then the deposition is realized. But in the design, the axis of the depositing rollers must be perpendicular to the direction of deposition at all times. The software and machinery designs for this situation would be quite demanding.

A simplified design is shown in Figure 2-18B. The depositing roller is replaced by an alignment ring i.e. nozzle. Its diameter is larger than the diameter of the towpreg. During the deposition step, the nozzle is pressed on the molten towpreg to help it adhere

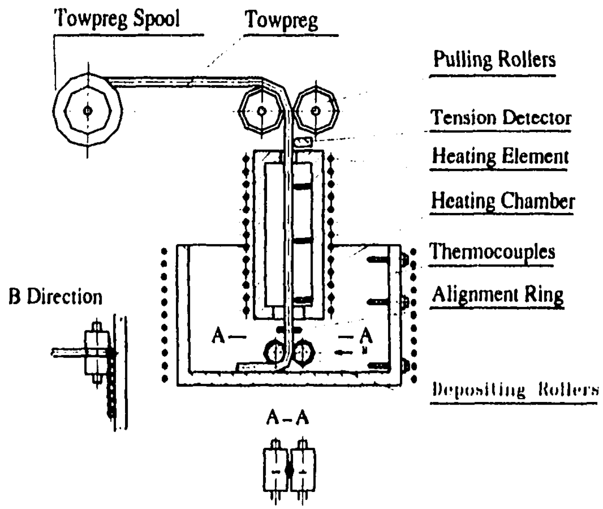

Fig 2-18A a couple of deposition roller is positioned near the bottom of the heating tube to pull the molten towpreg downward and to help the towpreg roll to a desired location.

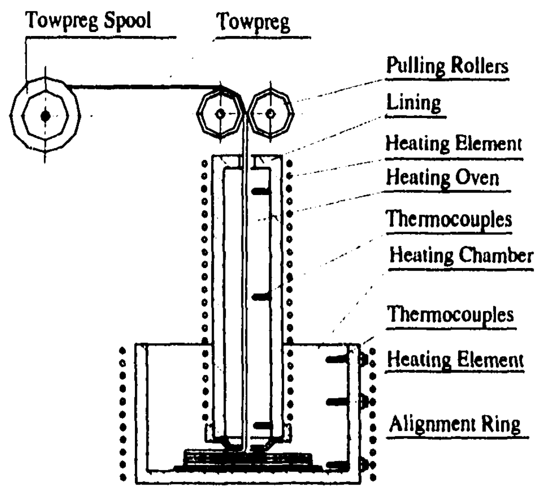

Fig. 2-18B The deposition roller is replaced by an alignment ring.

Fig 2-18 Passive and active material supplying deposition methods.

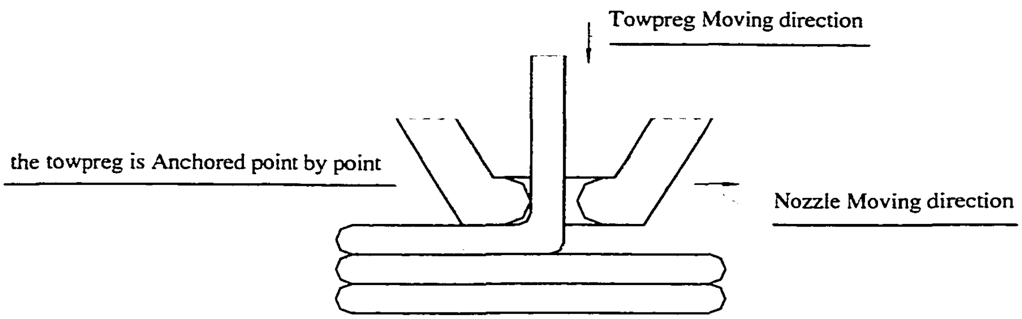

Fig. 2-19 the passive material supply mechanism.

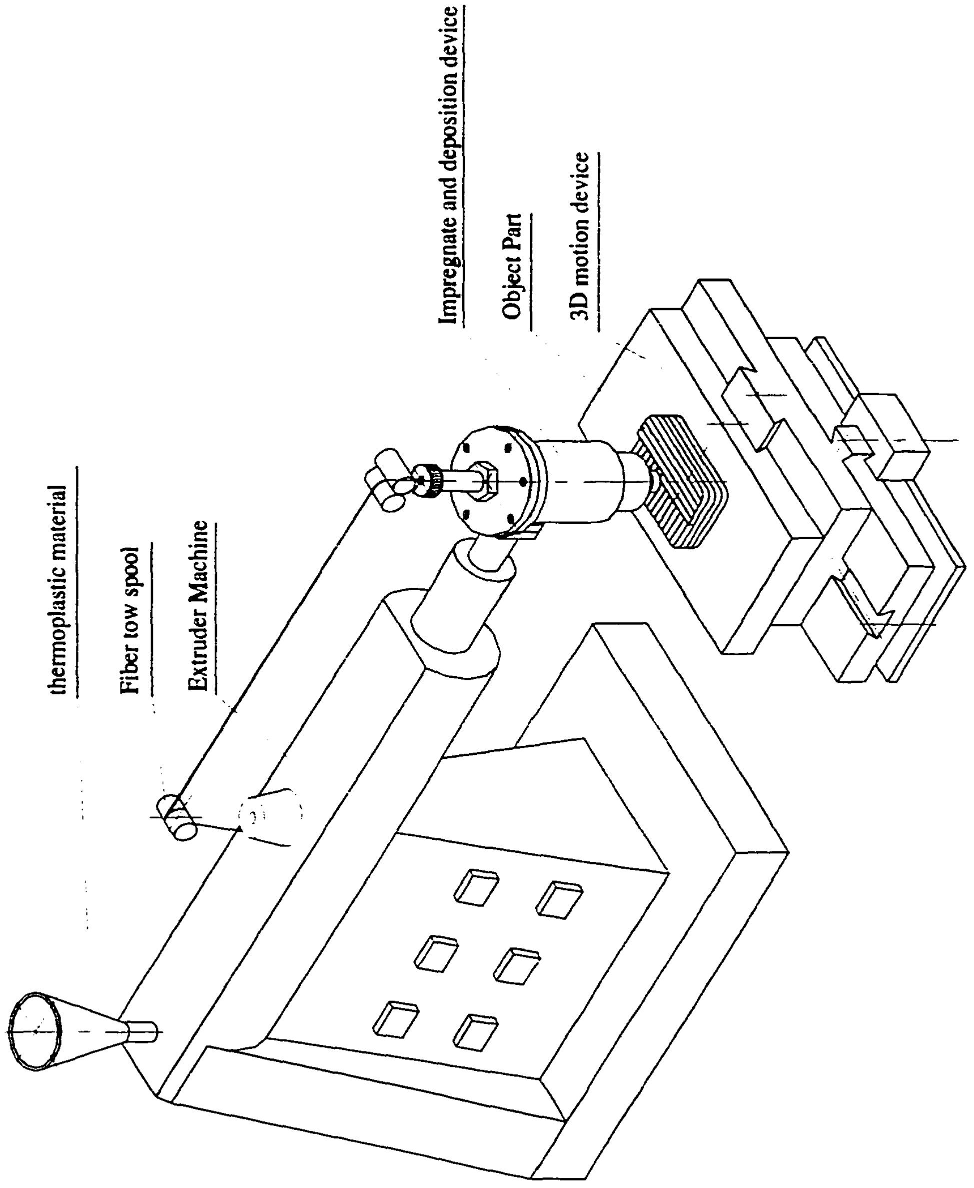

Fig. 2-20 the Active Material Supply method, a one-step forming process.

to the previous layer. The forming mechanism is depicted in Figure 2-19. When the molten towpreg is deposited on the previous layer, under the surrounding temperature, the towpreg is solidified and glued to the previous layer immediately. The towpreg forms a series of anchor points. Because the anchor points adhered to the object, the towpreg should be pulled automatically out from the nozzle when the nozzle is continuously moved relative to the object. Then the deposition procedures are repeated to form successive layers of an object.

Throughout the above analysis and based on a feasibility testing, the design called self-anchoring method, shown in Figure 2-18B, has been selected as the primary design.

Also, an Active Material Supplying method shown in Figure 2-20 has been selected. It is designed for the thermoplastic, one-step method. In addition, a lot of research and development have been done around the designs. More detailed explanations will be given in Chapter 4 and Chapter 5.

§ 2-6 CHAPTER CONCLUSIONS

1. The development strategy of a new technology has been analyzed, and a research outline for CLM has been presented.

2. The forming theories of the CLM and the material selection issues for CLM have been studied.

3. The new concept of Active and Passive Materials Supplying has been put forward to help categorize and create a new deposition method.

4. Several concept designs have been given and analyzed in this chapter.

5. Two designs are considered as the best plans.

CHAPTER 3 PRINCIPLES OF TOOLPATH DESIGN

§3-1 INTRODUCTION

The principle of CLM forming, concept design and developmental procedure have been discussed before. The methods of material delivery have been analyzed and are divided into two main kinds, which are Active Materials Supplying and Passive Materials Supplying discussed in Chapter 2. In this chapter the precision of deposition and the pre-design of mechanical properties will be studied. We will also investigate the requirements of software to control the toolpath in a certain deposition procedure.

The depositing method for CLM technology is different from any other method, in terms of the sources of error and how the system error can be reduced. These are problems unique to the CLM technology. Once the CLM precision question is answered, the rules for software development and tool path generation will be obtained.

How high should the precision be for a new forming technology? What are the mechanical properties for all the formed parts? How are the mechanical properties be achieved? These are questions to be answered for all new technology development efforts. So first of all, we should research the precision in more details.

§3-2 POTENTIAL SOURCES OF ERRORS AND CONTROL METHODS FOR CLM

3-2-1 Potential Origins of Errors

The forming process of RPT is realized by adding material layer by layer. Depending on how much material is added each time, the precision could be affected directly. The cross sections of complicated shape parts are not uniform. Because the dimensions of a cross-section can vary from layer to layer, no matter what RPT forming process is used, there will be a Staircase Effort. The Staircase Effect and its dependence on the layer thickness are illustrated in Figure 3-1.

The Staircase Effect between layers is influenced by the thickness of each layer. The thickness of layers at the left side of Figure 3-1 is two times that of the right side. Therefore, the difference between the theoretical contour and the formed part profile line at the left is larger than that of the right side. For example, in the LOM and SL technologies, each added layer is very thin. Furthermore, StereoLithography is currently approaching the point where *90%* of all the measurements on a commonly used accuracy standard test part will be within five mils (*0.005*") of their CAD value. The Staircase Effect is so small that it could not be recognized by the naked eye.

In the FDM technology the thickness of each layer is determined by the diameter of rods, which is deposited by a nozzle. If the orifice diameter of the nozzle, *Dn*, is *1mm*, the max error is ½ *Dn*, or *0.5mm* in principle. If the orifice diameter of the nozzle becomes small, the error could be reduced proportionately. But the orifice diameter of the nozzle could

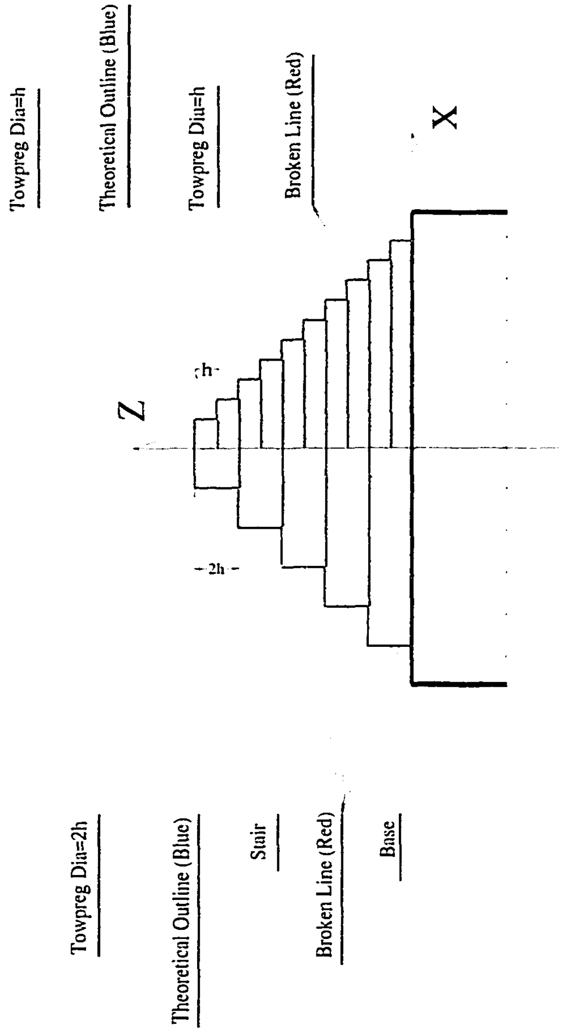

Fig. 3-1 Staircase effect and its dependence on the layer thickness.

not be reduced without a limitation. The limiting factors of the nozzle's orifice diameter are discussed as follows:

1. If the nozzle orifice diameter becomes small, the number of layers that are needed to build the whole part would increase, resulting in an increased part-building time.

2. If a pressure is needed to extrude the material, the nozzle supplied pressure, P_n, is inversely proportional to the reciprocal of the forth power of the nozzle's orifice diameter D_n, $P_n \propto 1/(D_n)^4$. The pressure that is needed to extrude materials out of the nozzle is increased dramatically with a smaller orifice. In other words, if the orifice diameter of the nozzle becomes too small, it may be come extremely difficult, if not impossible, to extrude out the material. The extrusion process may be come unstable and difficult to control. The smallest orifice dimension will be studied in Chapter 4.

Besides the staircase effect between layers and even inside a layer, there may also be the error that is called "In Layer Error". The sources of this type error are analyzed in the following:

1. The diameter of a towpreg could be a source of error. The two common kinds of In Layer Errors are shown in Figure 3-2.

Materials are deposited line by line to cover a whole layer; the deposition direction is along the X-axis direction and the towpreg line increment direction is along the Y-axis. An error occurs where a broken line replaces the arc, which is the theoretical contour (See Figure 3-2A). The towpreg size in the upper portion is two

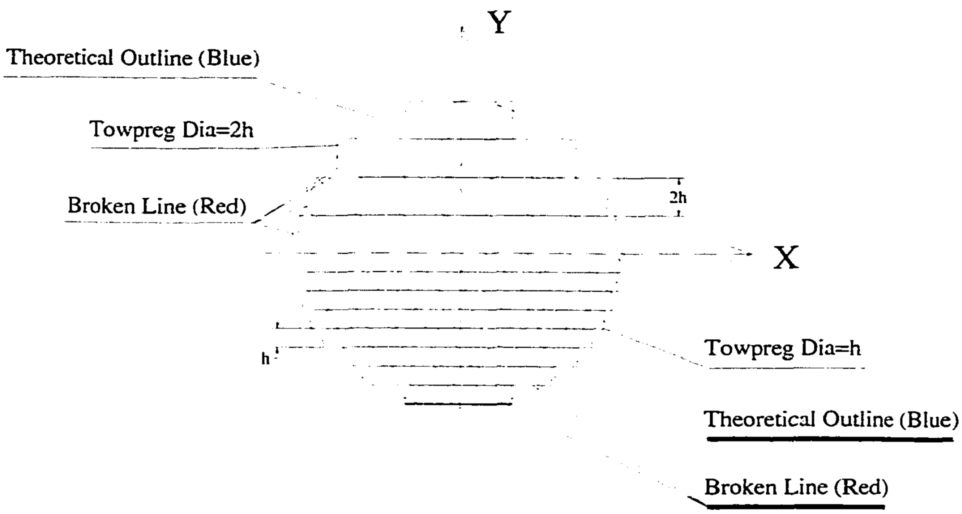

Fig. 3-2A In Layer Staircase Effect.

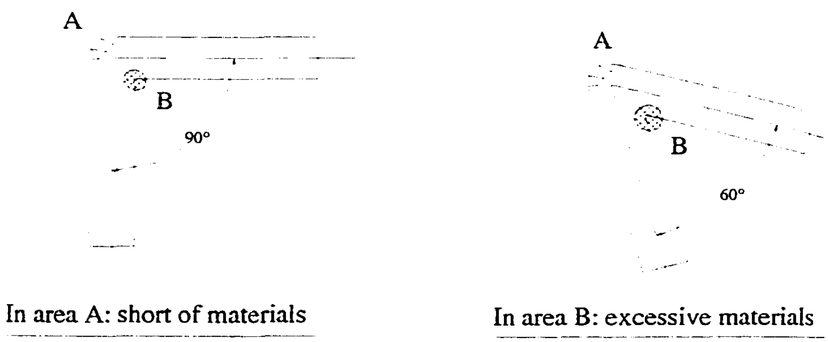

Fig. 3-2B Turn deposition direction induced errors.

Fig. 3-2 In layer errors.

times of that in the lower portion of Figure 3-2A. An influencing factor in this error is obviously the towpreg diameter.

An error is introduced during the deposition process and is shown in Figure 3-2B. When the deposition direction is changed and the towpreg is bent at an angle, at depositing direction-changing points, an error occurs. The error is more pronounced when the turn angle is larger and/or the towpreg is thicker.

2. In the case of towpreg extrusion as a way of active material supplying and under the assumption that 3D motion control error is negligible, the discrepancy between the material delivery speed and the motion device speed could also become a source of error.

3. An error is induced by material shrinkage, which is the problem many RP technologies could face. On CLM, the shrinkage error should be smaller since the fibers, which occupy at least *50%* by volume of the towpreg, do not shrink much within the common working temperature range.

4. An error could occur as a result of nozzle pressure variations. If a nozzle-supplied pressure fluctuates during deposition, the supplied material could also fluctuate particularly at the beginning and end.

5. A difference between the nozzle orifice diameter and towpreg diameter could also cause an error: In the case of Active Material Supply, material is pushed out of the nozzle, and the diameter of the towpreg is equal to the diameter of the nozzle's bore. If the Extruding Die Swell Effect of a plastic material is considered, the diameter of the extruded towpreg could be larger than the bore of the nozzle. But, in the case of Passive Material Supply, the diameter of the nozzle bore should be

larger than the diameter of towpreg. Otherwise, a frictional force between the orifice and the towpreg will be large and the force that is needed to pull the towpreg out of the nozzle will correspondingly be larger. If the friction force arrives at a certain value, the process could not be continued. The diameter difference between the nozzles bore and the towpreg is shown in Figure 3-3. These kinds of errors will be studied in the next subsections in more detail.

6. There is another error brought in during the deposition process for Passive Material Supply. When the deposited towpreg could not be immediately solidified and anchored to a previous layer, a larger error will be induced. These problems will be discussed in more depth in Chapter 4.

3-2-2 Controlling the Errors

1. In order to reduce the staircase effect, a general method may be followed which involves building a perimeter area (exterior or interior boundary) by using a smaller-bore nozzle and building the interior of a layer by using a thicker towpreg.

2. The forming precision is related to the forming speed, and one normally has to strike a balance between part accuracy and forming speed. When high accuracy is required, the deposition speed may have to be reduced.

3. The precision may change as the deposition direction is changed, so at the turning point of the of deposition direction, a reduced forming speed is necessary. When a straight line is formed, the forming speed could be increased as high as possible to reduce over-all the forming cycle time.

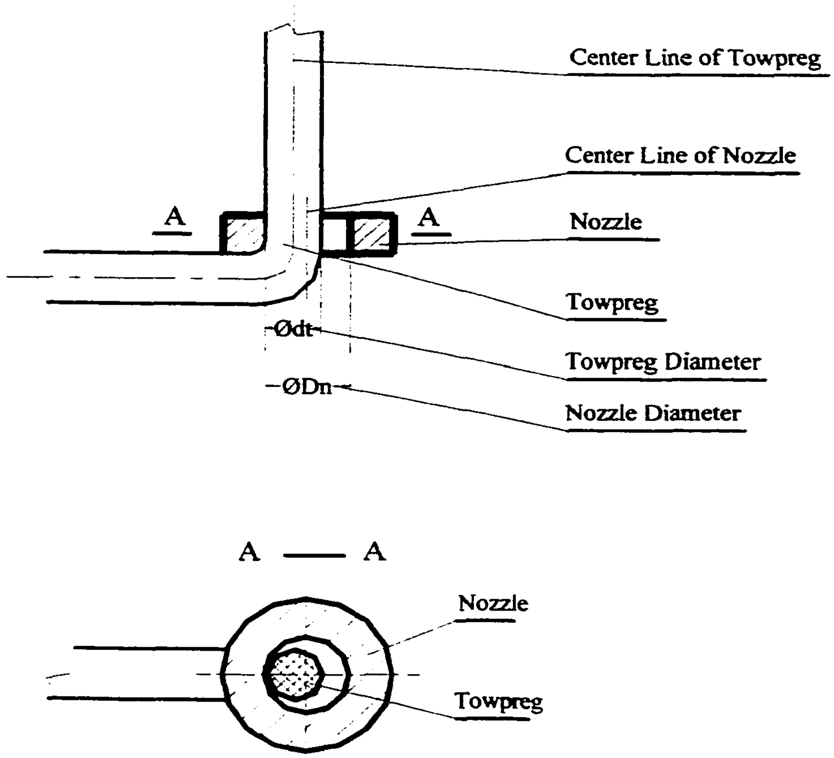

Fig. 3-3 Difference in Diameter of the nozzle bore and the towpreg.

4. The material compositions of the towpreg may be re-formulated to reduce shrinkage.

5. At starting points or stopping points, an error sometimes occurs especially in the case of Active Material Supply. Therefore, a materials compensation method may be considered by way of software or hardware variations.

§3-3 ERRORS CAUSED BY DEPOSITION DIRECTION CHANGES

In the self-anchoring method, using a device of Passive Material Supply, the bore diameter D_n of the nozzle is larger than the outside diameter of the towpreg d_T. During deposition, it is possible to make a big error, especially when the nozzle makes a big-angle turn. Situations in which an error could be induced include:

1. When the self-anchoring method or other Passive Material Supply methods are employed to deposit the towpreg,

2. When the diameter of the towpreg is less than the diameter of the nozzle's bore, and

3. When the deposition changes direction.

Figure 3-4 illustrates the latter possibility. The difference in diameter between the nozzle bore D_n, and the outside diameter d_T of the towpreg is shown in Figure 3-4A. According to the toolpath, the center of the nozzle is moved from point A to point B_0 and then is turn a right angle to move along $B_0 C$ direction, (which is perpendicular with line AB_0) to B_1, B_2, ... to point C. What is a moving regularity of the towpreg center point (X_0, Y_0)? If the regularity is found, the error can be figured out immediately. Now, the error can be

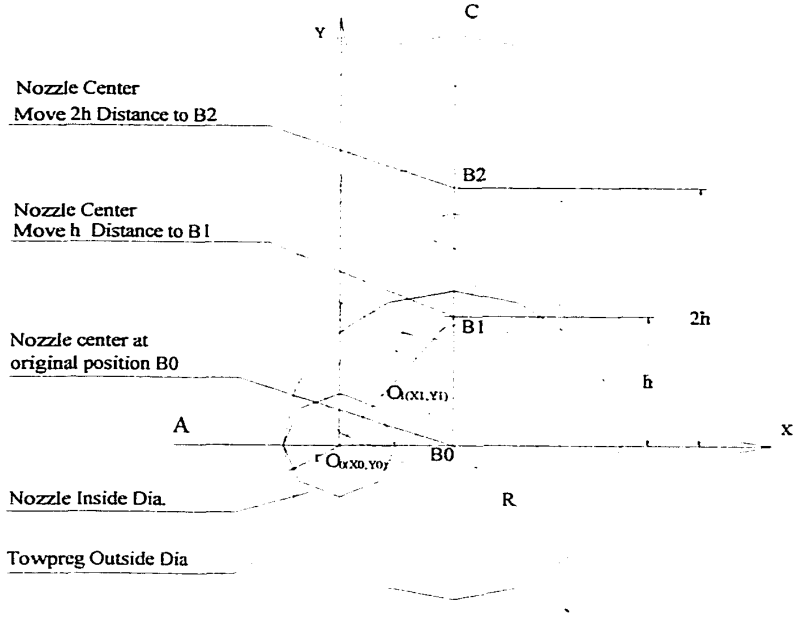

Fig. 3-4A.

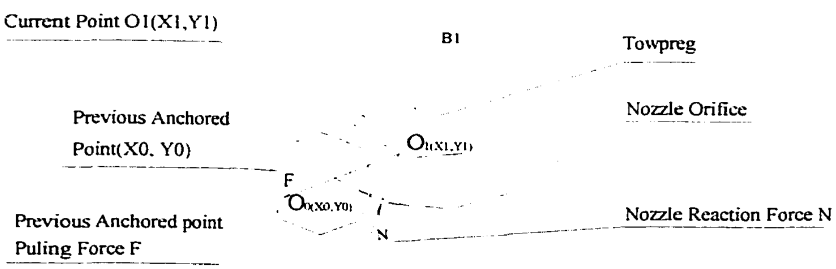

Fig. 3-4B Free Body Diagram.

Fig. 3-4 Right angle turn.

determined by the difference between the center track of towpreg and the center track of the nozzle.

3-3-1 A Mechanics Model

To set up a mechanics model, several assumptions are made:

1. Mechanics Assumptions:

a. All inertial forces are neglected.

b. Gravity and friction forces are not considered.

c. The forces imposed on the center of the towpreg are given only by the reaction force ***N*** from the nozzle and the pulling force ***F***, which is induced by the previous anchored point. The situation of forces is shown in Figure 3-4B.

2. Physics Assumptions:

a. The previous point is anchored completely at once, which means the solidification time should be very short.

b. In practice, if the deposition speed is slow enough, the assumption could be justified.

3. Geometry Assumptions:

a. It is supposed that the nozzle center point moves a distance H from B_0 to B_1.

b. In fact the nozzle is moved continuously, and the distance H should be infinitesimal. But in practice, a small value can be used for the distance H and the nozzle is assumed to move step by step.

3-3-2 A Derivation for the Towpreg Center Tracks

The question could be converted to determining the positions of the towpreg center with each moving step of the nozzle center. Suppose that the towpreg is at an original point (X_0, Y_0), at which the resin has been solidified completely and a reliable anchored point has been formed. According to the Force Balance Condition, a new towpreg center point should be judged to be a point of balance between the two forces, which are the nozzle reaction force ***N*** and the pulling force ***F*** at the original point O_0 (X_0, Y_0). When the nozzle center is moved from B_0 to B_1, a new towpreg center point O_1 $(X_1, Y1)$ must be on the point of intersection between the connection line O_0B_1 and the circle, whose center is set at B_1 and radius with R-r.

Based on the above assumptions and analysis, an equation can be derived to determine the towpreg center point O_1 (X_1, Y_1).

$$(h-y_1)^2+(R-r-x_1)^2=(R-r)^2$$
$$y_1=\frac{h}{R-r}X_1 \qquad (3-1)$$

where: R = bore radius of the nozzle,

r = towpreg radius,

h = the length of the nozzle moving step.

From equation (3-1), a coordinate O_1 (X_1, Y_1) of the towpreg center can be determined when the nozzle moves by one-step of length h. When the nozzle continuously moves along the toolpath B_0C to point B_2, O_1 (X_1, Y_1) is regarded as the new anchored point, and the position of O_2 (X_2, Y_2) could be found the in same way. Based on these rules, the track of the towpreg center point could be found. Equation (3-2) describes the track of the towpreg center point.

$$(i \times h - y_i)^2 + (R - r - x_i)^2 = (R - r)^2$$

$$yi = \frac{ih - yi - 1}{R - r - xi - 1}(xi - x_{i-1}) + y_{i-1} \qquad i = 2,\ 3,\ 4,..... \qquad (3-2)$$

where $i = i^{th}$ moving step of the nozzle.

3-3-3 Discussions of the Calculated Results

Equation (3-2) is a dispersion equation; the coordinate O_i (X_i, Y_i) of the towpreg center is determined by each moving step length h of the nozzle and by how many steps have been executed. A total moved distance of the nozzle is the product i times h. Equation (3-2) is also a convergence function. When the nozzle is moved to the i times, O_i (X_i, Y_i) is gradually converges to the toolpath line B_0C, and the line of B_0C is the infinite position of the track O_i (X_i, Y_i). The track of O_i (X_i, Y_i) could be obtained when a value for h is given. When the step length h is changed, the convergence value of each point O_i (X_i, Y_i) is not the same (Figure 3-5).

According to Equation (3-2), when the length of each step h is changed, the center point of the towpreg converges to different locations. In a real deposition process, the nozzle is moved continuously, which means that the length of step $h \rightarrow 0$, only when the length of each step is small enough, Equation (3-2) could describe the actual condition.

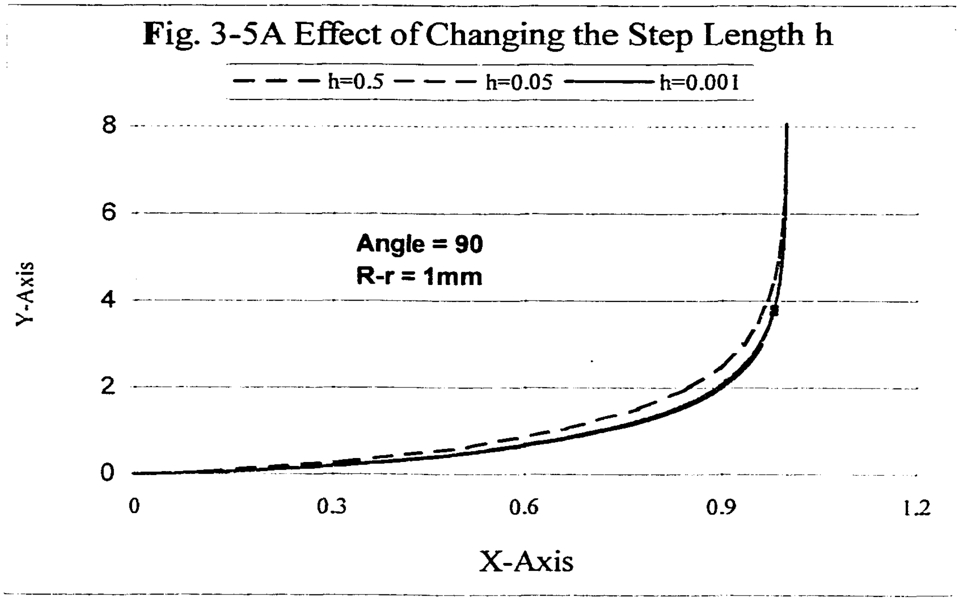
Fig. 3-5A Effect of Changing the Step Length h
h=0.5
h=0.05
h=0.001
Angle = 90
R-r = 1mm
Y-Axis
X-Axis
0
2
4
6
8
0
0.3
0.6
0.9
1.2

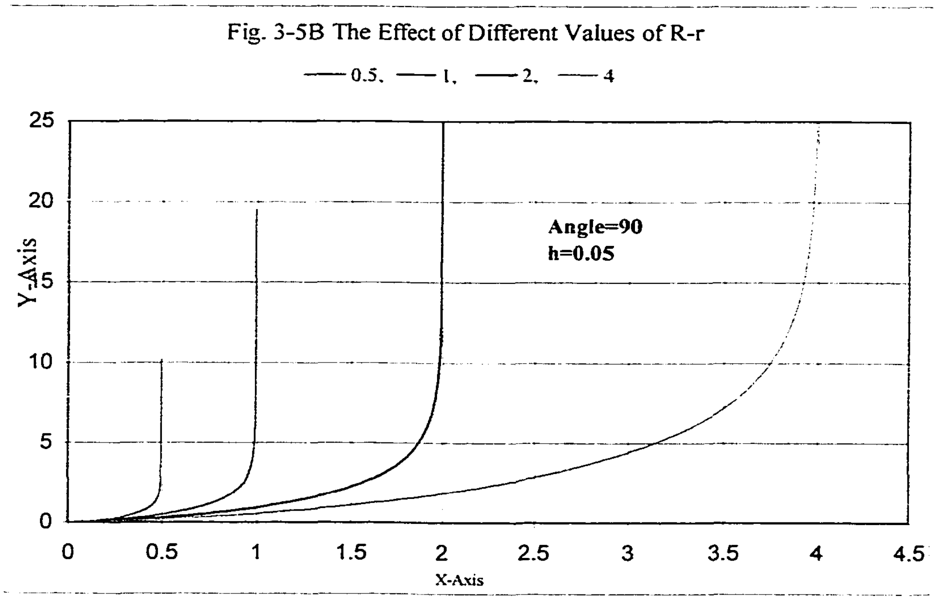
Fig. 3-5B The Effect of Different Values of R-r
0.5,
1,
2,
4
Angle=90
h=0.05
Y-Axis
X-Axis
0
5
10
15
20
25
0
0.5
1
1.5
2
2.5
3
3.5
4
4.5

Figure 3-5.

If a small value δ_x, a distance between the points O_i (X_i, Y_i) and the X-axis direction B_0C, is set as a controlling target, the value $\delta_x = 10^{-2}$ mm is accurate enough and could be regarded as coinciding with line B_0C. Then the step length h is set at $h_1=10^{-1}$, $h_2=10^{-2}$, $h_3=10^{-3}$ and is substituted into Equation (3-2), respectively, see Figure 3-5A. When $h<10^{-2}$ and the iterative times in Equation (3-2) are greater than the value $i\times h$, each track is always converged to a same δ_x.

The 3D motion device, which is employed for the CLM experiment, is driven by three stepper motors to move along the X, Y and Z-axes, respectively. The step length of these motors is a half-degree, *1/720*. The diameter of the driving shaft is *20 mm* and the pitch of screws is *3*mm. The moving length of each step for each of the linear motion devices is $3/720 \approx 4\times10^{-3}$ *mm*. When the simulation step length is set to 10^{-3} *mm*, the situation is more realistic. After proper values are assigned to the bore diameter of the nozzle, $D_n = 2R$, diameter of the towpreg $d_T = 2r$, the controlled value of error δ_x and the supposed length of step h, then the error of the towpreg center could be calculated by using Equations (3-1) and (3-2). An algorithm flow chart is shown in Figure 3-6A. Figure 3-5A and Figure 3-5B are then calculated results after the above parameters have been changed.

In Figure 3-5A, we could see the moving regularity of the towpreg. The moving direction of the nozzle is changed (new direction is perpendicular to the original direction) after appointing a new length value so that the nozzle can move along a new direction. The center of the towpreg converges very fast to the toolpath. Finally, only a value R-r, which is the difference between the track of the nozzle center and the track of the towpreg center, is reminded.

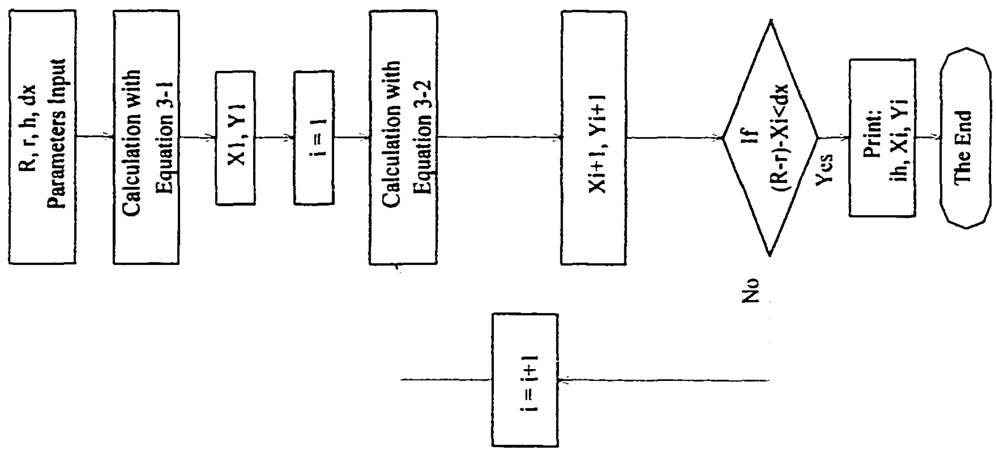

Figure3-6A Right Angle Turn.

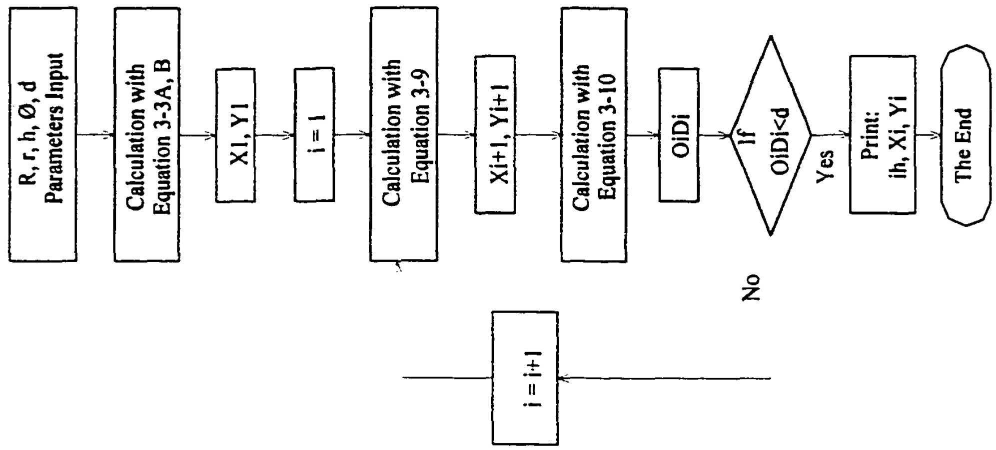

Figure3-6B Obtuse Angle Turn.

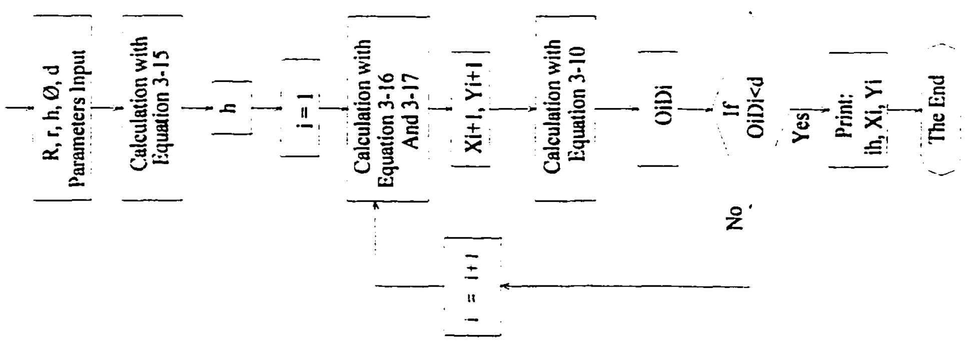

Figure 3-6C Acute angle turn flow chart.

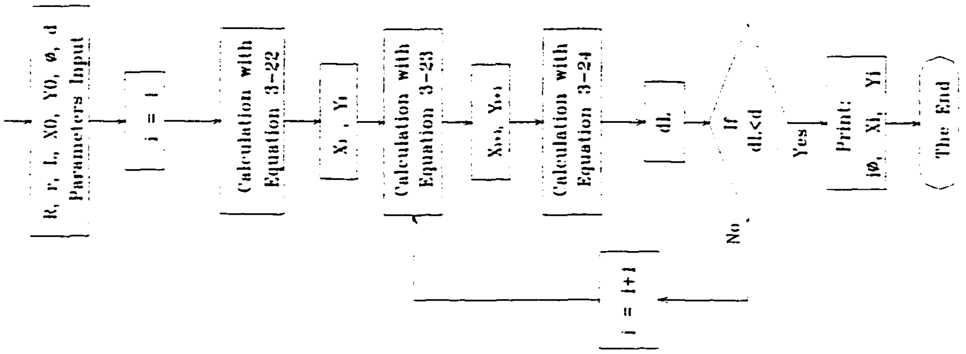

Figure 3-6D Error Evaluation for the case of depositing an arc.

When $h<0.05$ mm, the difference of the each towpreg center tracks is not obvious (In Figure 3-5A). With other conditions being the same and h being set at $h=0.05$, and $h=0.001mm$, the curved lines of the two towpreg center arcs almost overlap with each other. Figure 3-5B shows the variation of the towpreg tracks with a differing R-r value. The result shows that when R-r is larger, the error is bigger. Then, the distance that is needed to converge to the toolpath is larger.

3-3-4 Analysis of Case 1: Obtuse Angle Turn

The deposition direction of the nozzle could be change by an angle between $0°$ and $180°$. The resulting error will be discussed in the following sections. First, we will examine the case of making a turn in an obtuse angle; the situation is shown schematically in Figure 3-7. A nozzle is controlled to move from left A, to right B_0, and then at B_0, the nozzle is turned at an obtuse angle θ in order to move toward C. The same assumptions used in the previous section for the case of a right angle turn arc are employed in the present case.

For convenience, the initial conditions are presumed to be: nozzle center is placed at B_0, center of the towpreg located at O_0 (X_0, Y_0), and turned angle being ϕ. When the nozzle is moved by a one-step length h, the position of the towpreg center could be at O_1 (X_1, Y_1), which could be evaluated by equations (3-3A) and (3-3B).

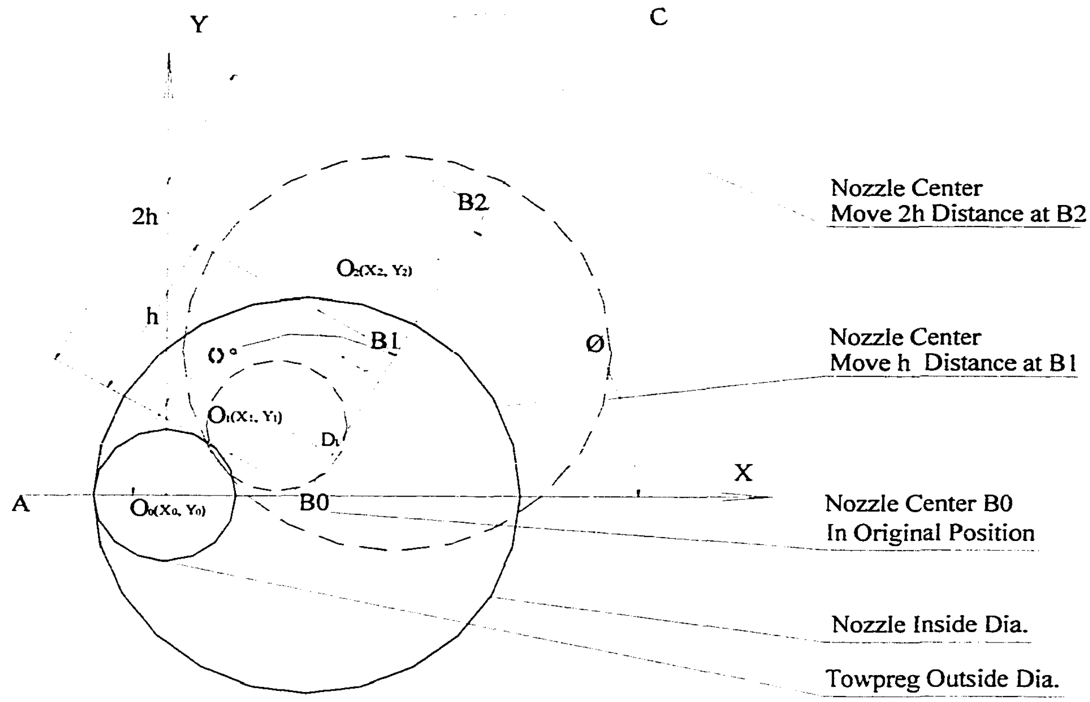

Fig. 3-7 Obtuse angle turn.

$$(h\cdot\sin\phi - y_1)^2+(R-r + h\cdot\cos\phi-X_1)^2=(R-r)^2 \quad (3\text{-}3A)$$

$$y_1 = \frac{h\cdot\sin\phi}{R-r+h\cdot\cos\phi} X_1 \quad (3\text{-}3B)$$

where: h = nozzle moving length of each step,

θ = an obtuse angle,

ϕ = 180°-θ.

Substituting Equation (3-3B) into (3-3A), one obtains Equation (3-4):

$$(h\cdot\sin\phi - \frac{h\cdot\sin\phi}{R-r+h\cdot\cos\phi}X_1)^2 + (R-r+h\cos\phi - X_1)^2 = (R-r)^2 \quad (3-4)$$

The value of X_1 can obtained from equation (3-4) and then the X_1 value can be substituted into (3-3B) to get Y_1. The point O_1 (X_1, Y_1) is a new location of the towpreg center.

To calculate the error (a distance between the point O_1 (X_1, Y_1) and line B_0C) a line O_1D_1 is drawn from point O_1 (X_1, Y_1) to be perpendicular to B_0C. See Figure 3-7. Equation (3-5) is a straight-line equation to indicate line O_1D_1.

$$Y = kX + b \quad (3-5)$$

Because $O_1D_1 \perp B_0C$,

$$Tan\phi \cdot k = -1, \qquad and \qquad k = \frac{X_1}{Tan\phi}$$

Substituting k into equation (3-5) to get b:

$$b = Y_1 + \frac{X_1}{Tan\phi}$$

Equation (3-5) is re-written as equation (3-6):

$$Y = \frac{1}{Tan\phi}(X - X_1) + Y_1 \qquad (3-6)$$

An equation for the straight line B_0C could be obtained at same time:

$$Y = Tan\phi[X - (R - C)] \qquad (3-7)$$

Combining Equation (3-6) and Equation (3-7) to have the intersection point D_1:

$$\overline{X}_1 = \frac{X_1 + Y_1 Tan\phi + (R - r) \times Tan^2\phi}{1 + Tan^2\phi}$$

$$\overline{Y}_1 = \left[\frac{X_1 + Y_1 Tan\phi + (R - r)Tan^2\phi}{1 + Tan^2\phi} - (R - r)\right] Tan\phi$$

The distance from point O_1 to point D_1 is given by:

$$\overline{O_1 D_1} = \sqrt{(\overline{X}_1 - X_1)^2 + (\overline{Y}_1 - Y_1)^2} \qquad (3-8)$$

So far, the first step has been finished and it is a very important step. The following track of the towpreg center points can be obtain in the same manner by using Equations (3-9):

$$(ih \sin\phi - Y_i)^2 + (R - r + h\cos\phi - X_i)^2 = (R - r)^2$$

$$\frac{Y_i - Yi - 1}{X_i - X_i - 1} = \frac{ih \cdot \sin\phi - Y_i - 1}{R - r + h\cos\phi - X_i - 1} \qquad (3-9)$$

where: $i = 1, 2, 3, \ldots\ldots$ and when $X_0 = 0,\ Y_0 = 0.$

Using the same principle as in step one, the distance between each point of the towpreg center to the nozzle center could be obtained by equations (3-10), (3-11) and (3-12):

$$\overline{OiDi} = \sqrt{(\overline{X}_i - X_i)^2 + (\overline{Y}_i - Y_i)^2} \qquad (3-10)$$

$$\overline{Y}_i = \frac{1}{Tan\,\phi}(\overline{X}_i - X_i) + Y_i \qquad (3-11)$$

$$\overline{Y}_i = Tan\,\phi\left[\overline{X}_i - (R - r)\right] \qquad (3-12)$$

A calculation algorithm is shown in Figure 3-6B.

Figure 3-8 shows the errors vs. turned angles ϕ and different *R-r* with other conditions being the same as before. From the diagram, the following observations can be made:

1. No matter how big the turn angle is, when the nozzle along the new direction moves a distance, which is 5~7 times of *(R-r)*, the track of the towpreg almost always coincides with the nozzle path. The deviation is less than 10^{-4} *mm*.

2. When the turning angle is smaller, the error is larger and the required converging distance is longer.

When the angle $\phi = 90°$, this is described previously in the condition for the nozzle turning at a right angle. When the turn angle that the nozzle makes is less than 90°,

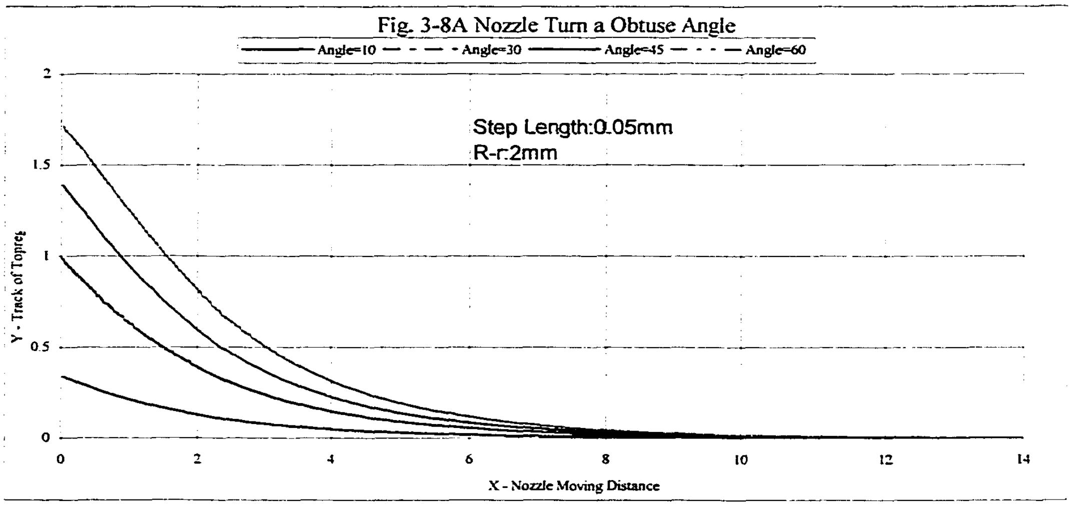

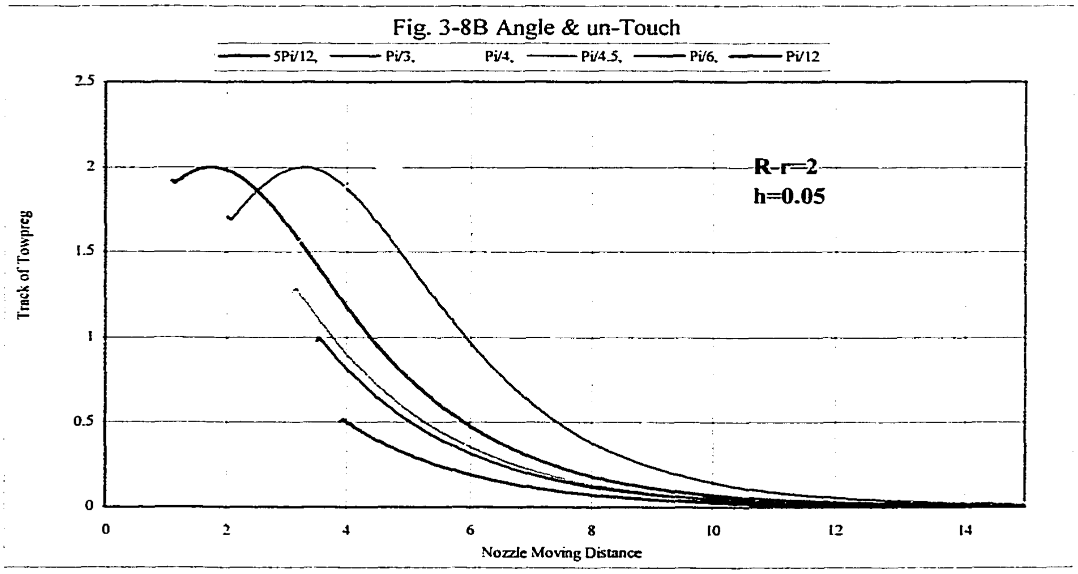

Figure 3-8. The toolpath has an obtuse angle turn.

Fig. 3-8A shows the towpreg track vs. different turned angles,
Fig. 3-8B shows the towpreg track vs. different value of *R-r*.

such a situation is complicated and will be studied in the next section. The reason is because during a short distance, the nozzle could not touch the towpreg.

3-3-5 Analysis of Case 2: Acute Angle Turn

For convenience, suppose that the nozzle moves from right side A to the left direction B and then turns at an angle, ϕ *to* C. The angle ϕ between the toolpath AB and BC is less than 90°.

Referring to Figure 3-9A. Point B is regarded as the original position where the towpreg center is at O_0 (X_0, Y_0), and the center of the nozzle is at $B(0, 0)$. When the nozzle at point B changes direction, during a certain period of time the nozzle could neither control nor touch the towpreg again until it comes to B_1. After B_1, the effect of the nozzle on the moving behavior of the towpreg is as same as in the case of an obtuse angle that was analyzed above. Therefore B_1, the nozzle center, should be found under the condition of turning an acute angle first.

Assume that the towpreg is kept at the original position until is touched again and the distance of BB_1 is h. The original coordinate of the towpreg center is:

$$X_0 = R - r, \qquad Y_0 = 0 \qquad (3-13)$$

Inside the nozzle, an equation of a circle, which is through the center of the towpreg could be written as:

$$(H\cos\phi - x)^2 + (H\sin\phi - y)^2 = (R - r)^2 \qquad (3-14)$$

Substituting equation (3-13) into (3-14) to get equation (3-15):

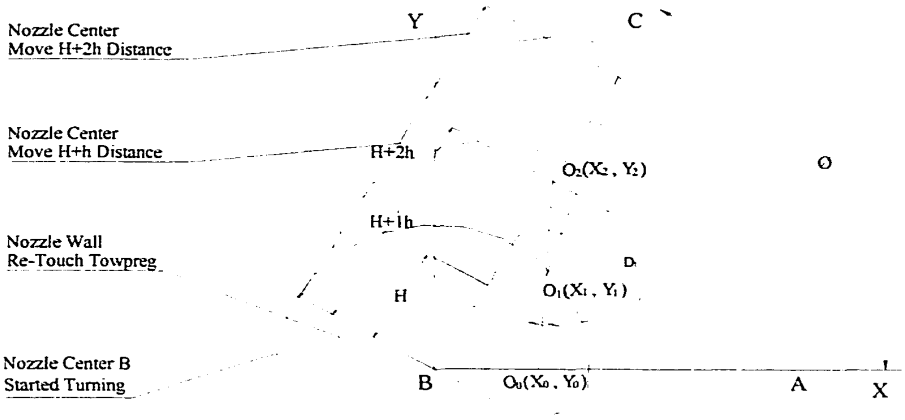

Fig. 3-9A.

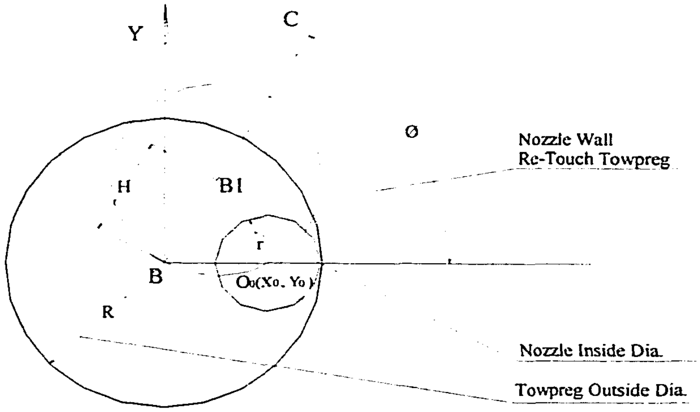

Fig. 3-9 B.

Fig. 3-9 Acute angle turn.

$$H = 2(R-r)\cos\phi \qquad (3-15)$$

When the nozzle center exceed the point *H*, and moves one more step, the track of the towpreg center can be described as:

$$[(H+ih)\cdot\sin\phi - Y]^2 + [(H+ih)\cdot\cos\phi - Xi]^2 = (R-r)^2 \qquad (3-16)$$

$$\frac{Y_i-(H+ih)\sin\phi}{X_i-(H+ih)con\phi} = \frac{Y_{i-1}-(H+ih)\sin\phi}{X_{i-1}-(H+ih)con\phi} \qquad (3-17)$$

$$Ki = \frac{Y_{i-1}-(H+ih)\sin\phi}{X_{i-1}-(H+ih)\cos\phi} \qquad (3-18)$$

Where i = 1, 2 , 3......

ϕ = turning angle,

h = one-step length of nozzle movement.

Substitution of $i = 1$, $X_0 = R\text{-}r$, $Y_0 = 0$, $H=2(R\text{-}r)\ Cos\phi$ into Equations (3-16), (3-17), (3-18) and simplify them to get X_1, K_1. Equation (3-19A) gives X_1:

$$K_1 = \frac{-(H+h)\sin\phi}{(R-r)-(H+h)\cos\phi} = -\frac{(R-r)\sin 2\phi + h\sin\phi}{(R-r)\cos 2\phi - h\cos\phi}$$

$$X_1 = (R-r)\cos 2\phi - h\cos\phi \pm \frac{R-r}{\sqrt{1+K_1^2}}$$

$$X_1 = (H+h)\cos\phi + \frac{R-r}{\sqrt{1+K1^2}} \qquad (3-19A)$$

Substitution of Equation (3-19A) into Equation (3-16) yields Y_1. Equation (3-19B) gives Y_1:

$$Y_1=K_1\,[X_1-(H+h)\cos\phi]+(H+h)\sin\phi \qquad (3\text{-}19B)$$

If set $i = 2$, then substitute Equations (3-19A) and (3-19B) into Equations (3-16) and (3-17) to get X_2 and Y_2 values and the track of the towpreg could be obtained. Using the same principle with obtuse angles, Equations (3-10), (3-11) and (3-12) are employed again to yield the deviations for each point of the towpreg center. A calculation flow chart is depicted in Figure 3-6C. A toolpath for turning at an acute angle is illustrated in Figure 3-8B. These angle directions are different with the obtuse situations and need to be specified in the diagram.

When the nozzle moves along a new direction by a segment, it does not touch with the towpreg. The segment is longer with a smaller turn angle of turn. When the turn angle is zero degree, nozzle go back to the opposite direction, and the length of the segment that the towpreg could not be touched is *2(R-r)*.

§3-4 ERRORS IN DEPOSITING AN ARC-SHAPED SEGMENT

3-4-1 Evaluation of Errors in Depositing an Arc

When the nozzle moves along an arc, the route of the towpreg is different from the route analyzed in the previous section. In building a part using CLM, the arc is the most commonly deposited shape, so a study for the nozzle moves along an arc is emphasized in this section.

A deposition along an arc is schematically shown in Figure 3-10. All assumptions are same as made before.

The toolpath is an arc with radius L and center at point O with turning in the

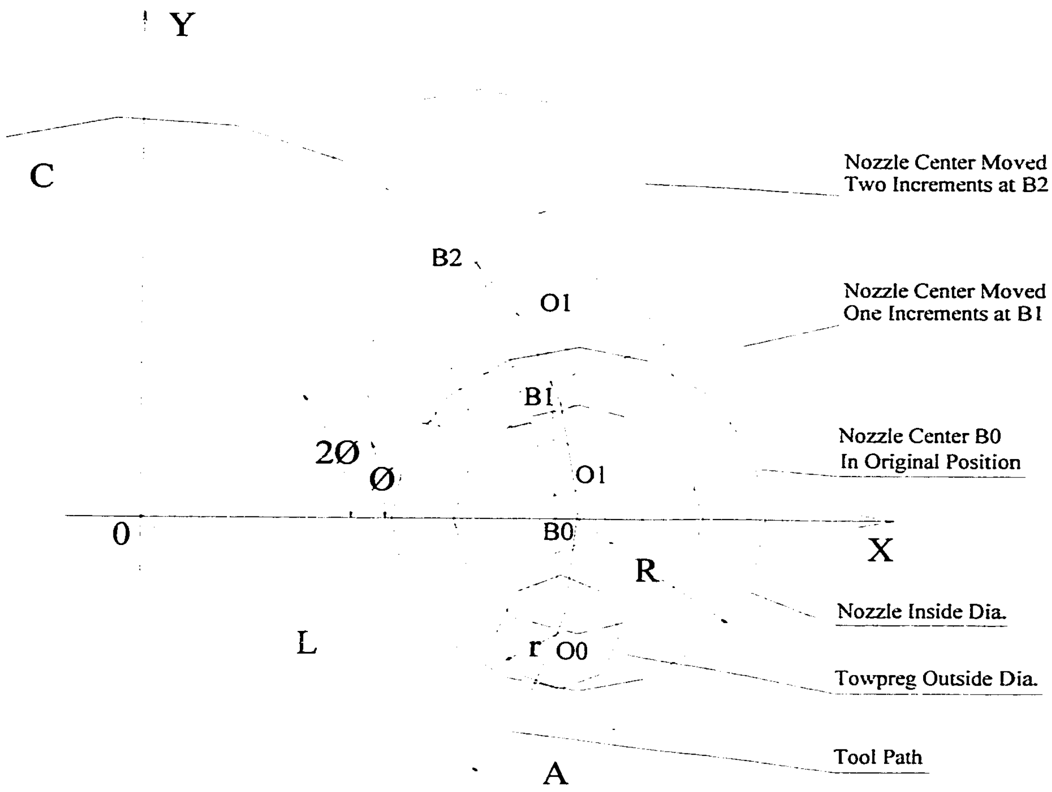

Fig. 3-10 Nozzle moving along an arc toolpath.

anticlockwise direction. The original position of the towpreg center is on the arc toolpath and is placed at O_0; the nozzle center is at B_0. Actually, throughout an analysis, no matter where the original position is when the towpreg moves an arc distance with the moving nozzle, the towpreg center could come to a balanced position. The balanced position is calculated in the following.

For convenience, assume that the radius L of the arc is a constant, which means that the nozzle moves along a circle. So, the coordinates of B_0 and O_0 could be written directly since for point O_0

$$\begin{aligned} &X^2 + Y^2 = L^2 \\ &(X - L)^2 + Y^2 = (R - r)^2 \end{aligned} \qquad (3-20)$$

And for point B_0: $X = L$, $Y = 0$.

where $R =$ the bore radius of the nozzle,

$r =$ the towpreg radius,

$L =$ the toolpath radius.

From Equation (3-20), X_0 and Y_0 can be solved:

$$X_0 = \frac{2L^2 - (R-r)^2}{2L}$$

$$Y_0 = \frac{R-r}{2L}\sqrt{4L^2 - (R-r)^2}$$

Here, let the angle ϕ be used as an increment for the nozzle moving along the toolpath, because this angle ϕ can be conveniently observed. In the software development, a length of the arc should be used as the increment. When the nozzle is moved along the arc to point B_1, based on the original position O_0 (X_0, Y_0) and the first increment turning angle step ϕ, the center position of the towpreg could be point O_1.

$$(X - L\cos\phi)^2 + (Y - L\sin\phi)^2 = (R - r)^2$$
$$\frac{Y - Y_0}{X - X_0} = \frac{L\sin\phi - Y_0}{L\cos\phi - X_0} \qquad (3-21)$$

where ϕ = increment angle for nozzle moving each step.

From equation (3-21) we can get the coordinates of point O_1:

$$X_1 = \frac{C_1K_1 + L\cos\phi}{1 + K_1^2} \pm \sqrt{\left(\frac{C_1K_1 + L\cos\phi}{1 + K_1^2}\right)^2 - \frac{C^2\cos^2\phi + C_1^2 - (R - r)^2}{1 + K_1^2}}$$
$$Y_1 = K_1(X_1 - X_0) + Y_0 \qquad (3-22)$$

where:

$$K_1 = \frac{L\sin\phi - Y_0}{L\cos\phi - X_0}$$

$$C_1 = K_1X_0 + L\sin\phi - Y_0$$

When the nozzle is moved along the circle with any angle $i\phi$, the position of the Towpreg center is:

$$Xi = \frac{CiKi + L\cos i\phi}{1 + k^2 i} \pm \sqrt{\left(\frac{CiKi + L\cos i\phi}{1 + K_i^2}\right)^2 - \frac{L^2\cos^2(i\phi) + C^2 i + (R - r)^2}{1 + K_i^2}}$$
$$Yi = Ki(Xi - Xi - 1) + Yi - 1 \qquad (3-23)$$

where:

$$Ki = \frac{L\sin(i\phi) - Yi - 1}{L\cos(i\phi) - Xi - 1}$$

$$Ci = KiX_{i-1} + L\sin(i\phi) - Yi - 1$$

$$i = 2, 3, 4, \ldots .$$

The deviation, a distance from the towpreg center point O_i (Xi, Yi) to the nozzle toolpath, is:

$$\Delta L = L - \sqrt{X_i^2 + Y_i^2} \qquad (3-24)$$

A calculation flow chart is given in Figure 3-6D and the results are charted in Figure 3-11A, B, and C. From these charts, a deposition error is obtained. When the nozzle is moved by a certain distance, the towpreg center reaches a balanced track, which is like another circle and its radius being smaller than the radius of toolpath. This is an important result, which should be considered during software development.

Figure 3-11A shows the errors vs. ϕ, the increment length.

Where: $R\text{-}r = 2mm$,

$L = 10mm$,

l = Arc length is conversed from ϕ with,

$$l = \frac{\phi\pi}{180}L$$

When $\phi = 1/5°, 1/10°, 1/100°$ and $1/1000°$,

then $l = 0.03491, 0.01745, 0.00171$ and 0.00017, respectively.

In Fig 3-11A, we could find that when step length l is smaller than 0.00171 ($1/100°$), the variation in error of the towpreg is not large, and the two curved lines of step length

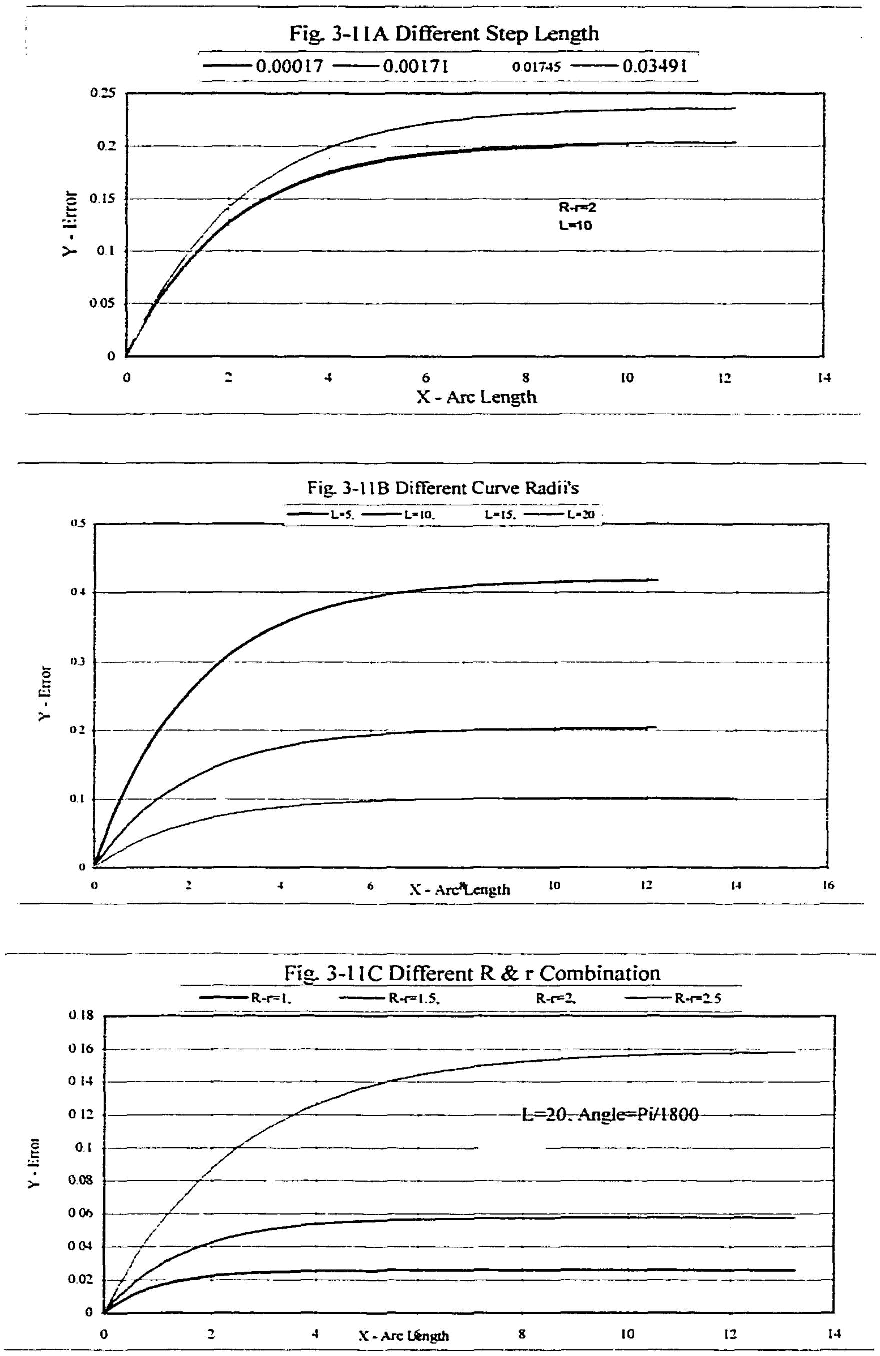

Figure 3-11. Calculation results for an arc toolpath.

0.01°and *0.001*°almost coincide.

Fig 3-11B shows the regularity with which the error changes as the changing radius of the toolpath varied. When the toolpath radius is small the error is large.

Fig 3-11C shows another effect that error changes with different *R-r* value. Then the larger the difference of *R-r* value is, the larger the error is.

3-4-2 Sources and Factors that Affect the Errors

In §3-3 and §3-4, the deposition errors induced in certain situations have been discussed and calculated. The original error sources and their effects are summarized in the following:

1. A toolpath is made up of a group of straight-line segments, when the nozzle moves along one of the lines and turns to move along another line, the error could be induced due to a difference in *R-r*. No matter how many degrees the nozzle has turned, the track of the towpreg could converge quickly over to the toolpath. Finally, the deviation is given by *R-r* only.

2. From point 1 it follows that the simulation step length does not affect the convergence result but the convergence shape. When the step length is smaller than an appointed value, (i.e. < *0.05*), the calculation result is not much different.

3. When a toolpath is an arc, the center of the towpreg could converge very fast on another circle at a balanced position. The radius of this circle is smaller than the radius of toolpath. The difference between the radius of

the balanced circle and the radius of the toolpath is determined by the *R-r* value, the radius of the arc toolpath.

4. From conclusion 3 it follows that, the simulation step length affects the balanced position. But, when the arc length is less than *0.00171*, the final result is not much different.

5. These errors, cited in Conclusion one and Conclusion three are small compared with toolpath dimension and will converged to zero or to a certain value quickly.

6. Because the method of depositing is unique, the mechanics model that describes this process is also unique. It was assumed that at any deposition point, the towpreg is anchored to the previous layer immediately, and the previous point and the nozzle moving direction determine the position of the next point. Hence, the equations, which describe the process, are the dispersion equations. If the step length is longer, realistic condition could not be simulated.

§3-5 DESIGN AND PREDICTION OF COMPOSITE MECHANICAL PROPERTIES PRODUCED BY CLM

A component made from a composite material normally has excellent mechanical properties [58-60]. Many composite materials scientists have experimentally studied mechanical properties and failure mechanism of various composite structures. Other have developed micro-mechanics and macro-mechanics models that are capable of predicting mechanical properties of a composite based on the properties, proportions, and orientations of its constituent phases. With the great computing capability of a modern computer, many complicated composite mechanics problems can be readily solved.

The forming flexibility of RP technology gives a possible way to build a structure with desired mechanical properties. This is another advantage for CLM technology.

Fiber reinforced composite materials are a kind of orthotropic materials. For example, a fiber-reinforced composite laminate structure is shown in Figure 3-12. A symmetric structure is arranged and shown in Figure 3-12A. When the laminates are over-layered and pressed together to form a panel, the panel will be a cross plied quasi-isotropic laminate .

This kind of structure could not be used as a part directly. But a part that is shown in Figure 3-12C is cut off from the panel and is indicated by the dashed line in Figure 3-12B. The part will process a quasi-isotropic character. Several methods to make the part with desired mechanical properties will be introduced.

3-5-1 Arranging Layer Directions with LOM

A good method to finish the cross permutation between different layers is to use LOM technology for forming a 3-D composite part. RPT has another important feature, which is the ability to regulate the mechanical properties during the forming process.
An improved LOM (Laminate Object Manufacturing) technology device is illustrated in Figure 3-13. The basic forming principle and structure are similar to traditional LOM. The differences are as follows:

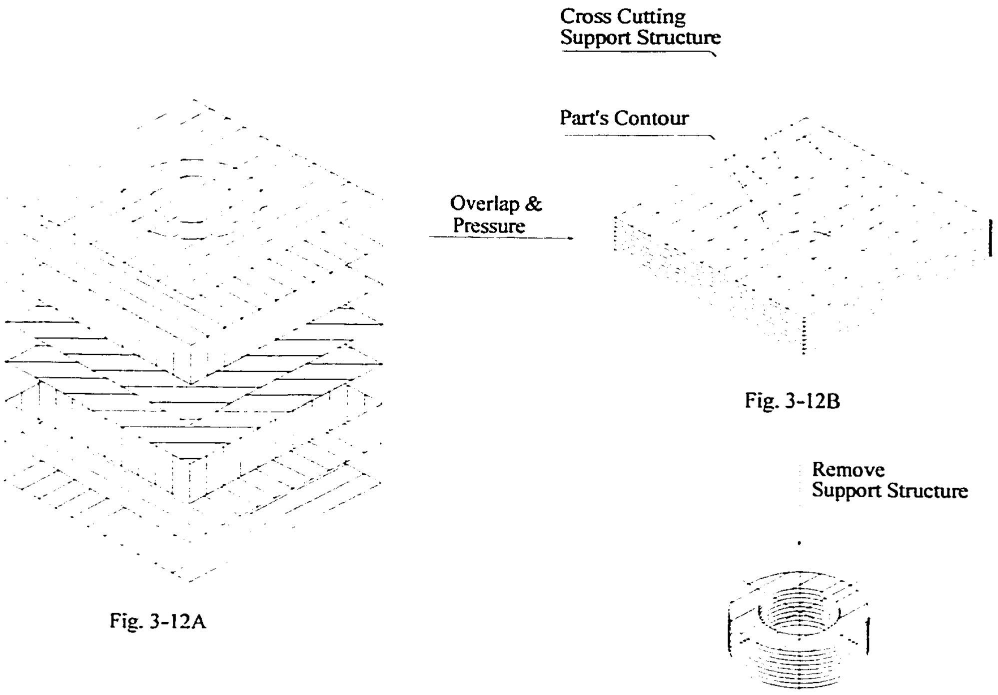

Fig. 3-12 Cross plied quasi-isotropic part.

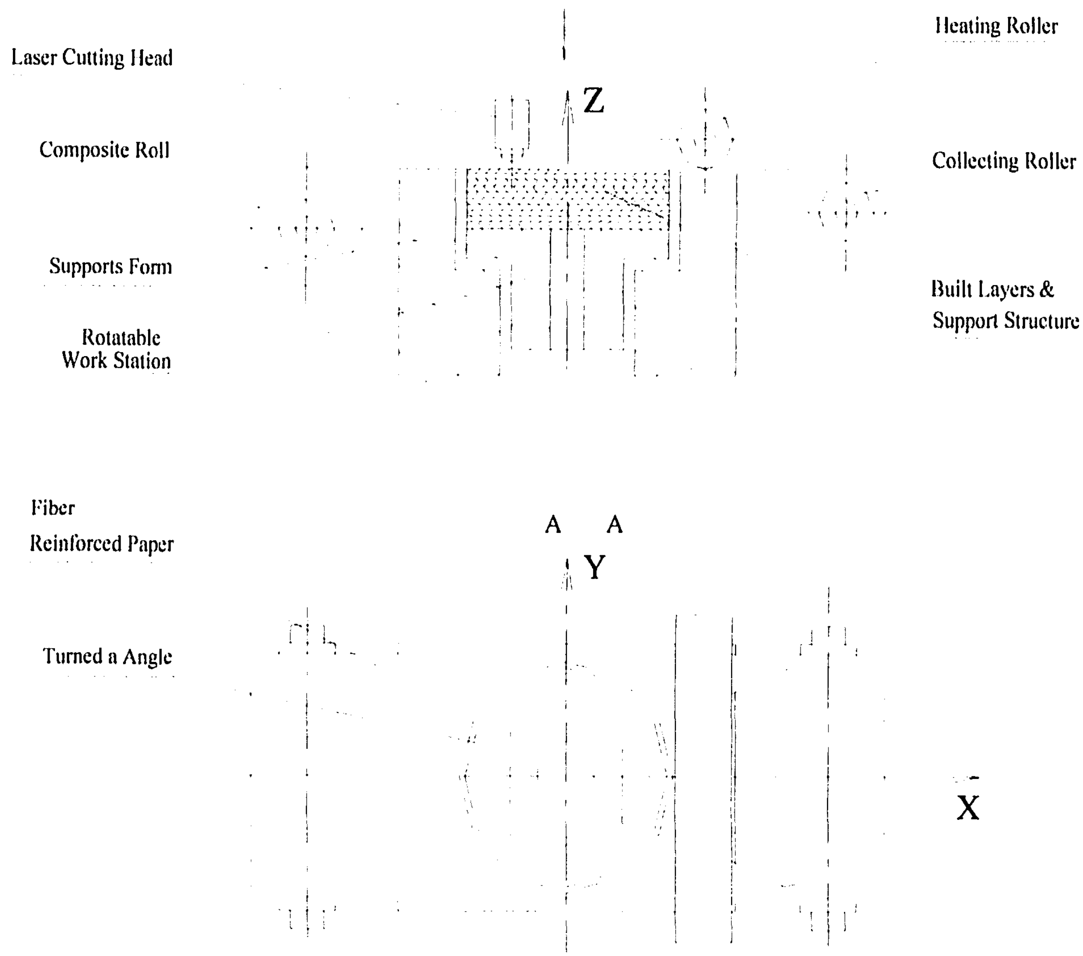

Figure 3-13 Composite forming process based on the LOM.

1. The material that is used is not paper with glue on its back, but is a kind of material that has a thickness similar to that of paper, for instance, a continuous fiber reinforced thermoplastic matrix where fiber direction is parallel with the feeding direction. Such a material could be made easily with a low cost.

2. Another difference is the working platform. In the common LOM technology, when a layer is formed at each time, the working platform is moved down one layer thickness. Then, a new layer could be carried in. In the improved LOM system, the working platform is not only moved up and/or down, but also could be rotated around the Z-axes to arrange the composite with a cross direction. With such a method, a part as shown in Figure 3-12C could be readily formed.

3. Software has to be modified: A computer-controlled laser cutting head is employed to cut the contour of a cross section for each layer. When the working platform is rotated at an angle, a new toolpath should be rotated at the same angle to match the required contour and make the required support structure.

4. The heating device is different. A heating roller or a heating plate is used to melt the thermoplastic materials and make the current layer stick to the pervious layer.

3-5-2 In Layer Mechanical Properties

On the improved LOM technology the orientation angle of all the reinforcing fibers in a layer is uniform throughout the layer. In contrast, in the present CLM technology, the fiber orientation can vary from spot to spot in a layer and can vary from one layer to another. This feature makes it possible to tailor-make the mechanical properties, essentially point by point and layer by layer. For example, two laminates that are subjected to the same force condition but are arranged in different fiber orientations are shown in Figure 3-14.

A stress field distribution exerted on the laminate is shown in Figure 3-14A. A stress concentration could be induced around a small hole as indicated with the dashed line in Figure 3-14A. However, along the Y-axes direction, the load-carrying capability is limited. Another fiber orientation arrangement style is shown in Figure 3-14B. A fiber reinforced towpreg may be deposited around the hole by CLM to reinforce the strength of the laminate in the vicinity of the hole. Another example is depicted in Figure 3-15, which shows an arbitrary plane of a component, along with its shear stress condition and fiber orientations. It is obvious that the stress concentrations are present in at areas A, B, and C, and a crack could be readily initiated at these areas. In contrast, if the towpreg orientation is arranged like that shown Figure 3-15B, this plane could exhibit a much higher strength.

The above analysis is only qualitative in nature. For a complex-shaped structure, which is loaded even with a simple force (i.e. tensile or compressive force) only, the stress condition could be difficult to determine for the whole structure and for individual layers. This is a challenging research direction in the future for the CLM technology.

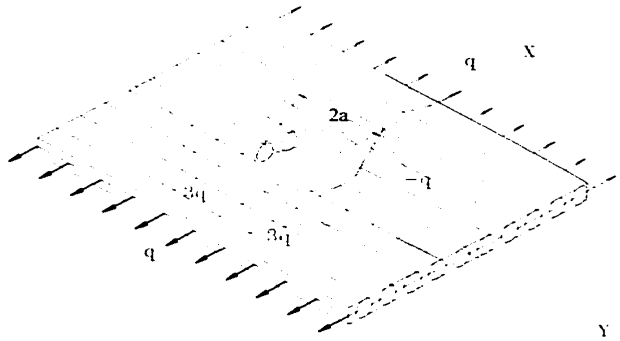

Fig. 3-14A

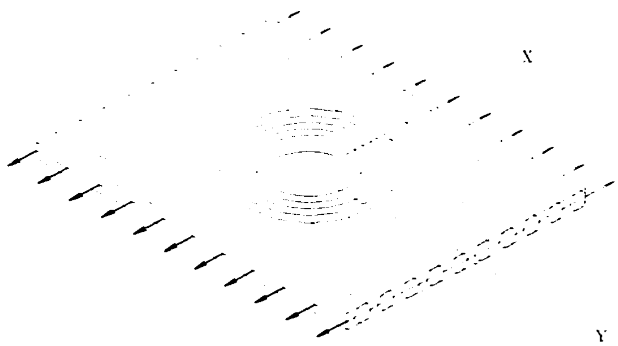

Fig. 3-14B

Fig. 3-14 In layer mechanical properties tailor.

Fig. 3-15A

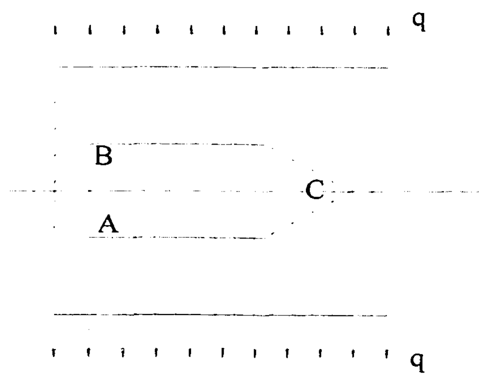

Fig. 3-15B

Figure 3-15 Toolpath orientation arrangement.

§3-6 SOFTWARE DEVELOPMENT STRATEGY

In the current software market, many specialized software packages for RPT development are available. These software packages are capable of automatically slicing a solid model to generate contours for each layer from a 3-D CAD file such as in STL file format. Then, according to the requirement for a specific system, the contours are converted to a programmed signal to control the toolpath. The toolpath signals are used to drive the work platform to move relative to a deposition head.

This software that is developed for several current kinds of RP technologies such as SLA, FDM, LOM, etc, is not suitable for CLM. Hence, new software needs to be developed to meet the specific requirements of CLM. Only the requirements for writing the software will be discussed here. The software development details for CML are introduced in other articles.

3-6-1 Software Development Considerations

The CLM forming principle and concept design have been studied in Chapter 2. Also the errors, depositing deviation, and mechanical properties have been analyzed in the previous section of this chapter. All these could be considered as the foundation requirement for the software development. There are several unique features associated with the deposition of continuous fiber composites:

1. Cutting off the towpreg: the function of cutting is important in the CLM system, and the function of the cutting device should be a simple and reliable design.

A monitoring sensor should be used to ensure that cutting is finished completely. The function could be written simply with the CNC G and M code to implement the cutting action.

2. After an intermittent cut-off, a towpreg must be re-attached to a spot in a different region of a layer or in a different layers, and a dwell time may be required to accomplish this function. The nozzle could stop on an initial point for 1/4-1/2 seconds. In practice the dwell time could be obtained by an experiment.

3. Optimization of cutting times: With the cutting times being reduced not only the complete forming cycle time could be reduced, but also the part forming precision could be improved. For example, three different toolpath designs for a layer of a part are shown in Figure 3-16. The toolpath direction design shown in Figure 3-16A requires the longest cutting times. A second longest cutting time is needed in Figure 3-16B, and the shortest cutting times are shown in Figure 3-16C. But the degree of difficulty in automatically generating a toolpath logic is just in the opposite order; in Figure 3-6A, the toolpath could be generated most easily.

4. Mechanics considerations: The software could be developed to generate a toolpath with desired mechanical properties, as suggested in the previous subsection.

5. To makes up the errors: The software could compensate for the errors that could occur in the process as analyzed in §3-3 and §3-4.

To generate a toolpath, a proper towpreg orientation could be used for a given layer for the purpose of optimizing the toolpath orientation and to minimize cutting times, as discussed in the following:

The required minimum cutting times for each layer and the needed fiber orientation with an angle for two adjoining layers could impose conflicting constraints on the toolpath design. In any structure, two adjacent layers almost have the same geometric shape. If one of the layers is optimized with a minimum cutting time but for another layer the toolpath could be turned at an angle in order to have proper mechanical properties. Under this condition, the cutting times for this second layer could not be minimized. To overcome the contradiction, the following strategy is suggested,

1. The mechanical property is the first priority consideration. Parts having excellent mechanical properties are one important reason to develop the CLM technology. The mechanical property is sensitive to the towpreg orientation. When a layer toolpath is created, the towpreg in the following layer should be first turned by an angle to rearrange the current layer direction.

2. Interlayer direction is considered first. The direction of the towpreg in a layer is considered second. When the towpreg direction is determined for a certain layer, according to the results analyzed in a previous section, a partial reinforcing orientation arrangement should be considered to protect the laminate against stress concentration.

3-6-2 A Method to Optimize the in-Layer Toolpath

Once a main orientation is determined for each layer, the partial reinforcing effect is then considered. If a structure is complicated, its cross-section should be complex also. To automatically arrange an in-plane towpreg orientation for each layer and to minimize cutting times through a general rule is still a challenge. Several methods have been studied, one of which, the region partition method, is introduced here.

A cross-section layer of a part is shown in Figure 3-17. A rectangular hole and a groove hole do not require any deposit of materials on it. A towpreg depositing direction is arranged parallel to the X-axis (See Figure 3-17A). When deposition proceeds near the rectangular hole area, the deposition order could be from point *A* to point *B*. It could be stopped during the towpreg being cut at point *B*. After that, towpreg could be jumped to and restarted at point *C* and then continue to processed until point *D*. Such a start – stop-cutting- restart procedure could occur many times in the rectangular slide area, and the same procedure will be repeated in the groove area.

A new depositing arrangement is shown in Figure 3-17B. The layer is divided into *6* solid regions. The dashed lines are used to indicate the boundaries and *1, 2, 3, 4, 5, 6* are assigned for each region, respectively. In each region, the deposition could be finished at one time by starting and stopping with one towpreg. There are six total starting and stopping times.

A direction of deposition being parallel with the Y-axis is shown in Figure 3-18A. According to the same principle, the layer could be divided into six regions by the straight lines, which are parallel to the X-axis. If the deposition direction is needed to be turned 45° degrees relative to the X-axis, another 6 regions are divided. The case is shown in Figure 3-18B.

Figures 3-17B, 3-18A and 3-18B, serve to illustrate the region-dividing method. This method can be carried out by a computer automatically. Figure 3-18C shows an optimized region dividing method, and the layer is divided into only two regions. Therefore, a deposition process should need only two starting and stopping times. But the dividing logic is complicated.

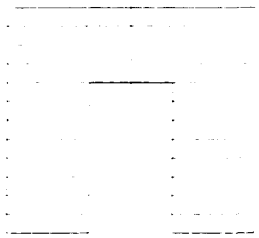

Fig. 3-16A

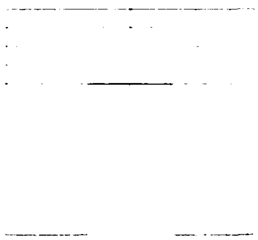

Fig. 3-16B

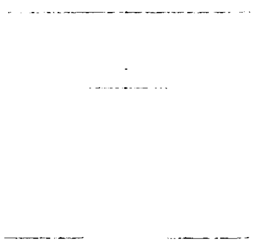

Fig. 3-16C

Figure 3-16 Different toolpath design.

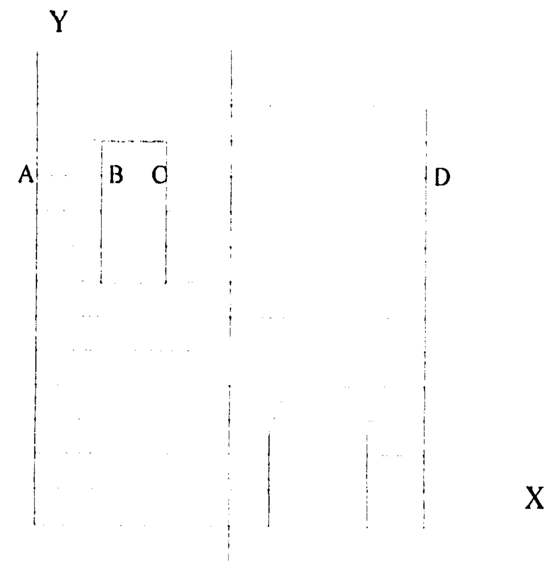

Fig. 3-17A

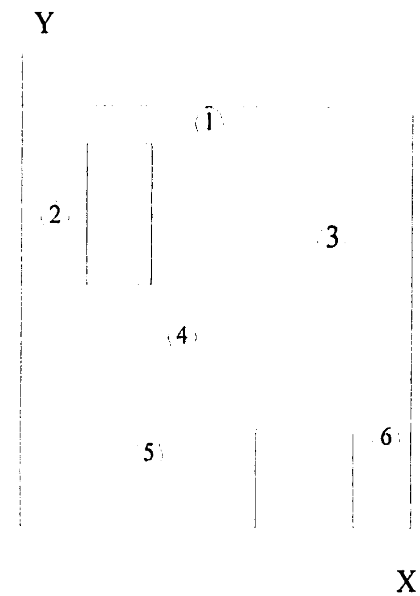

Fig. 3-17B

Fig. 3-17 To divide the deposition region.

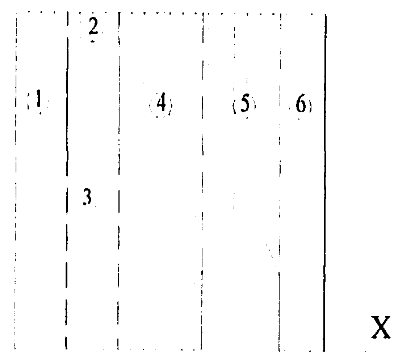

Fig. 3-18A Perpendicular to x-axis.

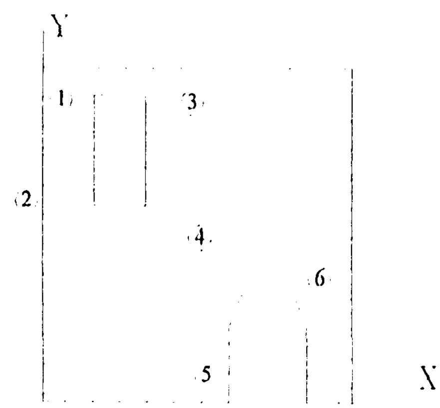

Fig. 3-18B An angle with respect to x-axis.

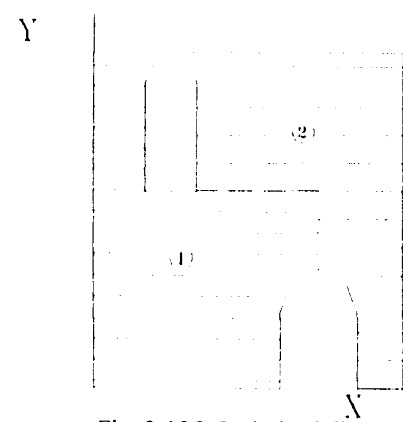

Fig. 3-18C Optimized dividing ragen.

Fig.3-18 Region dividing methods.

§3-7 CHAPTER CONCLUSIONS

1. The error sources, values, and governing factors in the CLM Technology have been analyzed and evaluated.

2. The method for in-priori design of mechanical properties and the method for reducing cutting time are introduced.

3. These results could be used in developing the software for CLM.

CHAPTER 4 THE SIMULATION OF THE CLM PROCESS

§4-1 INTRODUCTION

The fundamental theory for the CLM forming process has been studied in Chapter 2. The two forming strategies and related concept designs were selected because these forming methods have the greatest potential. In Chapter 3, the forming precision has been calculated to help on the design of a toolpath. In this chapter, the two forming methods will be numerically simulated and analyzed.

The reasons for simulating the CLM processes are:

1. The modeling of the process could lead to a betters understanding of the part forming theory.
2. The result of a simulation study could help confirm the feasibility of a forming method.
3. Proper process parameters could be found through a simulation study such as, the best temperature and the maximum forming speed.
4. The shape, dimension and the suitable position of a part could be optimized.

Computer simulation and optimization have been developed as essential tools in the theoretical research and for real applications. Simulation and optimization have been commercialized for the composite industry, such as for the optimization of composite structures, simulation of resin transfer molding, modeling of textiles, damage analysis etc. Computer software has played a key role in the development of the RP technology as a field. Specific software specifically for the CLM technology has to be developed for generating the toolpath and controlling the system. But, a process simulation by using a computer is still a challenging task. In this chapter, two models will be built and studied based on the existing CLM processes. These forming processes are complicated and are influenced by many factors. Therefore, several assumptions will be made to simplify the problem. These simulation approaches, although highly simplified, do provide deep insight into the CLM processes.

§4-2 SIMULATION OF THE SELF-ANCHORING PROCESS

4-2-1. Basic Theories

The self-anchoring method, a Passive Materials Supply Method, has been demonstrated to be an effective process for CLM. Its features and forming precision have been studied in the preceding chapters. How dose self-anchoring, basic forming mechanisms work? This will be investigated in more detail.

In the self-anchoring forming method, a towpreg made of a thermoplastic matrix is re-melted and deposited onto an object; the towpreg could be solidified to a certain degree and glued to a corresponding point of the base or the previous layer immediately to form a point of anchoring. Then, with the nozzle being moved forward, the anchored point of towpreg servers as a stationary point to pull the towpreg out of the nozzle. Thus, more towpreg could be deposited into the object. The sequence "towpreg deposited□ solidified □ anchored□ pulled out□ deposited again" is the basic procedural steps of the self-anchoring process, which is also called *Deposited and Anchored At Once* forming principle. The forming mechanism for self-anchoring is illustrated in Figure 4-1. Figure 4-1A shows an overall profile of the forming process; Figure 4-1B shows that the towpreg is in the deposited condition.

It is expected that these steps can occur immediately, continuously, repeatedly and simultaneously. It takes some time for any step to be accomplished. But, a time for each step should be within a reasonable range, so as a main task for simulation, the range of time would be found.

4-2-2 Some Preliminary Concepts about Thought on the CLM Process

A stepper motor drives a delivery roller to supply the towpreg, where the later stays free of tensile force and the towpreg inside the heating tube is tensile force free (see the Figure 4-1, the roller is not shown in this sketch). The friction force between the towpreg and the nozzle is neglected. The force acting on anchored points lies on the nozzle-moving plane. In order to simulate and optimize the self-anchoring process, the requirements and restrictions on this process should be considered first.

1. Part Quality Considerations:

   a. Errors induced by the different diameters between the towpreg and the bore of the nozzle have been analyzed in Chapter 3, and there errors could

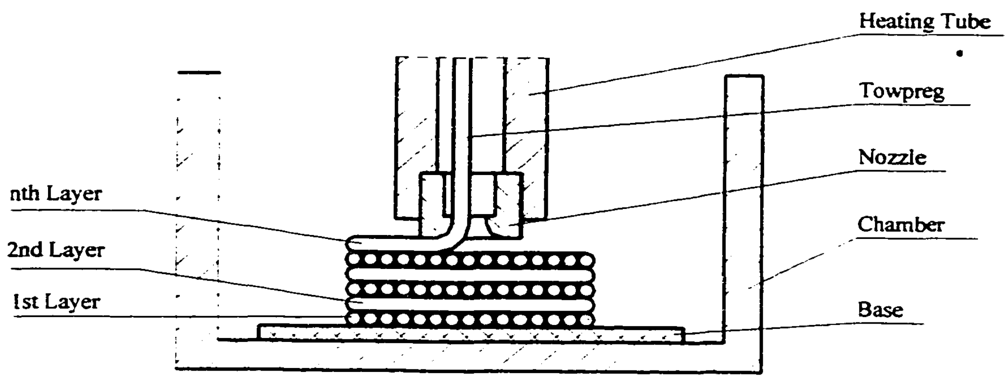

Fig. 4-1A

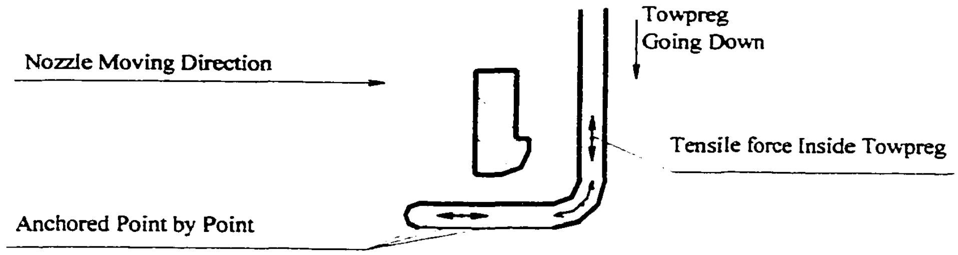

Fig. 4-1B

Fig. 4-1 Forming mechanism of the self- anchoring method.

be eliminated or compensated for by a modification to the software.

b. A toolpath error could be generated if an anchoring point is not formed properly. An arc toolpath is shown in Figure 4-2, and the nozzle is programmed to move along the arc toolpath from point *A* to points *B*, *C*, and *D*. Ideally, the towpreg is firmly anchored at point *A*. When the nozzle arrives at point B, the towpreg is supposed to be deposited and anchored at once to form a new anchoring point at *B*. Then the nozzle is moved to point *C* and so on to deposit the towpreg be following the path indicated with the broken line *ABCDE*···. However if the towpreg is not solidified to a certain degree and is not anchored completely at point *B*, the partially anchored point could not be serve as a stationary point to pull the towpreg out of the nozzle. With the nozzle being moved continuously to point *C*, a point in the towpreg that was supposed to be anchored at point *B* skids to B_1 and is anchored at *B1* instead. For the same reason, a point in the towpreg expected to be deposited at *C* is actually anchored at point C_1. Therefore, the real formed line $AB_1C_1D_1$ is deviated from the theoretical line *ABCD*.

The extent of this error depends on the forming condition, particularly the forming speed relative to the depositing speed or the nozzle moving speed. For example, in Figure 4-2, during the same period, as mentioned in the above paragraph, but with a higher nozzle moving speed, then when the nozzle arrived at point *E* instead of at point *C*, the towpreg is slid to B_2 instead of B_1. Therefore, the error is larger than the

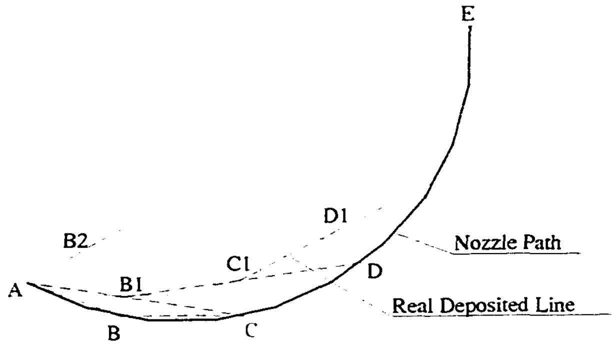

Fig. 4-2 An error is generated by the mechanism of the forming process.

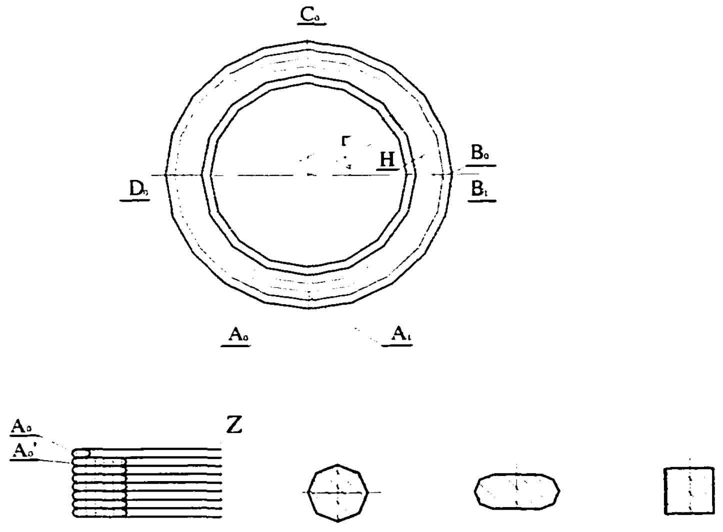

Fig. 4-3 Different boundary conditions for the thermal field.

case of deposition at a lower speed. In fact, in this situation the deposition is regarded as failure.

2. Speed considerations: as a matter of fact, the forming speed is relatively slow for most RPT processes. In the self-anchoring process, the forming quality is directly related to the forming speed, as has been analyzed in the preceding paragraph. However, the forming speed is limited by the present forming mechanism, and other influencing factors should be considered:

   a. The machine capability: any CNC machine has the maximum X-Y and/or Z interpolation speed, which is also the maximum depositing or scanning speed. For the Mini-Mill machine that is employed for the present CLM process, the maximum X-Y interpolation speed (G01, G02, G03 etc) is *6350 mm/min.*

   b. Towpreg melting speed: the self-anchoring process is a two-step method. In the first step, the towpreg is fabricated with the continuous fiber being impregnated with a thermoplastic material. During the deposition step, the towpreg is re-melted with a heating tube. The heating tube cannot be very long. If the towpreg is heated by radiation heating, it may take sometime for the towpreg to go from room temperature T_R to the melted point T_M. Thus, the delivery speed for the melted towpreg is restricted by:

$$V_m = \frac{L_t}{t_h} \qquad (4-1)$$

where V_m = Delivery speed of the melted towpreg, mm/s

L_t = Length of the heating tube, mm,

t_h = the time needed to heat the towpreg from T_R to T_M . s.

If $L_t = 150$ mm, $t_h = 30$ second, then $V_m = 5$ *mm/s,* this means that the forming speed could not exceed *5* mm per second. Optimizing the tube structure and/or raising the heating temperature of the tube could somewhat relax this restriction. In the following process simulation, the towpreg melting speed in the tube is not considered, but one must bear in mind that the melting speed could be a constraint.

According to the above analysis, the major concern is the forming speed. The simulation for the self-anchoring process is related to the forming speed.

4-2-3 Transformations and Simplification of the Problem

To investigate the *Deposited and Anchored At Once* forming principle, and optimize forming parameters, the forming speed is the priority consideration. But this problem may change into a research of a temperature field for the forming process because in the self-anchoring process, the durations of time required of solidification and anchoring are directly related to temperature changes.

As Figure 4-1 shows, the depositing process is done in a chamber that has closed surroundings and opened at the top. The interior of the chamber is at a constant temperature, which is a very important parameter. During the forming process, the molten towpreg is deposited line by line to form a layer, and layer by layer to build a whole part or structure. The temperature of the added new line or layer is higher than the temperature of the previous line or layer. The newly added line or layer is regarded as a thermal source, which can heat the previous layer. But after a short period of time, the chamber temperature and the surrounding temperature are in equilibrium with the temperature of the formed layers or lines.

The temperature inside a chamber could not be set too high because it is necessary to increase the solidification speed of the towpreg in order to anchor it into a previous layer as soon as possible. However, the temperature inside the chamber could not be set too low either. If the temperature is too low and the cross-section of a part is too large, then when a new segment of the towpreg is added onto the top of the object, the heat quantity of the towpreg may not be sufficient to melt the corresponding point of the previous layer, which is already in equilibrium with the low surrounding temperature. As a result, the newly added towpreg could not be glued effectively to the previous layer, and the formed part will have delamination defects.

Not only the temperature field of the chamber but also the sign and shape of the part affect the solidifying speed of the towpreg. The result is shown in Figure 4-3.

For example, in a layer, the tool path is from $A_0 \rightarrow B_0 \rightarrow C_0 \rightarrow D_0$ and then to $A_1 \rightarrow B_1 \ldots$. For the different points, their thermal boundary conditions are different, and the temperature of each point could not be the same. The results analyzed above show that the effects of different temperatures on the forming speed are much different. If a part is significantly larger and more complicated, and has a larger cross section than the others, then it should take more time to finish one layer. When a previous layer has been built and a new layer has started to form, the starting point A_0 in the new layer is supposed to be anchored to a corresponding point A_0', which is in the previous layer (Figure 4-3). Because the time is too long, the temperature of A_0' is much different from that of A_0. Perhaps the temperature of point A_0' has already reached the surrounding

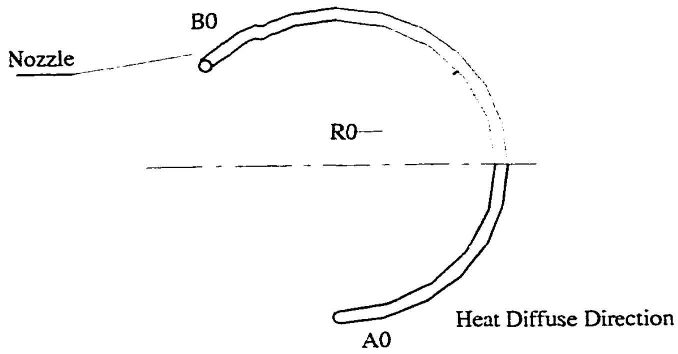

Fig. 4-4A Thermal transfer direction in a single towpreg line.

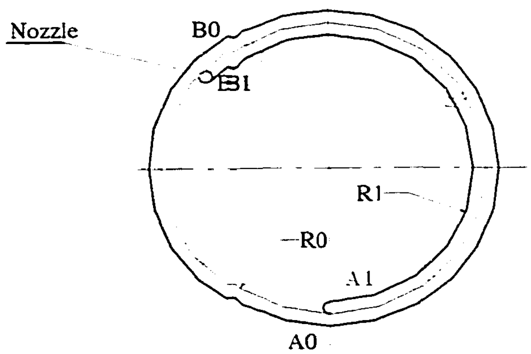

Fig. 4-4B Thermal transfer direction in the multiple line.

Fig. 4-4 Thermal transfer direction.

temperature, and point A_0 could not re-melt point A_0'. As a result, it could not be anchored to the point A_0'.

If a layer area is significantly smaller than other layer, then it is possible that the temperature of the starting point of a layer has not reached the equilibrium point before the nozzle returns to this point for starting to build the next layer. In this case, one may have an unsuccessful anchoring.

If the cross-section of a structure is more complex, the condition for heat dissipation and/or absorption may vary from point to point, such as point B_0 and point H in Figure 4-3. The cross-sectional shape of a part or structure varies from part to part; even in a particular structure, all cross-sections are not the same. But, it is practically impossible to adjust the chamber temperature and nozzle moving speed according to the different cross-section or different part shape. Therefore, it is necessary to make some assumption in order to simplify the problem:

1. The temperature is the same in each built layer and is different between different layers.
2. In a currently being built layer, the temperature is the same in each deposited line and is different between different lines.

§4-3 BASICS OF SIMULATION

4-3-1 Thermal Conduction Equations

The Fourier differentiation equation, a general heat transfer equation is given by [61]:

$$\rho(T)c(T)\frac{\partial T}{\partial t} = \frac{\partial}{\partial x}(k_x \frac{\partial T}{\partial x}) + \frac{\partial}{\partial y}(k_y \frac{\partial T}{\partial y}) + \frac{\partial}{\partial z}(k_z \frac{\partial T}{\partial z}) + \dot{Q} \qquad (4-2)$$

where $\dot{Q}$= the internal thermal sources density, $\rho(T)$, $c(T)$ are the density and specific heat of a material, respectively, k_x, k_y, and k_z are the coefficient of thermal conductivity along the X, Y, Z, directions, respectively. If the material is isotopic, $k_x = k_y = k_z = k$.

Equation (4-2) is a thermal balance equation, in which the left hand side is the needed heat quantity for a unit temperature increment. On the right hand side, the first, second and third terms indicate the inputted heat quantity from the *X*, *Y*, and *Z* directions, respectively, and the last term is the heat quantity generated by the internal thermal source. If only the 2-D problem is considered, and assuming no inside thermal source and material being isotropic, then Equation (4-2) can be simplified to

$$\rho \cdot c\frac{\partial T}{\partial t} = k(\frac{\partial^2 T}{\partial x^2} + \frac{\partial^2 T}{\partial y^2}) \qquad (4-3)$$

The equation governs the heat transfer behavior of a system. Further, the thermal field inside the material is determined by a specific boundary condition for a given situation.

$$T(x,y,z,t)_{t=0} = T_0(x,y,z) \qquad (4-4)$$

There are four types of boundary conditions:

1. The first boundary condition is that the temperature on surface S_1 is already known. The condition is:

$$T(x,y,z,t) = T_0(x,y,z,t) \tag{4-5}$$

2. The second boundary condition is the density of a thermal flow on surface S_2:

$$k\frac{\partial T}{\partial n} = -q \tag{4-6}$$

where $\frac{\partial T}{\partial n}$ is a directional derivative of a temperature, T, along the normal line direction.

q is the density of thermal flow.

3. The third boundary condition:

a. S_3 is a convection thermal exchange boundary:

$$k\frac{\partial T}{\partial n} = -\alpha(T - T_0) \tag{4-7}$$

where a is the thermal exchange co-efficient, T_0 is the outside temperature.

b. S_4 is a radiating thermal exchange surface:

$$k\frac{\partial T}{\partial n} = -\sigma\varepsilon F(T^4 - T_\infty^4) \tag{4-8}$$

where σ is the Boltzmann constant, 1.380662×10^{-23} J/K, ε is the radiation ratio (thermal emissive), F is a shape coefficient, and T_∞ is the temperature of the thermal radiating source.

4. The fourth boundary condition is that a surface S_5 is a heat insulation boundary:

$$\frac{\partial T}{\partial n} = 0 \tag{4-9}$$

where $\boldsymbol{n}$ is the outside normal direction of the surface S_5.

For any system, the boundary condition should be S and

$$S = S_1 + S_2 + S_3 + S_4 + S_5 \qquad (4-10)$$

where S includes all the boundaries of the system.

4-3-2 Basic Assumptions

According to the existing CLM system operating in a self-anchoring mode, the following boundary conditions can be assumed:

1. At the bottom of the forming chamber, the surface is thermally insulated. Thus, it is the fourth boundary condition, and Equation (4-9) can be used.

2. Connecting thermal exchange exists between the deposited towpreg and the air of the inside chamber. Hence, the third boundary condition; Equation (4-7) can be used.

3. The temperature inside the chamber is set to be constant and uniform.

4. The radiation direction is along the longitude of the deposited towpreg line. The cross-section direction does not radiate. See Figure 4-4.

4-3-3 Basic Parameters

The most important parameters used for the present simulation work are listed in Table 4-1 (see Appendix A). In the Self-anchoring process, Kevlar-49 fiber and polyethylene matrix are used. The parameters listed in Table 4-1 are for these two materials. If other materials replace these materials, the simulation process does not need to be changed. Only the inputted parameters need to be changed [62, 63].

4-3-4 An Analytical Solution for a Single Towpreg

An analytical solution should be used to describe the results of the simulation study.

A unit cube is shown in Figure 4-5. Assume that

1. The temperature inside the cube is uniform, and is not a function of the X, Y, and Z coordinates.

2. There is no heat source inside the cube and only the heat quantity change on the cube surface influences the heat quantity change inside the cube.

3. Furthermore, only a change of the heat quantity could changes the temperature inside the cube.

4. The temperature change in the cube surface follows the third boundary condition. Equation (4-7) should be used.

5. No thermal exchange occurs on the bottom, front and rear surfaces. Only the top, left, and right surfaces experience thermal exchanges, (Figure 4-5).

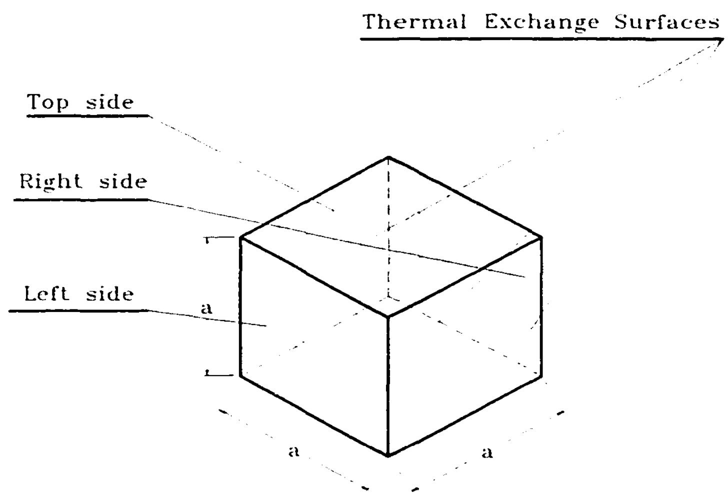

Figure 4–5 A Unit cube of thermal exchange.

The area of the thermal exchange surfaces is $3a^2$, and the cube volume is a^3. According to the principle of energy conservation, one can establish an equation that describes the thermal exchange in the micro-cube:

$$\rho c \frac{\partial T}{\partial t} a^3 = -\alpha (T - T_c)(3a^2) \qquad (4-11)$$

where T_c is the temperature of the chamber, α is the thermal convection exchange coefficient.

In the left hand side of Equation (4-11), the item indicates the heat quantity varies with the temperature, which changes with the time inside the micro-unite. The right hand side item is related to the quantity of the thermal exchange at the boundary.

Simplifying and changing the order of Equation (4-11) we have Equations (4-12) and (4-13):

$$\frac{dT}{dt} = -\frac{3\alpha}{a\rho c}(T - T_c) \qquad (4-12)$$

$$\frac{d(T - T_c)}{T - T_c} = -\frac{3\alpha}{a\rho c} dt \qquad (4-13)$$

and upon integration of both sides of Equation (4-13), one obtains

$$T = Ae^{-\frac{3\alpha}{a\rho c}t} + T_c \qquad (4-14)$$

From an initial condition:

when $t = 0$, $T = T_0$, we have $A = T_0 - T_0$.

Substituting the value A into equation (4-14) results in:

$$T = (T_0 - T_c)e^{-\frac{3\alpha}{a\rho c}t} + T_c \qquad (4-15)$$

Figure 4-6 An analytical solution for the single- towpreg-line heat transfer.

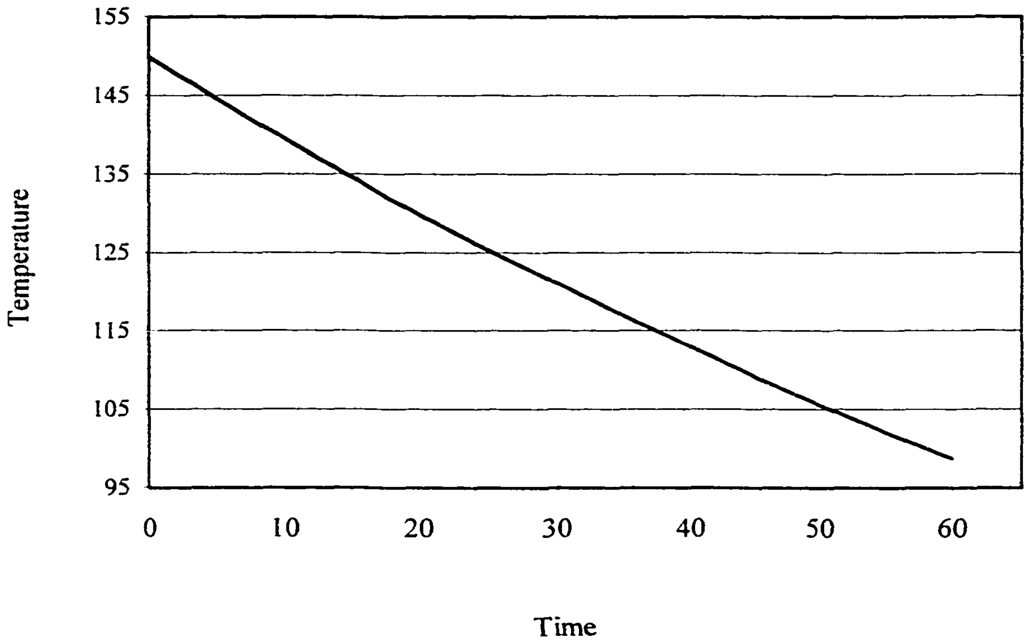

According to Equations (4-14), and (4-15) and the length of the cube $a = l^{-3}\ m$, a diagram of the temperature vs. the time is shown in Figure 4-6. By comparing Figure 4-6 with Figure 4-9 and Figure 4-10, we can find that the temperature change pattern is almost the same. The temperature change for a single towpreg can be simulated and calculated, but in a complicated problem, only the simulation is useful.

§4-4 TEMPERATURE SIMULATION FOR A SINGLE TOWPREG

4-4-1 Introduction to the ANSYS

It is hard to find an analytical solution to Equation (4-3), even if it is a 2D problem. For most of the thermal field problems, a numerical solution is used. Many software packages are commercially available for thermal field simulation. The ANSYS is one of the most successful software packages. ANSYS can be used to solve the problems such as structure analysis, thermal transfer, electromagnetic field and fluid flow analysis.

Conduction, convection, and radiation, the three basic heat transfer processes could be treated by the ANSYS program package, which can be used for linear, nonlinear, steady state, and transient thermal analysis.

According to the forming characteristics of the CLM process, the current problem requires nonlinear and transient thermal analysis. Thus, thermal conduction, convection, and radiation should be considered.

4-4-2 Simulations for a Single Towpreg

First let us evaluate the influence of a towpreg's cross-section. A towpreg is dispensed from a nozzle, which has a circular cross-section. When the towpreg is deposited onto a surface, its cross-section could be changed into a square or other shapes, see Figure 4-3A, B, and C. Two shapes are shown in Figure 4-7. Figure 4-7A shows a shape with round corners. Figure 4-7B shows a square shape. Now, an error is evaluated when the shape effect is negligible.

Five points were selected for each shape (see Figure 4-7). It is assumed that the chamber temperature is *20℃* and the initial temperature of the towpreg is *150℃*. A calculation result is shown in Figure 4-8. Figure 4-8A shows the temperature changes with time at each point for the shape that has round corners, Figure 4-8B shows the same thing but for a square shape. As demonstrated in Figure 4-8, the shape does not influence the temperature variation too much. Therefore, in the following calculation the towpreg is treated as a square cross-section.

Second, consider the effect of fiber. Figure 4-8 shows the result for the case of a pure matrix in witch the fiber effect is not considered. for the case of a *50%* fiber volume fraction, the result is shown in Figure 4-9. By comparing Figure 4-8 and Figure 4-9, we can see that the temperature change trend is almost the same, but the value is different. The specific heat of the Kevlar fiber is lower than that of the PE matrix. When heat is lost, the temperature of the Kevlar-PE towpreg will fall faster than that of the pure material.

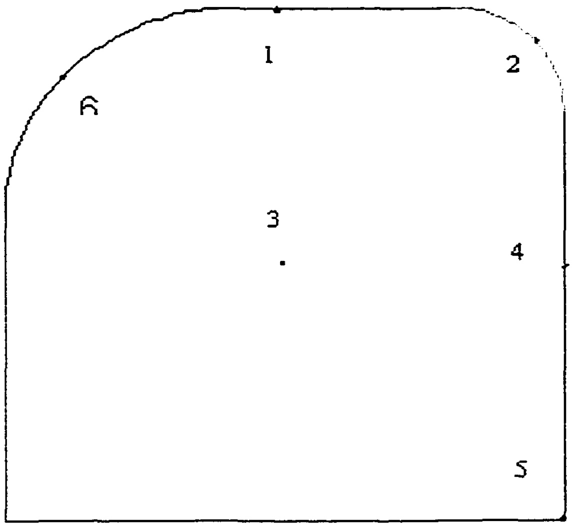

Figure 4-7A A cross-section of the towpreg has round corners.

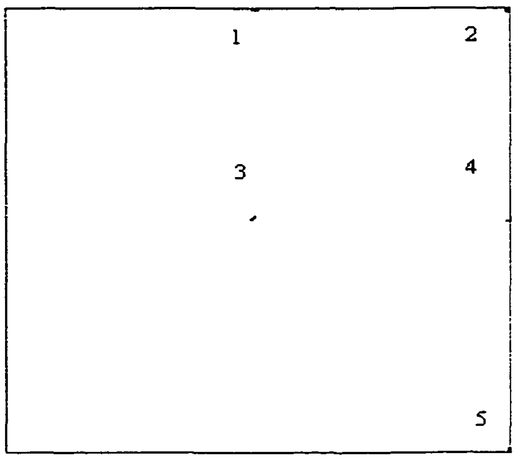

Figure 4-7B A cross-section of the towpreg has right-angle corners.

Figure 4-7 Cross-section shapes and the calculated points.

1, 2, 3, 4, 5 and 6 are the selected points for evaluation.

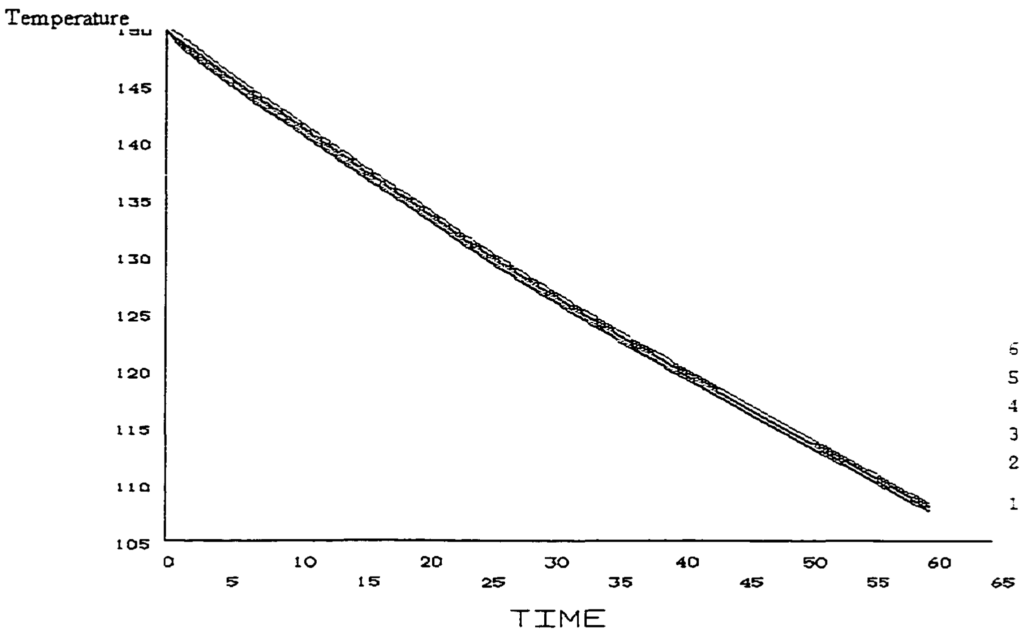

Figure 4-8A Temperature changing with time at each point for the round-corners shape.

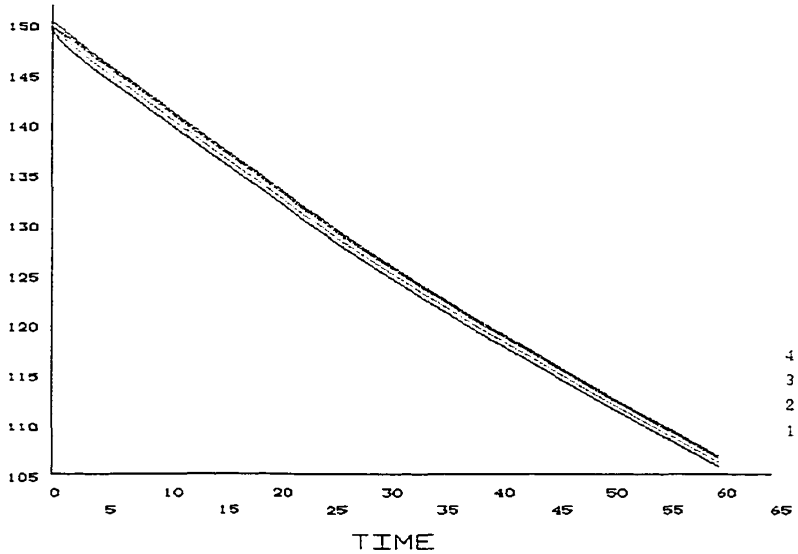

Figure 4-8B Temperature changing with time at each point for a square shape.

Figure 4-8 Temperature changing for each point.

An ANSYS model for a composite material is complicated. The model is built up with two different components, the fiber and the matrix. These components are assumed to be evenly distributed inside the model. Through separate Boolean Operations, the fiber and the matrix properties were inputted to the units, respectively. Then, they were marked with different number to build the final model. If equivalent heat transfer properties of the material are found, the model can be readily built.

According to the heat transfer principle, the equivalent conductivity $\bar{k}$, specific heat $\bar{c}$, and density $\bar{\rho}$ of the composite are [64]:

$$\bar{k} = \frac{k_f k_m}{k_f V_m + k_m V_f} \qquad (4-16)$$

$$\bar{c} = c_f V_f + c_m V_m \qquad (4-17)$$

$$\bar{\rho} = \rho_f V_f + \rho_m V_m \qquad (4-18)$$

where K_f, K_m are the thermal conductivity of fiber and matrix, respectively, V_f, V_m are the volume fraction of the fiber and matrix, respectively, c_f, c_m are the specific heat of the fiber and matrix, respectively, and ρ_f, ρ_m are the density of the fiber and matrix, respectively.

Assuming that $V_f = V_m = 0.5$, and that the fiber is well dispersed in the matrix. according to Table 4-1 and Equations (4-11) ~ (4-13), the equivalent parameters are:

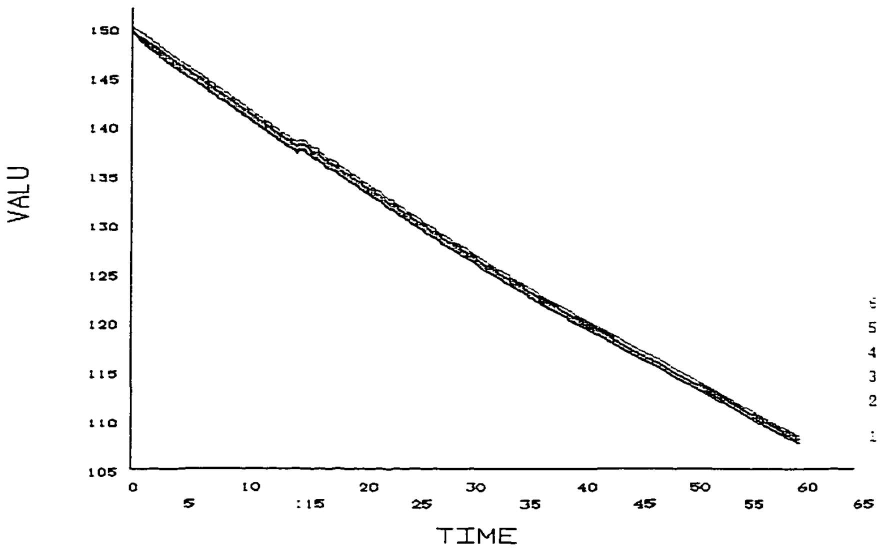

Figure 4-9 Temperature changes of the towpreg having a 50% by volume of fibers.

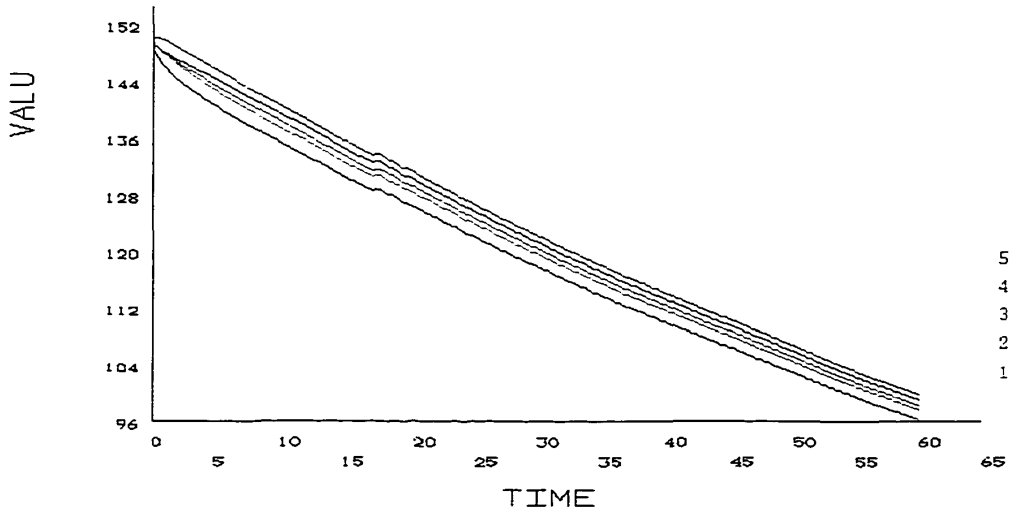

Figure 4-10 Temperature changes with time (with equivalent parameter values incorporated).

$$\bar{k}=0.07\frac{w}{mK},\qquad \bar{c}=1465\frac{J}{kg\,K},\qquad \bar{\rho}=1231\frac{kg}{m^3} \qquad (4-19)$$

According to the equivalent parameters, a simulation result is shown in Figure 4-10. The numbers 1, 2…5 indicate different investigation points in the towpreg cross-section (See Figure 4-7)

By comparing Figure 4-10 with Figure 4-9 on the surfaces and corners of the towpreg (points 1, 3, 4 and 5), we can see that the temperature change trend is almost the same. Only in the inside of the towpreg (point 3) the temperature change trend is a little different. During the forming process, a temperature change on the towpreg surface is a major effect for anchoring. Therefore, the equivalent parameters can be used to substitute for the composite parameters and make the simulation simple.

§4-5 TEMPERATURE SIMULATION FOR MULTIPLE TOWPREGS

4-5-1 Forming and Heat Transfer Model

As indicated in the analysis in §4-1, the temperature of the towpreg is influenced by many factors. During the earliest stage of the simulation, the influencing factors should be simplified. A part of a forming process is selected for the simulation to find a general regularity of the whole forming process. As an example, the structure of a part may be built with nine towpreg circles. A cross section of the nine-towpreg circles is shown in Figure 4-11. There are three towpreg lines in each layer and three layers in the structure. In Figure 4-11, the different colors indicate different lines and layers, and the depositing sequence is $A_1 \rightarrow A_2 \rightarrow A_3 \rightarrow \cdots\cdots \rightarrow A_9$.

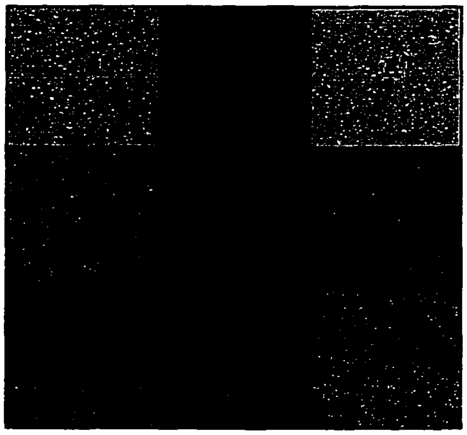

Figure 4-11 Deposition sequence of the nine towpregs (a cross-section).

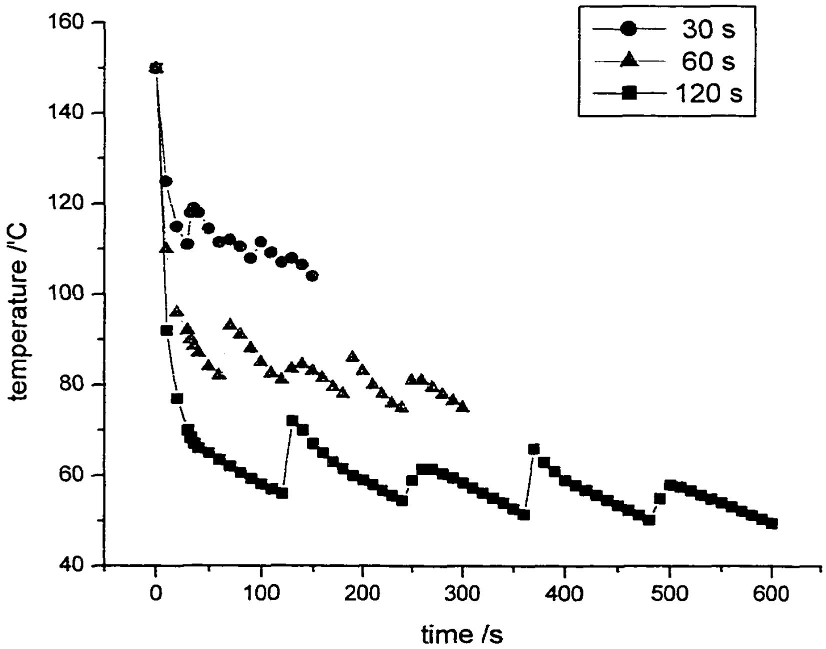

Figure 4-12 Temperature vs. depositing interval.

The deposition interval between two towpreg lines is the same everywhere and the interval is in inverse proportion to the nozzle moving speed. Assume the temperature of the chamber is 20^o *C*, and the convection coefficient is 5 N/m^2sk. Based on this forming and heat transfer model, the temperature change of the fifth towpreg is investigated under the different chamber temperature, nozzle moving speed, and convection coefficient conditions.

4-5-2 Temperature Field Simulations

The effects of depositing speed, chamber temperature, and convection coefficient will be simulated in this subsection. Figure 4-12 shows the fifth towpreg's temperature vs. different interval or depositing speed. The following observation are made:

1. At the beginning, the temperature decreases in a more drastic manner. With the towpreg is being added, the temperature is undulated. The temperature undulation is larger when the temperature is lower. The maximum fluctuation is up to approximately 16°C. After that, the temperature decrement is slower.
2. The sixth and eighth towpregs have the largest influence on the temperature of the fifth towpreg.
3. If the interval is longer, or the depositing speed is slower, the temperature falls faster.

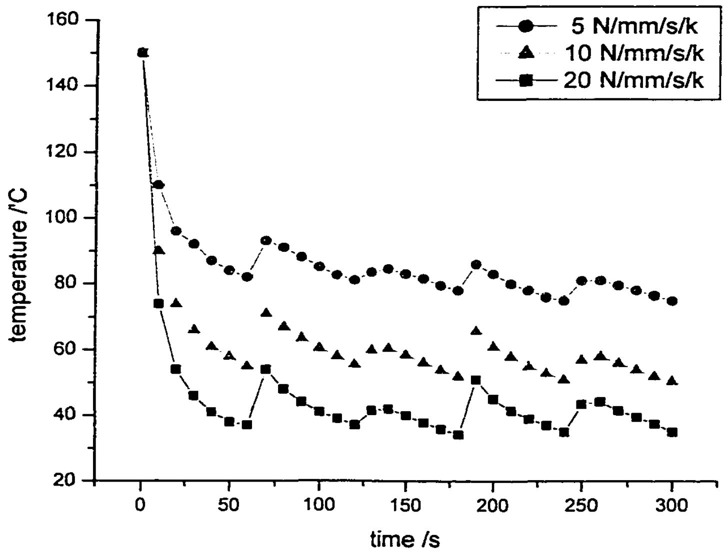

Figure 4-13 Temperature vs. convection exchange coefficient.

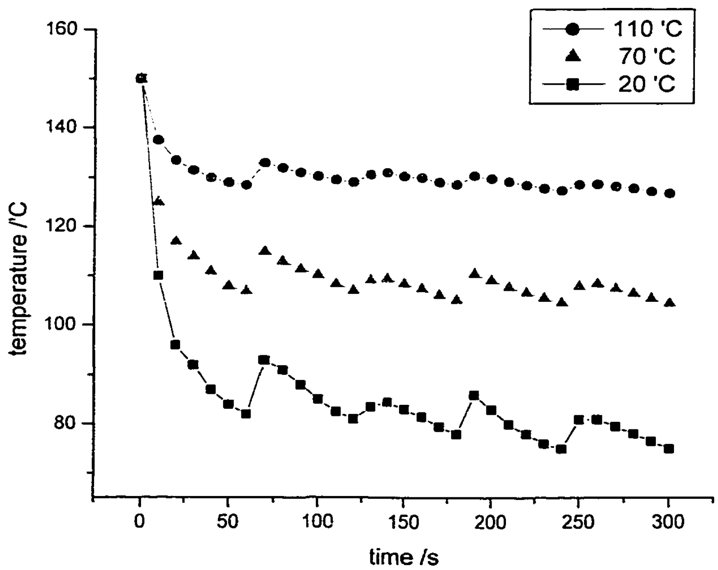

Figure 4-14 Temperature of the fifth towpreg vs. different chamber's temperature.

When the chamber temperature is *20℃* and the interval is *60* seconds, the temperature vs. the convection exchange coefficient, α, is shown in Figure 4-13. The temperature undulation is not much different for the different convection conditions.

When the convection exchange coefficient is $5 N/m^2\ s\ k$, and the interval is *60*, the temperature vs. the different chamber temperatures is shown in Figure 4-14. The undulation of temperature does not vary much with the different environment temperature.

In the preceding subsections, the temperature fields were simulated under different conditions. A future task should be to investigate the conditions of the towpreg's solidification speed in relation to the temperature fields, and then, according to the different towpreg's solidification degrees, to find the various bond strength of the towpreg, and finally to calculate the effect of the forming speed on the towpreg's bond strength. With this knowledge on hand, the max forming speed can be evaluated for different towpreg materials.

§4-6 ANALYZING AUTOMATIC EXTRUSION

4-6-1 Principle of Automatic Extrusion Method

The self-anchoring forming method was studied in the previous sections. It was found that the forming speed of the self-anchoring CLM method is limited. So, other effective forming methods are highly desired and must be investigated. The advantages of the one-step forming method and the Active Material Supply method were introduced in Chapter 2. One of the advantages is that the forming speed is not limited by the solidification condition of the towpreg during the forming process. But, a challenge of the one-step forming method mentioned before is to continuously deliver the fiber tow into a pressure vessel and to seal the fiber entrance to prevent leakage.

A one-step forming method is shown in Figure 2-20. In this system, an extrusion machine supplies melted thermoplastic material to an impregnating and depositing device. The device impregnates a continuously supplied fiber tow where the melt deposits the towpreg onto a work surface, which is located on a 3D-motion system. A key component in this forming system is the impregnating and depositing device. A layout of this device is shown in Figure 4-15. In the design, a flange joins the device to the extruder machine to receive a pressurized polymer melt there from; the fiber tow is drawn into the pressure chamber through a regulating rod and regulating head and is impregnated with the polymer melt inside the nozzle area. The regulating rod could be risen or lowered to adjust the distance between the regulating head and the nozzle. The nozzle and regulating head are changeable to match different towpreg requirements and to find the best shape and dimension.

A proposed fluid flow model is shown in Figure 4-16 [65, 66]. When the melted polymer is squeezed in the pressure vessel, in zone *A*, the fluid flow speed is steady and uniform, see Figure 4-16A. In zone *B*, the matrix impregnates the fiber tow, and the speed of the distributing matrix flow is complicated. However, a dead zone *C*, where the pressure is equal to zero, could be generated at the end of the regulating head. In zone *C*, the polymer flow speed is higher than that in zone *A*, and the towpreg is driven out of the

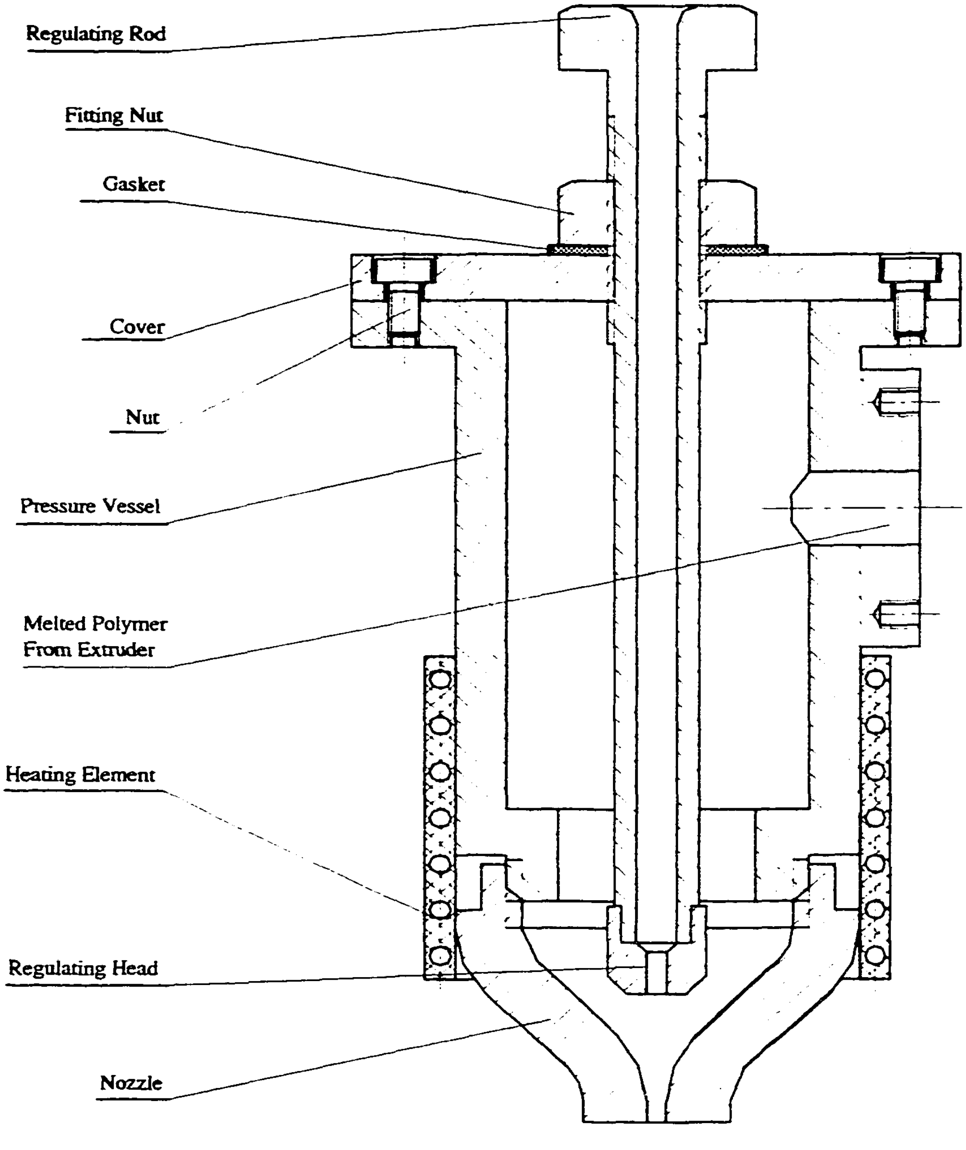

Fig. 4-15 An impregnation and deposition device.

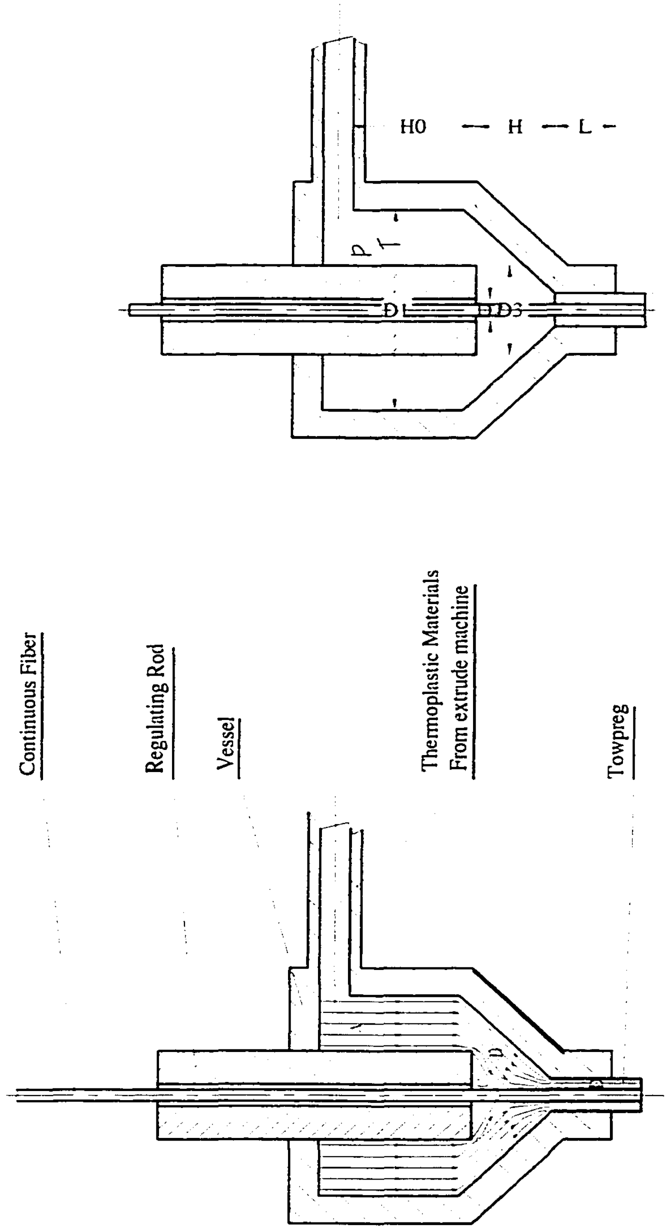

Fig. 4-16A

Fig. 4-16B

Fig. 4-16 The fluid flow model.

nozzle by shear stress. Because a dead zone is formed near the entrance of the fiber tow, the melted polymer could not go up. Therefore, the fiber is drawn into the chamber for impregnation and is deposited onto the work surface continuously and automatically. This is the mechanism of the forming method, which is called Automatic Impregnation and Deposition Mechanism (AIDM).

The factors that influence the AIDM are shown in Figure 4-16B. Physical properties that are influencing are material viscosity μ, chamber pressure p, and temperature T. The geometry factors are the shapes of the regulating head and nozzle. The dimension factors are shown in Figure 4-16B. The following simulation and analysis procedures were used to study their factors for the purpose of determining the best parameters for the AIDM forming method. The feasibility of the AIDM method has been demonstrated by experiments.

4-6-2 Simplification and Estimation of the Best Parameters

Figure 4-16A shows a distribution profile model of the fluid flow lines. In zone A, the fluid flow could be treated as a non-Newtonian fluid inside coaxial cylinders. This is a commonly encountered situation in the industry. Therefore, many scientists have tried to solve the problem with an analytical solution. Bird [67-72] has done much investigation in this field. The results of Bird's work provide some solution to the AIDM problem. Before analyzing the fluid flow, the following assumptions are made:

1. The fluid is incompressible (constant density).
2. The flow is under steady state conditions (i.e. time-independent).

3. **Stationary boundary condition (the two cylinders do not slide or rotate during the simulation).**

4. **The cylinders are sufficiently long, so that the effect of the cylinder ends could be neglected.**

5. **The gravitational force is neglected.**

The stress distribution for the axial laminar flow of an arbitrary inelastic, non-Newtonian fluid through a concentric annulus is known as:

$$\tau_{rz} = \frac{PR}{2}(\xi - \frac{\lambda^2}{\xi}) \qquad (4-20)$$

$$p = \frac{P_O - P_L}{L} + \rho g \qquad (4-21)$$

Where p = the total pressure loss per unit length L, τ_{rz} = the shear stress, $\xi = \frac{r}{R}$ and R = the Radius of the outer pipe of the annulus as illustrated in Fig4-17.

The constant of integration is chosen so that: when $r = \lambda R$, $\tau_{rz} = 0$.

In a laminar flow this corresponds to the location of maximum velocity. The power-low rheological model could be represented as:

$$\tau_{rz} = -m\left|\frac{dv_z}{dr}\right|^{n-1} \times \left(\frac{dv_z}{dr}\right) \qquad (4-22)$$

where: m, n are the parameters in power-low model and $s = 1/n$.

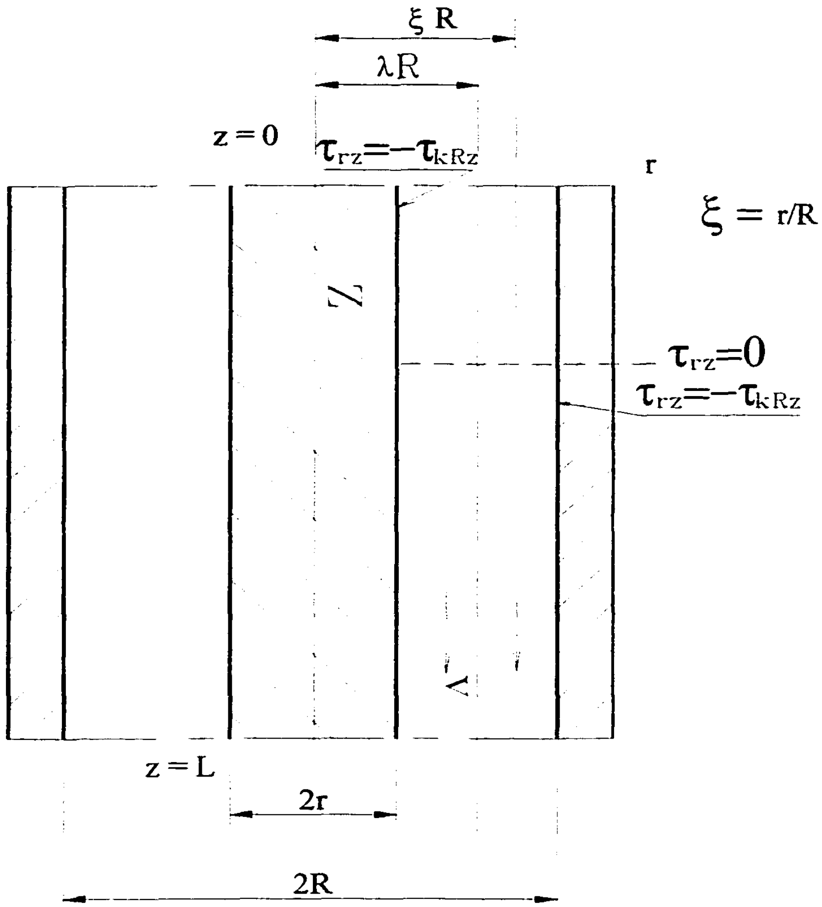

Figure 4-17 A fluid flow model.

Combining Equations (4-20) and (4-22) and considering the boundary conditions that, when $\xi = K$, $v_z = 0$, and when $\xi = 1$, $v_z = 0$, we obtain Equations (4-23) and (4-24):

$$-m\left|\frac{dv_z}{dr}\right|^{n-1}\frac{dv_z}{dr} = \frac{PR}{2}\left(\xi - \frac{\lambda^2}{\xi}\right) \qquad (4-23)$$

Or:

$$\mathrm{v}_{zi} = R\left(\frac{PR}{2m}\right)^s \times \int_K^{\xi}\left(\frac{\lambda^2}{x} - x\right)^s dx \qquad K \le \xi \le \lambda$$

$$v_{zo} = R\left(\frac{PR}{2m}\right)^s \times \int_{\xi}^{1}\left(x - \frac{\lambda^2}{x}\right)^s dx \qquad \lambda \le \xi \le 1 \qquad (4\text{-}24)$$

where: k = the ratio of the radius of inner cylinder to that of outer cylinder,

λ = a value of a dimensionless radial coordinate,

μ = Newtonian Viscosity,

μ_0 = "Plastic-viscosity" of the Bingham plastic.

The value of λ is determined by the condition:

$$v_{zi}(\lambda) = v_{zo}(\lambda)$$

Or: $$\int_K^{\lambda}\left(\frac{\lambda^2}{x} - x\right)^s dx = \int_{\lambda}^{1}\left(x - \frac{\lambda^2}{x}\right)^s \qquad (4-25)$$

A volume flow rate is

$$Q = 2\pi R^2 \int_K^1 \xi v_z d\xi \qquad (4-26)$$

Substitution Equation (4-24) into (4-26) yields:

$$\frac{Q}{\pi R^3} = 2\left(\frac{CPR}{2m}\right)^s\left[\int_K^{\lambda}\xi d\xi \cdot \int_K^{\xi}\left(\frac{\lambda^2}{x} - x\right)^s dx + \int_{\lambda}^{1}\xi d\xi \cdot \int_{\xi}^{1}\left(x - \frac{\lambda^2}{x}\right)^s dx\right] \qquad (4\text{-}27)$$

Integrating Equation (4-27) yields:

$$Q = \frac{\pi n R^3}{1+3n}\left(\frac{PR}{2m}\right)^{\frac{1}{n}} Y \qquad (4-28)$$

Or: $$\frac{PR}{2} = \left(Q\frac{1+3n}{Y\pi n R^3}\right)^n \times m$$

where $$Y = (1-\lambda^2)^{1+\frac{1}{n}} - k^{1-\frac{1}{n}}\left(\lambda^2 - k^2\right)^{1+\frac{1}{n}} \qquad (4-29)$$

The value of λ can be calculated by Equation (4-25), or the Table of λ (n, k) [73].

Thus, Equation (4-28) shows the relationship between pressures drop and flow quantity. When the m, n values and the dimensions of the concentric annulus are known, Equation (4-28) can be used to compute *PR/2* if *Q* is given.

According to the design of the impregnation and deposition device, the parameters could be *R=15 mm*, and $K \approx 0.3$. For polyethylene, values of *n=0.5, m=0.3* can be assumed

From the values of the table for $\lambda(n, k)$, the value of λ can be obtained: λ = *0.5970*. Substituting those parameters into Equation (4-29) we obtain $Y \approx 0.511$. If the extruder machine supplies a flow rate of melted polymer with

Q = 0.001cubic foot per second

$$p = 2\left(Q\frac{1+3n}{Y\pi n R^3}\right)^n \times m / R = 0.125$$ pound per square foot.

The above analytical solution can be used to describe the flow behavior in zone A of the impregnation and deposition device if the device is long enough (see Figure 4-16A). Several articles that introduced the analytical solutions for an Apex Tapered concentric annulus can be used to evaluate the wire coat and plastic blowing process. But for such

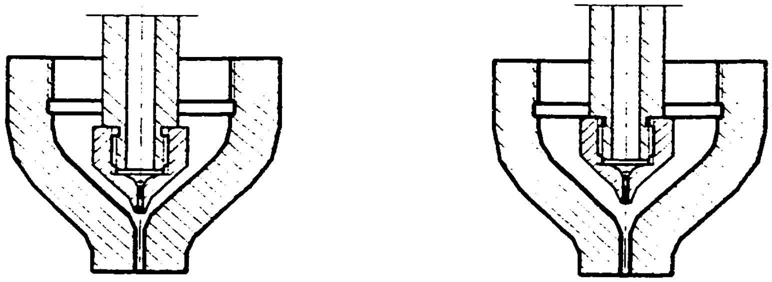

Fig. 4-18 A Different positions for tapered head.

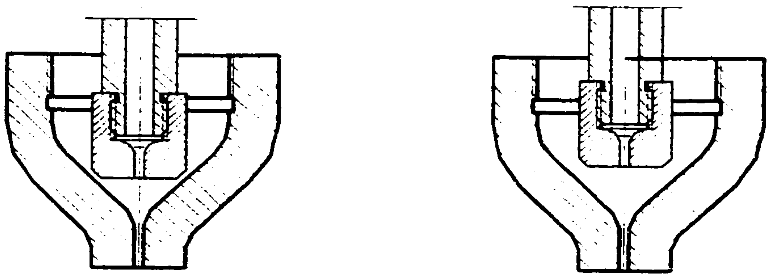

Fig. 4-18 B Different positions for flat head.

Fig. 4-18 The relative position of the heads and nozzles.

complicated shapes in zone B, C and D it is impossible to get the analytical solutions; the numerical solution is useful in this situation.

§4-7 NUMERICAL SIMULATION OF THE AIDM METHOD

4-7-1 The Numerical Simulation Model

The fluid flow could be assumed to be nonlinear, and steady-state, and the assumptions concerning physical properties are the same as those made in the previous subsection period, In fact, no matter how one selects the parameters of the matrix, the simulation result will not change too much. Hence the simulation will be focused on the geometry and dimensions of the regulating head and nozzle.

1. Two regulating heads are selected to be studied, referring to Figure 5-11. Figure 5-11A shows a flat head, Figure 5-11B shows an apex-tapered head, called tapering head. The heads are positioned inside the nozzle as shown in Figure 4-18.

2. The distance between the regulating head and the nozzle is an important parameter. It is called *h*, and several *h* values are investigated.

3. The diameter of the nozzle bore ϕ and a depth ξ of the bore need to be evaluated. See Figure 5-10.

4-7-2 The Fluid Flow Simulation

In this subsection, several simulation tasks are discussed.

1. **The *h* effect: the tapering head is used with a nozzle of ϕ = *2* mm.** Figure 4-19 shows a pressure distribution diagram near the nozzle exit for h = *1, 2, 3, 5* mm, respectively.

2. The effect of the diameter of the nozzle bore ϕ: In this case, using the tapering head, and setting h = *1, 2, 3, 5* mm, for four positions, three ϕ values have been simulated. Figure 4-20, 4-21 and 4-22 shows the results for ϕ = *3, 4, 6*, respectively.

The simulation results show that when the regulating head is adjusted near the nozzle exit, h is shorter and a zero pressure zone appears near the end of the regulating head. With increasing ϕ, the h needed to build a dead zone is going to be longer. When ϕ is smaller, the pressure inside the nozzle will be higher. The regulating head needs to be closer to the nozzle exit to form a small environment in which the pressure is equal to zero.

This simulation result is consistent with the result of an experiment that will be introduced in Chapter 5.

3. The effect of the regulating head: Figure 4-23 shows the simulation results in which the flat head is employed. One can see that when the regulating flat head is adjusted closest to the nozzle exit and ϕ is larger than *8mm*, a zero pressure zone will be established around the fiber tow entrance. The result is a little different from the experiment at result. Because in the simulation, only the steady state is considered. Actually, once a steady fluid flow is formed and the flat regulating head is adjusted up to some distance, the flow is still stable, and no melted

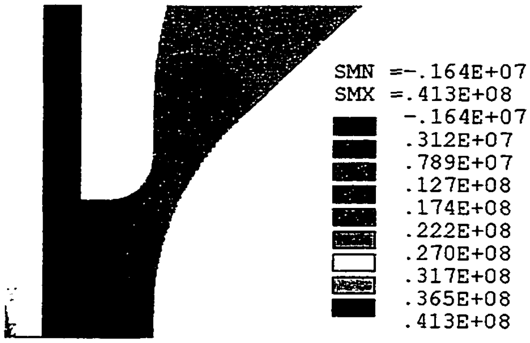

Figure 4-19A *h = 1 mm*

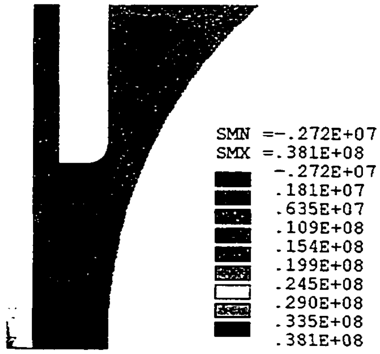

Figure 4-19B *h = 2 mm*

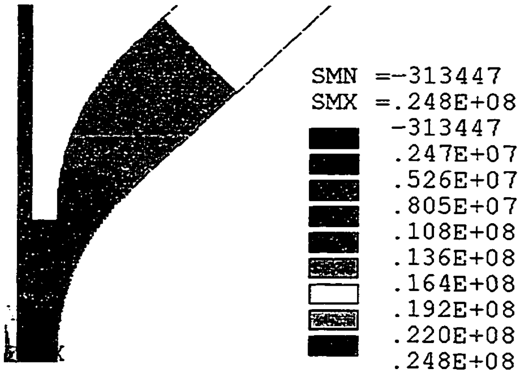

Figure 4-19C *h = 3 mm*

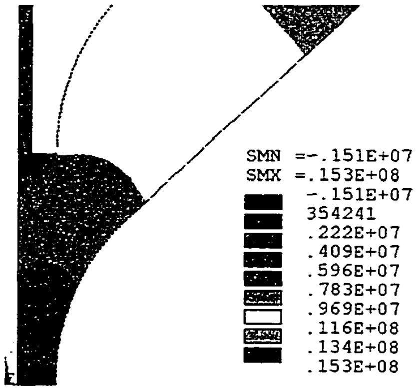

Figure 4-19D *h = 5 mm*

Figure 4-19 the pressure distribution with different *h* values.

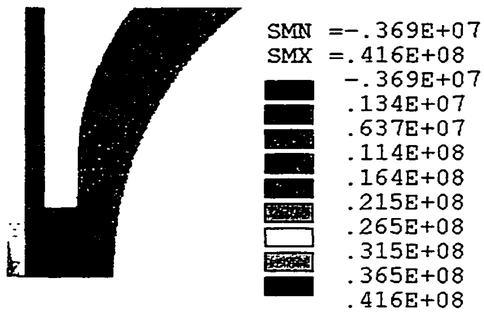

Figure 4-20A *h = 1 mm*

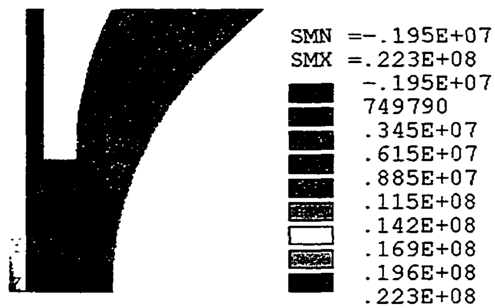

Figure 4-20B *h = 2 mm*

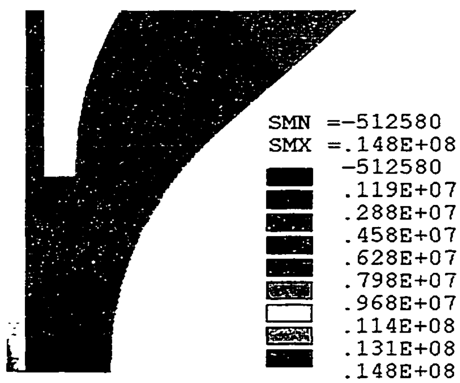

Figure 4-20C *h = 3 mm*

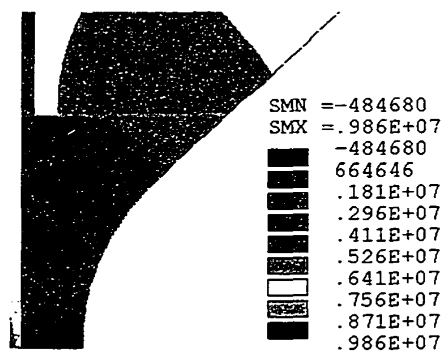

Figure 4-20D *h = 5 mm*

Figure 4-20 the pressure distribution when $\phi = 3$ *mm.*

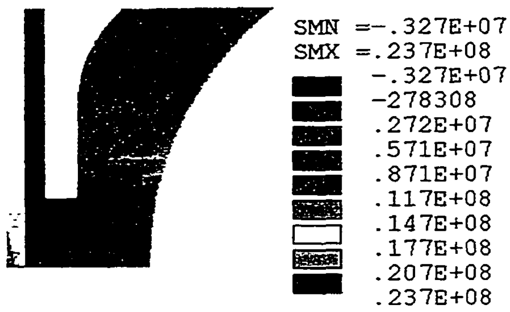

Figure 4-21A *h = 1 mm*

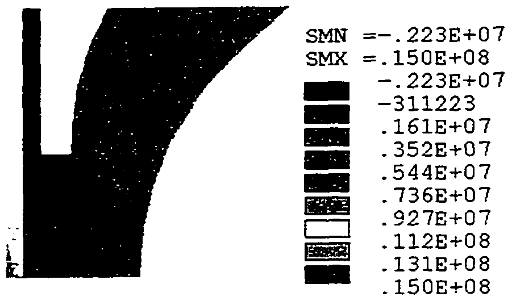

Figure 4-21B *h = 2 mm*

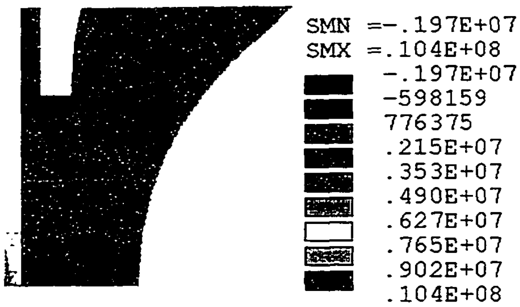

Figure 4-21C *h = 3 mm*

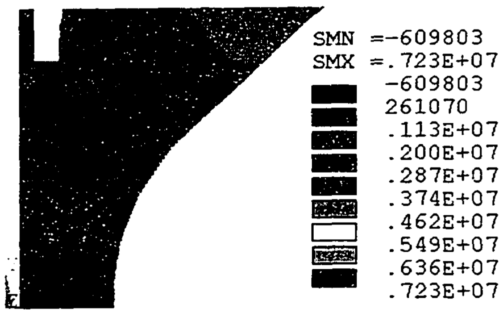

Figure 4-21D *h = 5 mm*

Figure 4-21 the pressure distribution when $\phi = 4$ *mm*.

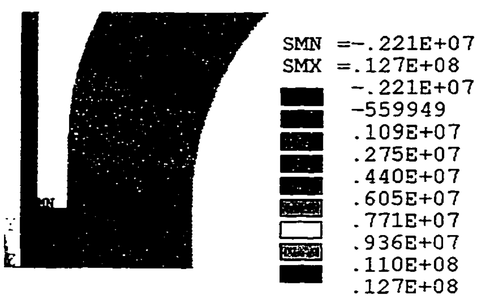

Figure 4-22A *h = 1 mm*

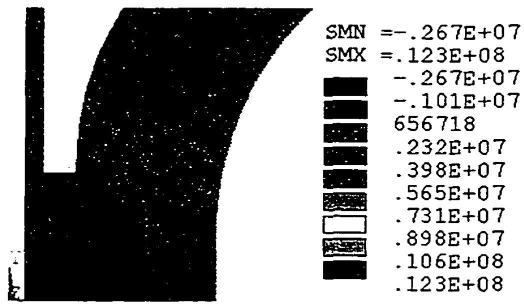

Figure 4-22B *h = 2 mm*

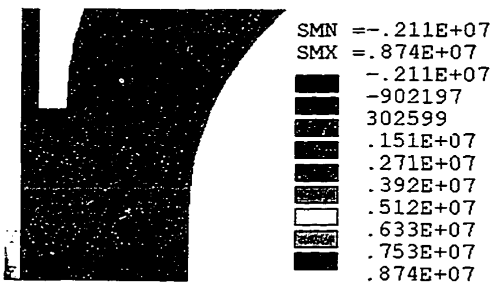

Figure 4-22C *h = 3 mm*

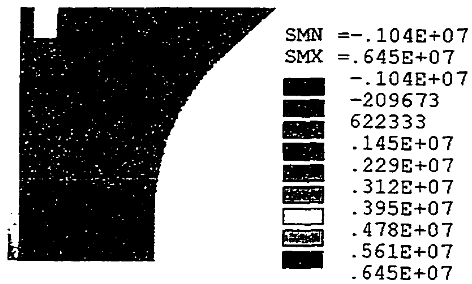

Figure 4-22D *h = 5 mm*

Figure 4-22 The pressure distribution when $\phi = 6\ mm$.

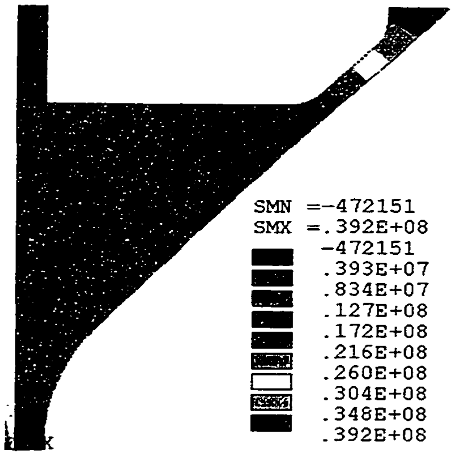

Figure 4-23A $\phi = 2\ mm$

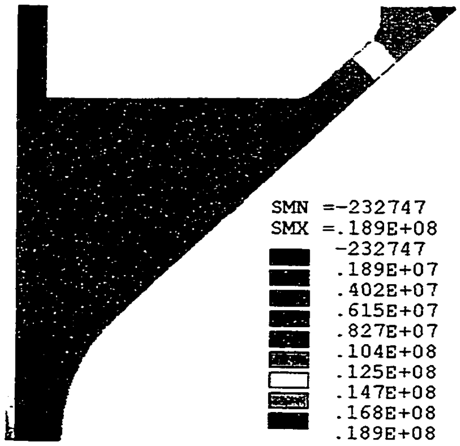

Figure 4-23B $\phi = 3\ mm$

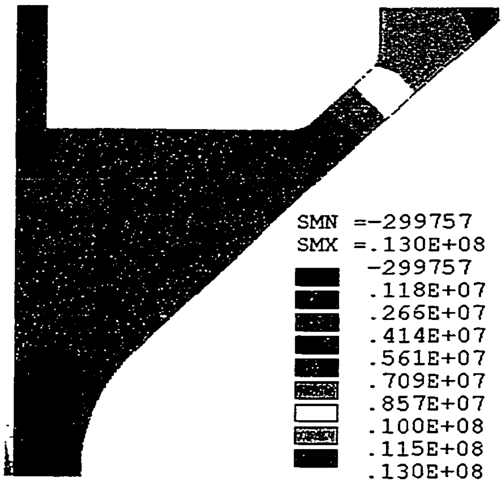

Figure 4-23C $\phi = 4\ mm$

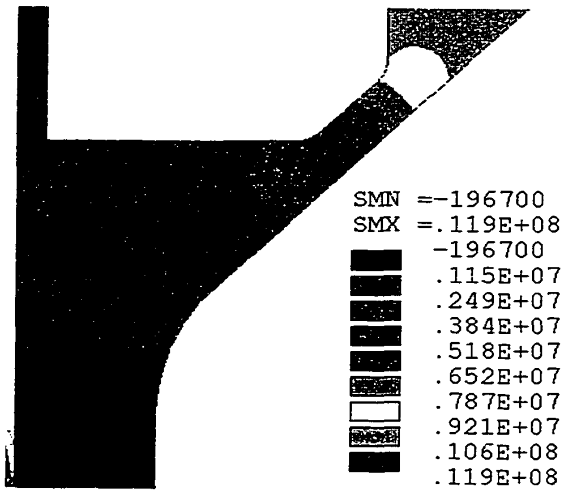

Figure 4-23D $\phi = 8\ mm$

Figure 4-23 the pressure distribution when $\phi = 10\ mm$ and using flatting head.

Figure 4-23 the pressure distribution when $\phi = 10\ mm$ and using flatting head.

polymer goes up through the regulating rod. More detail will be introduced in Chapter 5.

§4-8 CHAPTER CONCLUSIONS

1. In this chapter, the Self-Anchoring Process and Automatic Impregnation and Deposition Mechanism have been analyzed in more detail and analytical solutions methods were obtained that describe simplified processes.

2. The temperature fields for the Self-Anchoring Process were simulated by using ANSYS. The results could be used in the future for optimizing the whole process.

3. Numerical simulations were also obtained for the Automatic Impregnation and Deposition process. Again, the results could be used to optimize the process.

CHAPTER 5 CLM SYSTEM DEVELOPMENT AND EXPERIMENTAL ANALYSIS

§5-1 INTRODUCTION

The investigation of Composite Layer Manufacture (CLM) has been a four-year project, starting from the creation of original ideas, concept design demonstration, complete design for the CLM process, and the construction of the present prototype machine.

In this chapter, several important experiments, key part design principles, and CLM system components will be discussed. The mechanical properties of several parts fabricated through CLM will be analyzed in order to evaluate an important feature of this process.

A system developing process is a tedious procedure; the whole development process (including successes and failures) could not be completely covered in one chapter. Throughout the development process, no matter how big or small a component design is, several different plans were presented, analyzed, and compared to determine their pros and cons before making a decision.

Although the prototyping CLM system appears to work reasonably well, however, there is room for improvement and better systems will be coming in the future.

§5-2 THE EXTREMUM EXPERIMENT

The methodology used in the development of the new CLM technology has been introduced in Chapter 2. Numeric analysis is an important method used in the development period. Hence, a great amount of concept design, numeric simulation, and analysis work has been done and the results have been presented in Chapter 3 and Chapter 4. These results could be used as a guide to direct the hardware and software development of a CLM machine. But some key problems were hard to study with a numeric method or a numerical solution was impossible to get. So, from time to time, experiments were carried out to provide additional insight into the CLM process. With the sole purpose of reducing the required amount of simulation and modeling work an "Extremum experiment" were conducted.

5-2-1 The Concept of Extremum Experiments

In the early stage of development for a new technology, when a design is carried out or a method is proposed, many parameters should be considered, and many possibilities need to be analyzed. So, a lot of experiments need to be done in this period. Given the requirements and characteristics of the technology, Extremum experiments could be used to get an initial result quickly so that the whole technology development procedure can be conducted efficiently and effectively.

An Extremum experiment is done to investigate the result under a certain situation in which all influencing factors and parameters are set on the maximal or minimal value.

The Extremum experiment is one of the feasibility experiments, and it is used to yield a qualitative result to determine if the investigated object is possible or impossible. The Extremum experiment could be separated into two different experiments, which are Confirming Extremum Experiment and Denying Extremum Experiment:

1. Denying Extremum Experiment: To determine whether or not a design or a method could be employed, all parameters or positions are set in the best conditions. Then the experimented result is evaluated.

   a. If the result yields a negative conclusion, the design or method is not useful at all. Even in the best situation, the method is not workable, so it could not be used in a common situation. Therefore, the design or method should be discarded.

   b. If the result yields a positive conclusion, the design or method could not be rashly inferred as a good one in a common situation. Further experiments are required to determine the real conclusion.

2. Confirming Extremum Experiment: The experiment condition is set just opposite to the denying extreme experiment. All parameters and/or positions are set at the worst value or location.

   a. If a result yields a positive conclusion, the investigated design or method could be taken as a good one at once.

   b. If a result yields a negative conclusion, the investigated object could not hastily be regarded as a bad one.

The Extremum experiment could be used to find a correct research direction, or a region of parameter values only. But the direction could be modified, and the region could be compressed with a continuous Extremum experiment. When a series of Extremum Experiments is being done, the best point should be achieved, and/or the optimized value could be obtained. Several Extremum Experiments will be introduced in the following section.

5-2-2 Automatic Extrusions of Thermosetting Materials

The Extreme Experiment 1 was introduced in Chapter 2 briefly and is shown in Figure 2-6. In the concept design period, a material delivery method was proposed in which the fiber impregnation and towpreg deposition were meant to be done automatically and simultaneously. In order to test the designed method, a Deny Extremum Experiment was employed. All parameters and positions were set on the best conditions. If the towpreg could not be extruded out automatically, the design should be abandoned.

The influencing factors were simplified and the experiment was set up, as shown in Figure 2-6A. A segment of fiber tow was placed inside a hypodermic in where it was pilled out along with epoxy resin. The thermosetting resin was used as a matrix because its viscosity would not change too much at room temperature during a short period of time. When the plunger is pushed down, the impregnated towpreg could be squeezed out of the needle connecter. In such a set up, we assume that

a. A seal effect does not need to be considered,

b. Friction does not need to be considered,

c. The viscosity, μ of the polymer is not changed, so the shear stress could be regarded as a constant.

Throughout the present study, Kevlar-49 was used as the reinforcing fiber. There were *12K* filaments in one tow. In this experiment, *1* tow, *2* tows, or *3* tows were jointed together, respectively in *3* separate runs. The result indicated that when *2* tows were combined together, the impregnated Kevlar-49 fiber tow was readily squeezed out of the syringe. The volume fraction V_f could be evaluated as:

$$V_f = \frac{S_f}{S_n} \qquad (5-1)$$

where: S_f = the total cross section area of fibers, and

S_n = the cross-section area of the needle.

The diameter of a Kevlar 49 filament was $9 \mu m$, so

$$S_f = 2 \times 12000 \times \frac{9^2}{4} \pi \times 10^{-6} = 1.53\ (mm)^2$$

The inside diameter of the needle connecter was around *1.8mm*, so,

$$S_n = \frac{1.8^2}{4} \pi = 2.54 \quad (mm)^2$$

$$V_f = \frac{1.53}{2.54} \approx 0.6 = 60\%$$

When *2* tows were used, $V_f = 60\%$ is the best volume fraction for effecting the automatic extrusion. The viscosity μ of the thermoplastic is higher than that of the thermosetting materials, so *50%* volume fraction is chosen for the thermoplastic matrix composite.

For the case of *3* fiber tows, the total diameter of the fibers was larger than the orifice diameter of the syringe and the friction force was too large for the towpreg to be squeezed out.

In the case of using *1* tow of Kevlar-49, the fiber volume fraction was around *30* percent, $V_f = 30\%$. The automatic extrusion process did not work well for this case. One specimen of the extruded towpreg is shown in Figure 5-1. The speed of resin extrusion was not uniform and excess amount of resin was extruded out intermittently.

The conclusion was that the method for impregnation and deposition implemented at the same time is possible in certain situations. But further experiments need to be done to well define these situations.

5-2-3 Automatic Extrusions with Thermoplastic Materials

In the previous experiment, a thermosetting resin was used for the matrix. In the case of using thermoplastic materials, the viscosity μ is $50 \sim 400$ times higher than that of a thermosetting resin [74]. A device for extruding a thermoplastic melt and a continuous fiber tow is shown in Figure 4-7. Because many parameters influence the final result, several experiments had to be done. The result had not been was satisfactory, so a different extremum experiment had to be conducted, explained as follows.

To simplify the attempt to identify identifying influencing factors, the device was re-designed, as shown in Figure 5-2. The regulating rod and regulating head were removed, and a seal screw was used to seal off the hole of the top cover. Then a small shaft, which was entwined with the fiber, was placed in the cylinder. The volume fraction was set

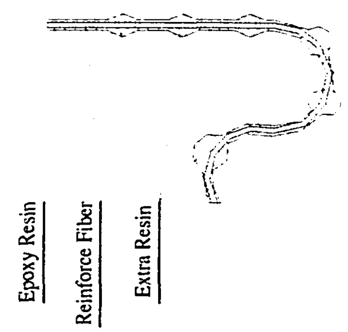

Fig. 5-1 The extrusion speed was not uniform.

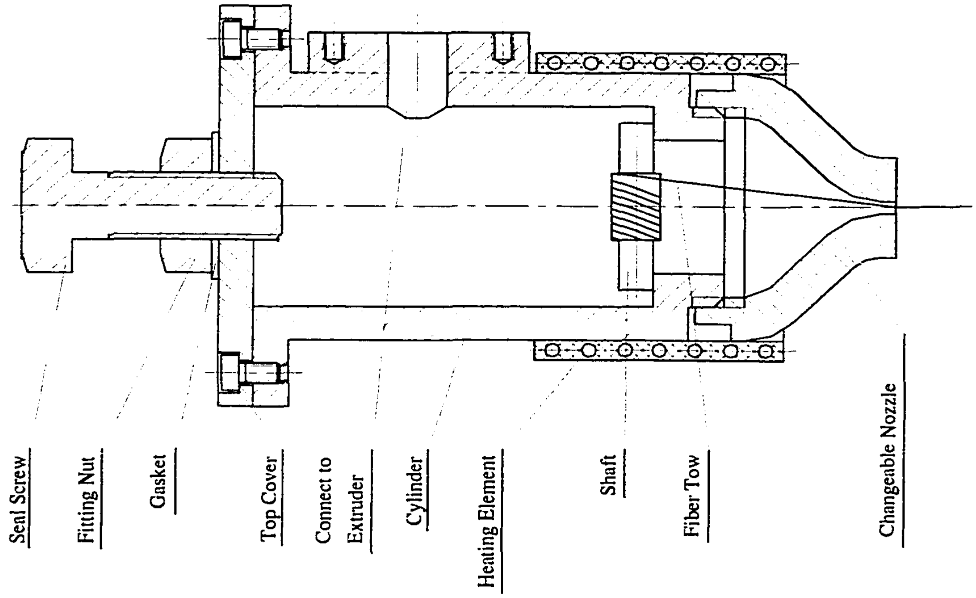

Fig. 5-2 An Extremum experiment.

at *50%* by selecting a proper bore diameter of the nozzle. After that, the device was installed on the extruder machine that supplied the required melted thermoplastic. This configuration was operated to determine if the towpreg could be extruded. The extremum experiment was successful, which means the method was useful provided that proper processing parameters could be found.

In order to find a correct parameters range, an experiment similar to the extremum experiments was carried out, such as indicated in Figure 4-7. To find the best distance between the regulating head and the nozzle, other influencing factors were kept at the same values or positions, which were supposed to be in the right region. Then, the effect of this distance was investigated. Initially, when the distance was not set in a correct position, the melted polymer would climb up through the center hole of the regulating rod to sometimes block the channel for the incoming fiber tow, and the polymer could not be sent back to the cylinder. As a result, the experiment could not be continued. A series of operations had to be carried out before the experiment could be resumed. These included cooling the device, disassembling the regulating rod, cleaning the polymer from the channel, and re-installing the rod, etc. But, if the regulating rod was set at the extremum position before the thermoplastic was extruded in the device, the phenomena of melted polymer climbing up should not happen. If in this situation, the polymer still goes up, the effectiveness of the method could not be proven.

A portion of the device is enlarged and shown in Figure 5-3. Figure 5-3A shows the setting position, with the regulating head being set in the lowest position and the end of the regulating head being at the exit of the nozzle to ensure no melted polymer could enter into the regulating head. But in this position, the impregnating time is very short,

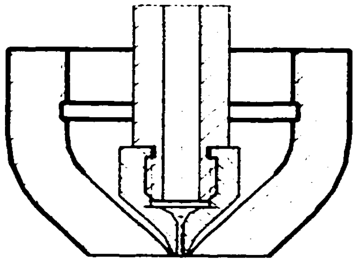

Fig.5-3A The original position.

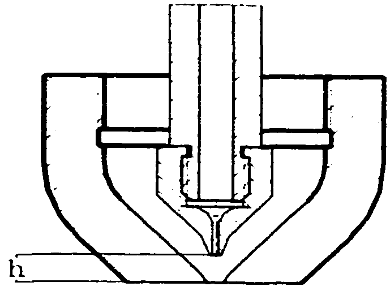

Fig.5-3B The head was ride.

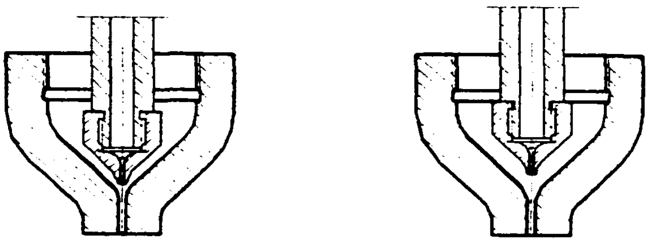

Fig.5-3C The two positions for a long-nozzle with the tapered head.

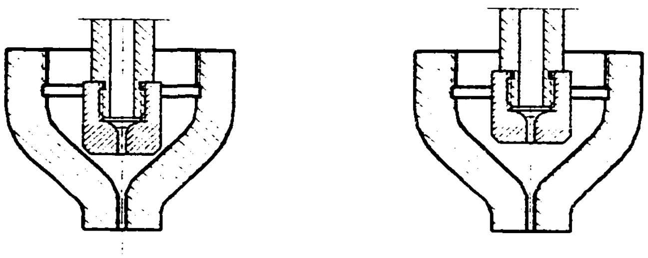

Fig.5-3C The two positions for a long-nozzne with the flat head.

Fig. 5-3 Extremum position experiment.

because when polymer is extruded outside of the nozzle, no shear stress is exists to assist the fiber impregnation. So, the regulating rod was raised to have the regulating head back in the nozzle. During the experiment, the regulating rod was rotated and raised slowly until the fiber was driven down automatically while no polymer went up through the regulating head. The situation is shown in Figure 5-3B. It was observed that, when h = *1~3* mm, the fiber tow was driven out automatically.

§5-3 "PISTON EFFECT" EXPERIMENT

In the FDM process, a wire made of thermoplastic materials is driven by rollers to work as a piston to push the melted materials out of the nozzle to implement the deposition process. Inspired by this FDM concept, in the early stage of development for CLM, a method was proposed that involved a concept design as shown in Figure 2-14. Several devices have been designed for the concept and a series of feasibility experiments have been conducted.

5-3-1 Experimental Set Up

The proposed CLM process, as indicated in Figure 2-13 and Figure 2-14, is a two-step forming method. In the first step, a towpreg that is a composite wire made of continuous fiber, and a thermoplastic are pre-formed. A towpreg forming device is shown in Figure 5-4. In the second process step, the towpreg is deposited onto a work surface just like in the FDM.

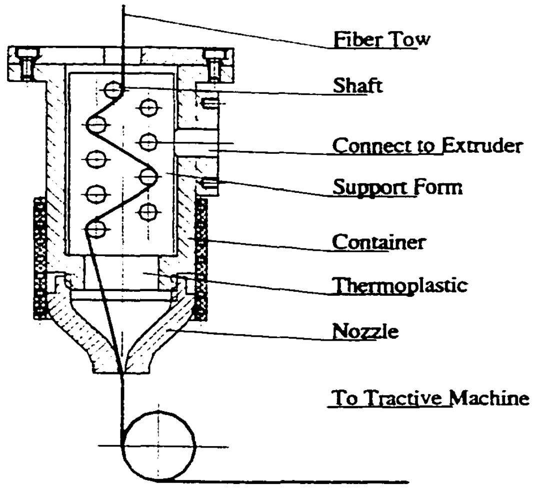

Fig. 5-4 A simple impregnating device.

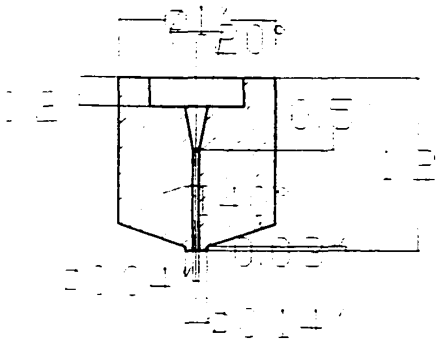

Fig. 5-5A

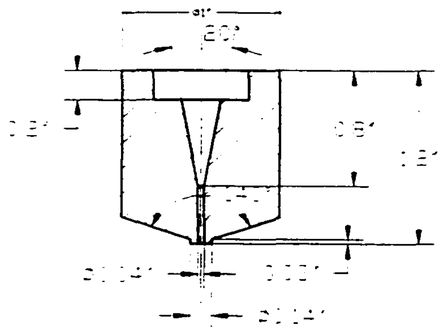

Fig. 5-5B

Fig. 5-5 The nozzles were designed for piston effect.

The 3D motion device, work-platform, heating and cooling device are considered to be similar to those in the FDM. The selection of a towpreg delivery method and the design of an effective nozzle are the key tasks in the development of the CLM process. Two nozzle shapes and dimensions are shown in Figure 5-5. The differences between the two designs are the lengths of the heating zone, entrance shape of the nozzle and the guiding distance for the towpreg.

The diameter of the towpreg is *1mm*; it is a little bit smaller than the orifice of the nozzle in order to ensure the towpreg could be pushed into the nozzle first. It is considered that the towpreg is heated up to above the resin melting point in the nozzle and the solid towpreg in the rear is used like a piston to push the melted towpreg out of the nozzle.

During the experiment, the towpreg was hard to push into the nozzle. What happened was that when the towpreg was forced to enter the nozzle as shown in Figure 5-6. the towpreg was bent or zigzagged to avoid entering the nozzle. The phenomena were analyzed as follows:

1. The diameter of the towpreg was too small so that the rigidity of this materials is not sufficient for it to serve as a piston.

2. At the nozzle entrance, the towpreg was heated and softened and hence it lost its stiffness.

3. The dimension and shape of the towpreg are not uniform and the fiber tow was not well impregnated.

4. The surface finish of the nozzle orifice is too low to allow the towpreg to go through smoothly.

Based on these considerations and experimental results, we believed that an improved design was much needed. Two such designs were layed out as shown in Figure 5-7 and Figure 5-8. These two designs were developed based on the following considerations:

1. A cooling sleeve may be used to keep the entrance at room temperature or lower.

2. The exit diameter of the nozzle is half of the entrance diameter. If the exit diameter is *1 mm*, a towpreg of *2 mm* diameter could be used.

3. In the FDM process, the entrance is three times larger than the exit diameter. The larger entrance ensures that the thick wire can be used as a piston, and a small exit is to ensure the precision of the deposited object. But, there are fibers inside a towpreg, and the fiber dimension could not be reduced. Because the towpreg is melted in the melting zone, segment by segment, and is supplied segment by segment, a branched-out orifice could be use to drain out the extra matrix materials.

4. Detailed designs of towpreg dispensing nozzles are shown in Figure 5-8. In order to evaluate the influence of shape and dimension, 12 different nozzles have been designed. The dimensions are shown in Table 5-1 and 5-2 (see Appendix B).

5. The fiber impregnation device was redesigned in order to make the towpreg uniform.

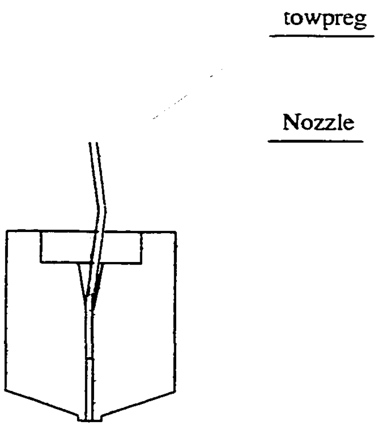

Fig. 5-6A The towpreg was bent.

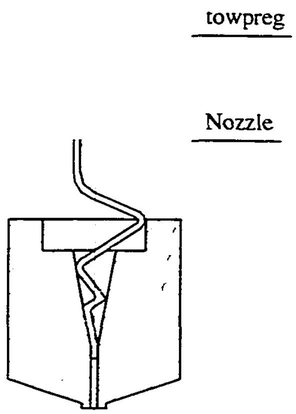

Fig. 5-6B The towpreg zigzagged.

Fig. 5-6 The towpreg can not be pushed into the nozzle properly.

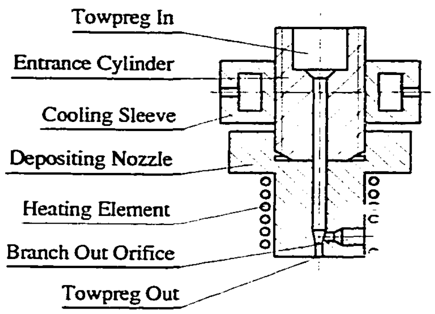

Fig. 5-7A The nozzle core was separated.

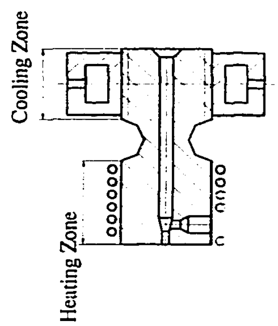

Fig. 5-7B The nozzle core has a groove.

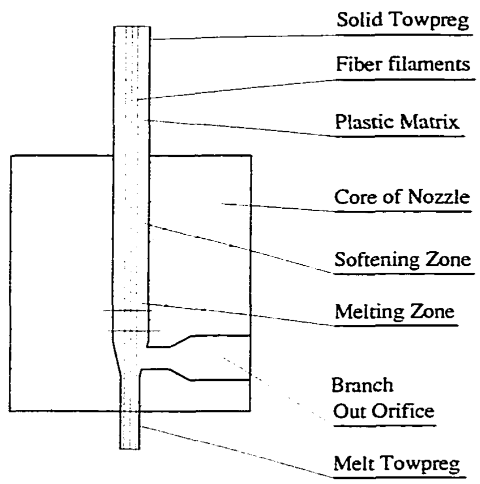

Figure 5-7C A divided exit for extra polymer.

Fig. 5-7 The nozzles designed for the "piston effect".

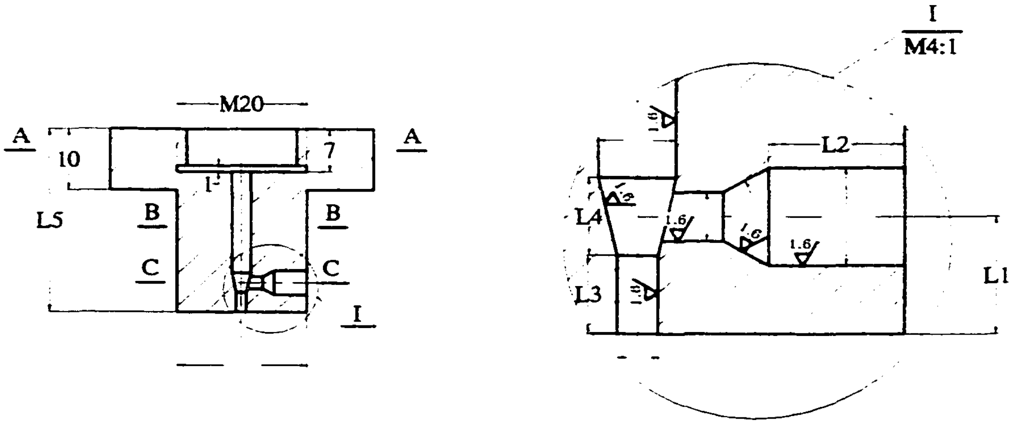

Fig.5-8A.

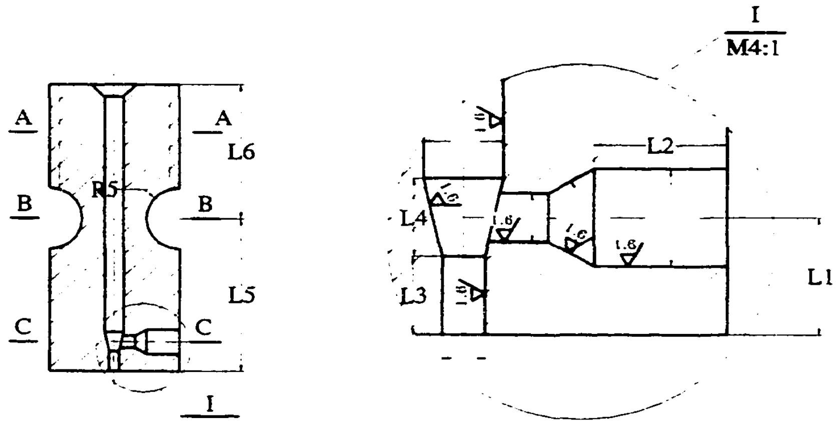

Fig.5-8B.

Fig. 5-8 Detailed Designs of the deposition nozzle shown in Fig. 5-7.

5-3-2 Results and Discussions

After conducting a series of experiments with these nozzles, we obtained the following results:

1. The towpreg could be melted within the nozzle when the towpreg was carried into the nozzle through a distance.

2. The cooling sleeve cooled the entrance of the nozzle, so the towpreg was delivered through the entrance with enough rigidity.

3. The towpreg was supposed to branch out near the exit of the nozzle; but did not.

These results indicate that a challenge still exists in the case where a solid towpreg is used to provide the piston effect to push the melted towpreg out of the nozzle. Other parameters and shapes could be improved to achieve successful results.

1. The fiber volume fraction of the towpreg could be made smaller. If the diameter ratio of the nozzle entrance to exit is *3:1*, and the fiber volume fraction of the towpreg in the exit of the nozzle is intended to be *50%,* at entrance, the fiber volume fraction at the entrance could not be in excess of *5.5% (1/18)*.

2. The temperature of the nozzle could be raised to decrease the needed heating distance in which the towpreg is touched with the nozzle. The smooth surface finish of the bores of the nozzle could be improved to decrease friction.

3. For a large structure or part, the towpreg could be slightly larger, but still keeping a reasonable precision. In this case, the nozzle exit diameter

could be made as large as the entrance, and the shape of the nozzle could be made very simple. The effect of the nozzle is only for heating up and guiding the towpreg to a certain location. Then, the diameter of the towpreg does not have to be reduced and the towpreg could be pushed straight through the nozzle.

§5-4 "AUTOMATIC EXTRUSION" EXPERIMENT

In Chapter 2, an Active Materials Supply method was introduced. See Figure 2-20 and Figure 4-7. The advantages of the one-step method have been analyzed in Chapter 2 and feasibility testing has been done successfully as discussed in §5-2. In order to find the best forming parameters, a numeric simulation procedure has been used to imitate the process of the one-step method with the results being analyzed in §4-3. To validate the method and to find the best range for the important parameters, a device that simulates a real system was set up and investigated.

5-4-1 Experimental Set Up

The experimental set-up was shown in Figure 2-20. The 3D motion device was not installed because the experiment was for testing the concept of automatic push-out in order to integrate the two processes, impregnating and depositing, into one step.

1. Pressure Control: The vessel pressure value is considered as an important parameter for this method, because the flow shape of the melted polymer fluid is influenced by the pressure directly. The extruder used in the

present study was a Killion extrusion machine (*Series Number 10881*), the pressure was regulated by controlling the volume of the extruding material. A fine-tuning resistor is used to control the volume. Actually the pressure value depends on the load also. A digital pressure meter is installed on the connector between the extruder and the impregnating and forming device. The displayed number approximately reflects the pressure value inside the device. At a stable fluid flow, a value of *150 Psi ~ 250 Psi* was shown on the display screen.

2. Temperature Setting: Temperature is also considered as an important parameter, because the viscosity μ of the polymer fluid depends on temperature. The effect of viscosity is complicated for a non-Newtonian fluid. For shear thin plastic materials, its viscosity is influenced by the shear stress also. Viscosity has two effects on the movement of a towpreg in this method. If the viscosity increases, the shear stress near the exit of the nozzle could also increase. That is an advantage for pushing automatically towpreg out. But if the viscosity μ is increased too much, the fiber could not be impregnated very well or could not be impregnated during a short period.

The above considerations led us to set the temperature at a certain value, which did not change during the experiment. A temperature of was selected *360°F* for the extrusion machine, and the temperature setting for the device was *370° F*.

3. The distance h between the regulating head and the nozzle: the distance could change continually (See Figure 5-4). Determination of the distance h was one of the targets for the experiment and it was set at three different values to evaluate its effect.

4. Shapes and dimension of the nozzle: The shape of the nozzle was not varied by much. But the ratio between the diameter and depth of the nozzle orifice was considered an important parameter because the stress distribution depends on the ratio:

$$R = \frac{D_n}{L_n} \qquad (5-2)$$

where: D_n = diameter of the nozzle and

L_n = depth of the nozzle.

In the experiment, R was set at eight different values, respectively.

5. The shape and dimension for the regulating head: Two different head shapes were designed in order to determine a preferred shape. The two designs are shown in Figure 5-9 and 5-10.

6. The fiber volume fraction: Each Kevlar fiber tow has *12,000* filaments and could not be separated, but several tows could be combined together. In the experiment, *1, 2, 3,* and *6* tows have been employed in *4* separate runs. The cross sectional area for each tow is around $1.53\ mm^2$. The volume fraction is determined with the number of fiber tows and the orifice diameter of the nozzle.

5-4-2 Results and Discussion

This experiment had many different effects. If each and every combination of items *3 - 6* above is evaluated, there would be $128\ (4 \times 4 \times 4 \times 2)$ different experiments that must be done, and it could take a long time. Instead, only representative combinations have been studied, which led to several significant findings or observations.

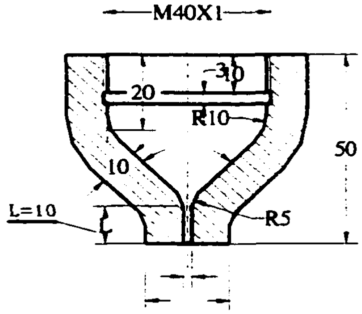

Fig.5-9A The long nozzle.

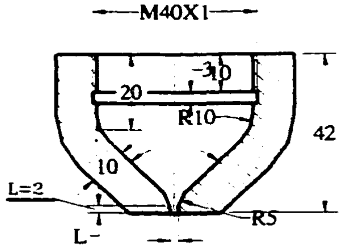

Fig.5-9B The short nozzle.

Fig. 5-9 The dimensions of the long and short nozzle.

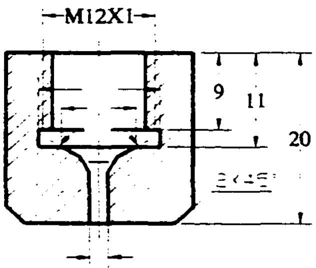

Fig. 5-10A The flat head.

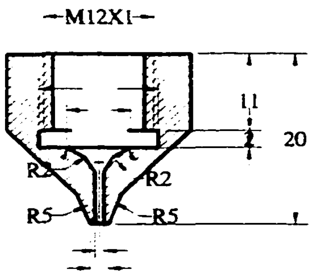

Fig. 5-10B The apex tapered head.

Fig. 5-10 The dimensions of the regulating heads.

The conditions for these experiments are listed in Table 5-3 (see Appendix C) and key observations shown are as follows:

1. The proposition that the towpreg could be delivered automatically was achieved under certain situations.

2. Some positions and parameters are not critical; a stable fluid flow could be established under a wide window of parameter values. For example, the distance between the regulating head and the nozzle was discussed before; actually the head was initially set outside of the nozzle, as shown in Figure 5-10. In this position, the fiber was readily guided through the device and it was ensured that the melted polymer would not go up into the regulating rod. When the regulating head is raised slowly, the melted polymer should be squeezed out by the vessel pressure. At the beginning, a gap between the head and the nozzle was small, so not much polymer was extruded out, and there was not enough force to push the towpreg out of the nozzle just yet. But, when the head was raised, the gap was larger and the volume of polymer flow was also larger. When the distance reached a certain value h, the polymer flow had enough shear stress to drive the towpreg out. Depending on the different ratio R, the distance h could be varied over a wide range. Some times, even when the head was still outside of the nozzle, the towpreg was driven to start moving.

3. The established stable flow: Once a stable flow is established, even if some conditions are later changed, the flow remains stable.

For example, when the head was raised to a distance h, say $h = 3mm$, the towpreg was driven downward. During this situation, if the head is raised up by additional *3~5 mm* more, no polymer is going up through the regulating rod. In another direction, if the head is lowered down by *1~2 mm* more, the towpreg was still driven downward by the polymer flow.

But, if the head was set at the same stable position $h = 3mm$, before the polymer was extruded, then even after the polymer was extruded, with the pressure slowly getting larger, the towpreg was not driven down and some polymer was going up through the regulating rod.

4. The ratio *R*: The ratio *R* between the diameter and the depth of the nozzle orifice was an important parameter. For the polymer fluid flow, the larger *R* is the more stable the flow is. But if *R* is smaller than a certain value, say $R<0.5$, a stable flow state is never reached.

5. The minimum diameter of the nozzle: In this experiment, the nozzle bore diameter ϕ was selected at $\phi = 4mm$, $\phi = 2.5mm$, $\phi = 2$, and $\phi = 1mm$, respectively. If $\phi > 2mm$, with the different depth of the nozzle and the ratio *R* not smaller than *0.5*, a stable flow is observed.

6. The fiber volume fraction: The fiber volume fraction did not influence the stable flow too much. But, in general, when the fiber volume fraction is larger the flow is more stable.

7. The regulating head: the shape of the regulating head did not have a significant effect on the stable flow. A flat head shown in Figure 5-10A could not be set outside of the nozzle. If the flat head was set at the lowest position in the beginning, the bottom edge of the flat head was touched the nozzle inside surface to

be service as the function of a seal, the polymer did not goes up. Then a similar operation that like conducted in the apex tapered head could establish a stable flow.

5-4-3 Design Features and Further Improvements

The "two in one" method (impregnation and deposition being integrated in one process step) was demonstrated by the experiments as a viable method. Compared with the "two in two" method (impregnation and deposition being conducted in sequence), the features of the "two in one" method are summarized as follows:

1. Advantages:
    a. The process is simple, and the time and cost will be saved.
    b. It is an Active Materials Supply method. The forming condition of the current layer being deposited is not influenced by the quality of a previous layer.
    c. The deposition speed is higher.
    d. The towpreg diameter is equal to the diameter of the nozzle bore. When the depositing toolpath turns at an angle or follows an arc, the errors analyzed in §3-3 and §3-4 could be neglected.
2. Disadvantages:
    a. A pressure is requires to drives the towpreg out of a vessel, but the pressure is hard to control, especially at the beginning of the forming process.

b. The bore or orifice diameter of the nozzle could not be too small and the deposited towpreg is somewhat thick. As a result, the part precision could not be high.

3. Improvement:

a. Redesign the "two in one" devices. The volume of the cylinder could be reduced, and a flow balance should be maintained; i.e., the polymer-entering rate equals to the polymer-exiting rate. The cylinder, the shape of the regulating rod, and other parts could be optimized to let the polymer flow more fluently and to let no extra polymer cumulate inside the cylinder.

b. The operating parameters of the extruder machine could be improved. The volume flow rate could be smaller and steadier.

c. One should select different matrix materials to impregnate Kevlar quickly and completely during a short period of time.

At the end of this section, another design will be introduced, which is supposed to improve the stability of the "two in one" method. A concept design is depicted in Figure 5-11. The melted polymer is supplied into a container by an extruder machine, which is used for shear thinning the viscosity μ. The container is divided into a top region and a bottom region by an annular seal that is made of rubber or some material that could not damage the fiber. In the top region, the pressure is higher than the atmospheric pressure. In the bottom region, there is a circulating pressure region. An annular Pulse Air Bag could be blown up or shrunk down by a circular pressure source to induce a circular pressure in the container. The annular seal could be controlled to open and close just like

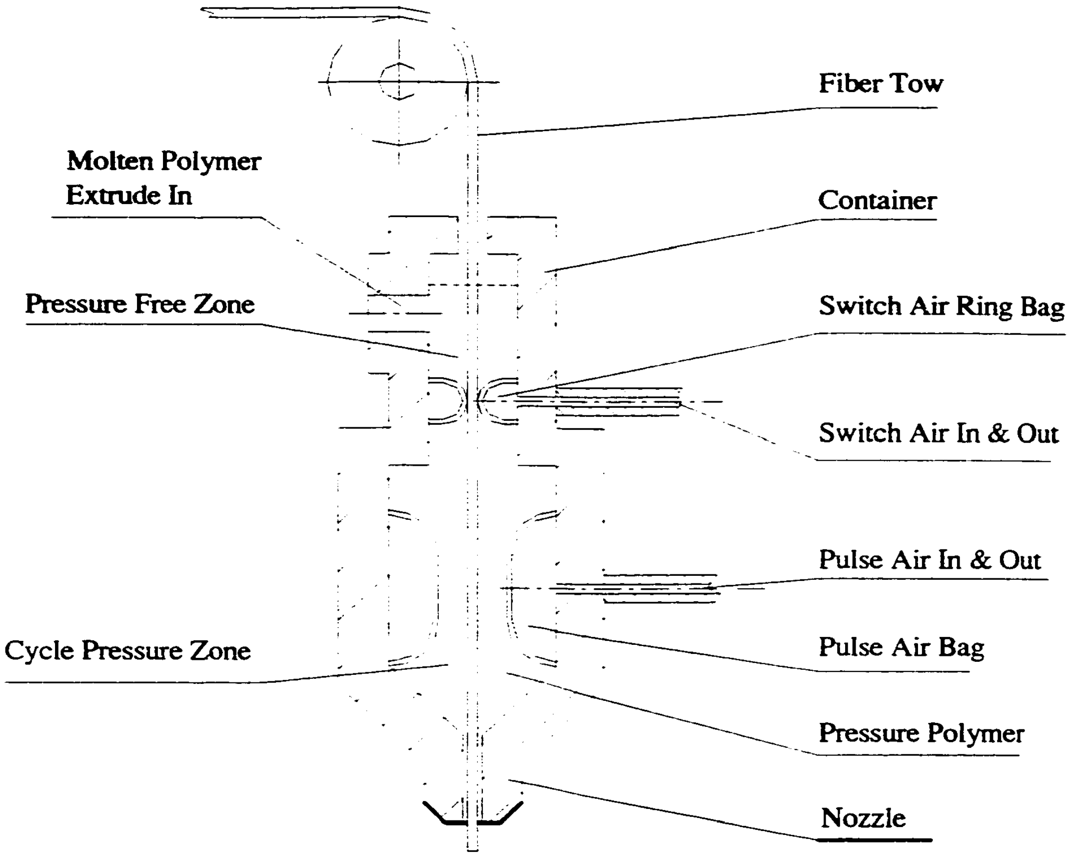

Fig.5-11 A proposed pulsating air method.

a door could be opened and closed. When the door is open and the Pulse Bag shrinks, a negative pressure is induced in the circular pressure region. Then the fiber tow and matrix materials, which are in the pressure free region, could be drawn into the circulating pressure region. When the door is closed and the Pulse Bag is blown up, a positive pressure is induced in the bottom region. The fiber is gripped and the polymer in the bottom region could not go up but could go out of a nozzle due to the positive pressure.

If the frequency of the circulating pressure is *100~ 200* times per second, the continuous towpreg will be delivered smoothly. Actually, other means could be employed to get the same function.

§5-5 SYSTEM DEVELOPMENT OF THE CLM WITH SELF-ANCHORING

The concept of self-anchoring was introduced in §2-5. Potential of this method capability were analyzed in §3-2 ~ §3-4, and the forming mechanism was studied in §4-2. A system for this forming method has been developed, and various simple parts and structures have been produced with this system.

This is a two-step method with thermoplastic materials: a towpreg making system was used to form the towpreg, a semi-finished composite product. Then, another machine system was used for deposition process.

5-5-1 The Towpreg Making System

The towpreg forming system is schematically shown in Figure 5-12. Four main units were lined up from right to left. An impregnating die fixed on the extruder machine was the first unit. A cooling water trough and a position trimmer constituted the second unit. A drawing machine and the winding machine were the third and fourth unit, respectively.

A towpreg made with the unsophisticated device mentioned before (See Figure 5-4) had many defects:

1. The geometric defects:
    a. The diameter of the towpreg was not uniform.
    b. Defects of creases, tumors, and ripples were induced sometimes because the extruder-supplied pressure fluctuated, and the impregnating device was designed roughly.
2. Impregnation defects:
    a. The fiber tow was not fully impregnated with the matrix in some sections because the viscosity μ was too high. The affinity between the fiber and the matrix was low.
    b. The fiber was not uniformly soaked.
3. Eccentric defect: The fiber tow filaments were not well dispersed in the matrix, even in segments where the fiber was soaked completely. This defect happens especially when the fiber volume fraction is lower. The filaments were not located at the center of the towpreg, as shown in Figure 5-13. The eccentric defect shown in Figure 5-13A has the characteristic that the impregnated filaments were pulled to one side of towpreg and,

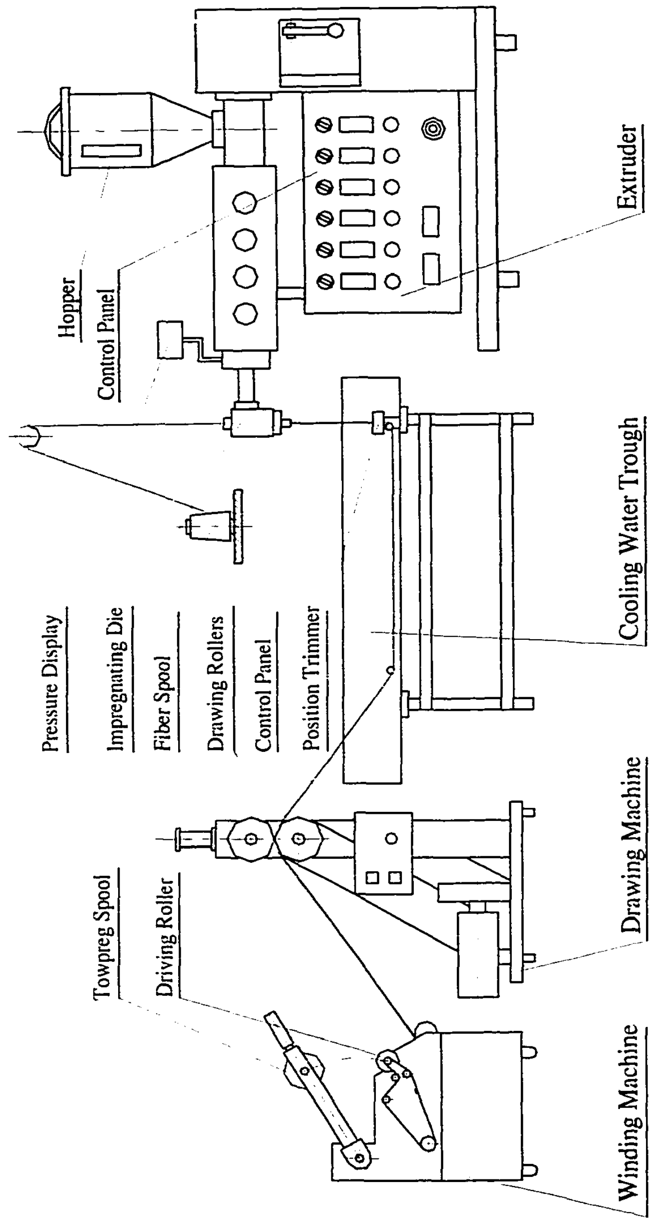

Fig.5-12 The towpreg forming system.

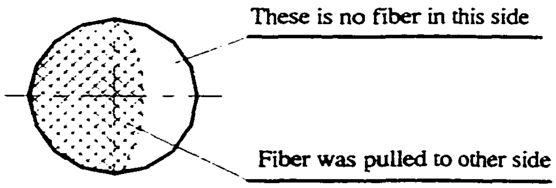

Fig. 5-13A A cross-section of the towpreg.

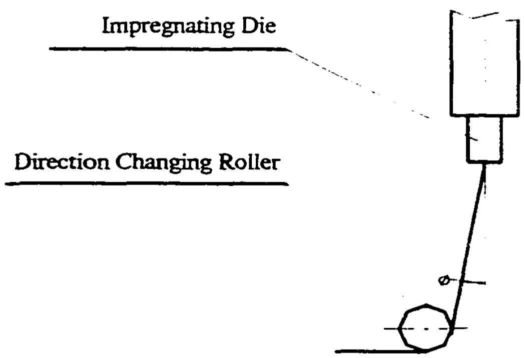

Fig. 5-13B The device was alignment properly.

Fig.5-14 An analysis diagram of the towpreg eccentric.

in another side, there was no filament.

A cause for the defect was that an angle ϕ existed between the impregnating die and the drawing device. The angle ϕ is shown in Figure 5-13B. In order to eliminate the angle ϕ, a position trimmer was designed, fabricated, and installed to align the towpreg line with the central axis of the impregnating die. The position trimmer is shown in Figure 5-14. Where the position trimmer is located in the whole impregnation system can be found in the Figure 5-12. The trimmer was fixed in the water trough first, and its position was roughly adjusted. Next, the core was aligned with the impregnating die by meticulously turning the three core-adjusting pins in order to ensure the towpreg be pulled concentrically with the impregnating die.

The device in the system was the impregnating die, which is shown in Figure 5-15. The die was designed and built based on the experience and knowledge acquired from previous experiments on polymer fluid flows. The design principle and the required calculations for the impregnating die are too complicated to be described in a short paragraph [75,76].

The main parts, which are the guider tip, and the cores of forming die, were designed into different dimensions and shapes so that the effects of shape and dimension could be readily accommodated. With this system, towpreg samples with a dimension range from *0.8 mm* to *2 mm* have been successfully formed with different forming dies. The linear forming speed was from *20* to *50* meter per minute (*20m/min. ~ 50m/min*).

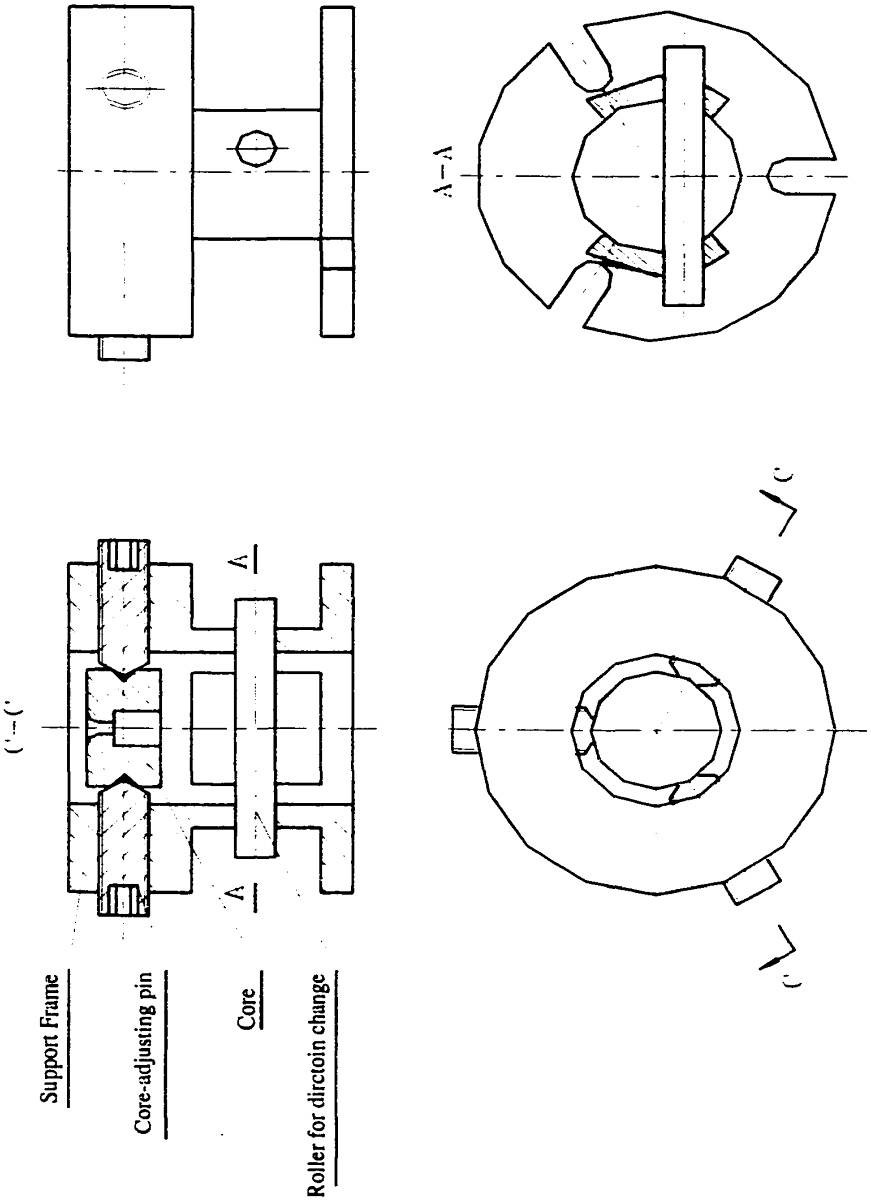

Fig. 5-14 The towpreg alignment device.

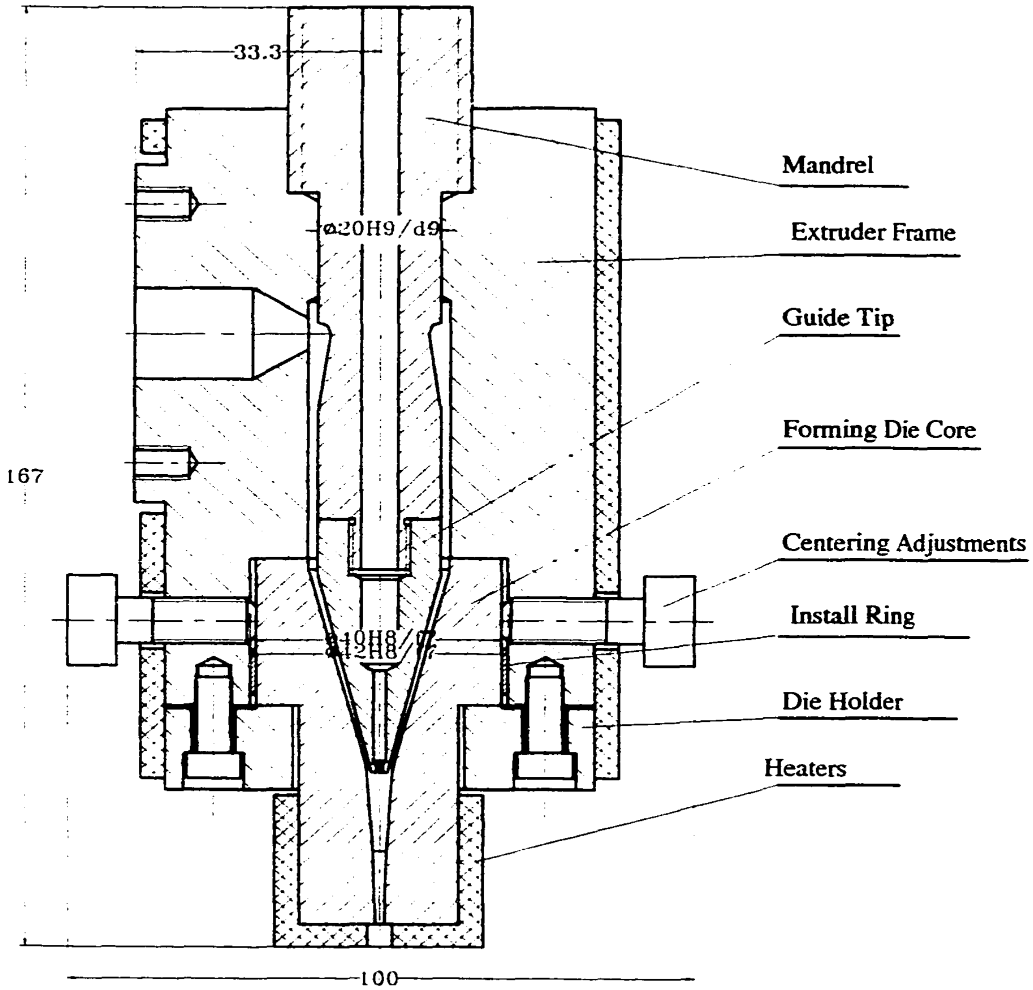

Fig. 5-15 The towpreg forming die assembly.

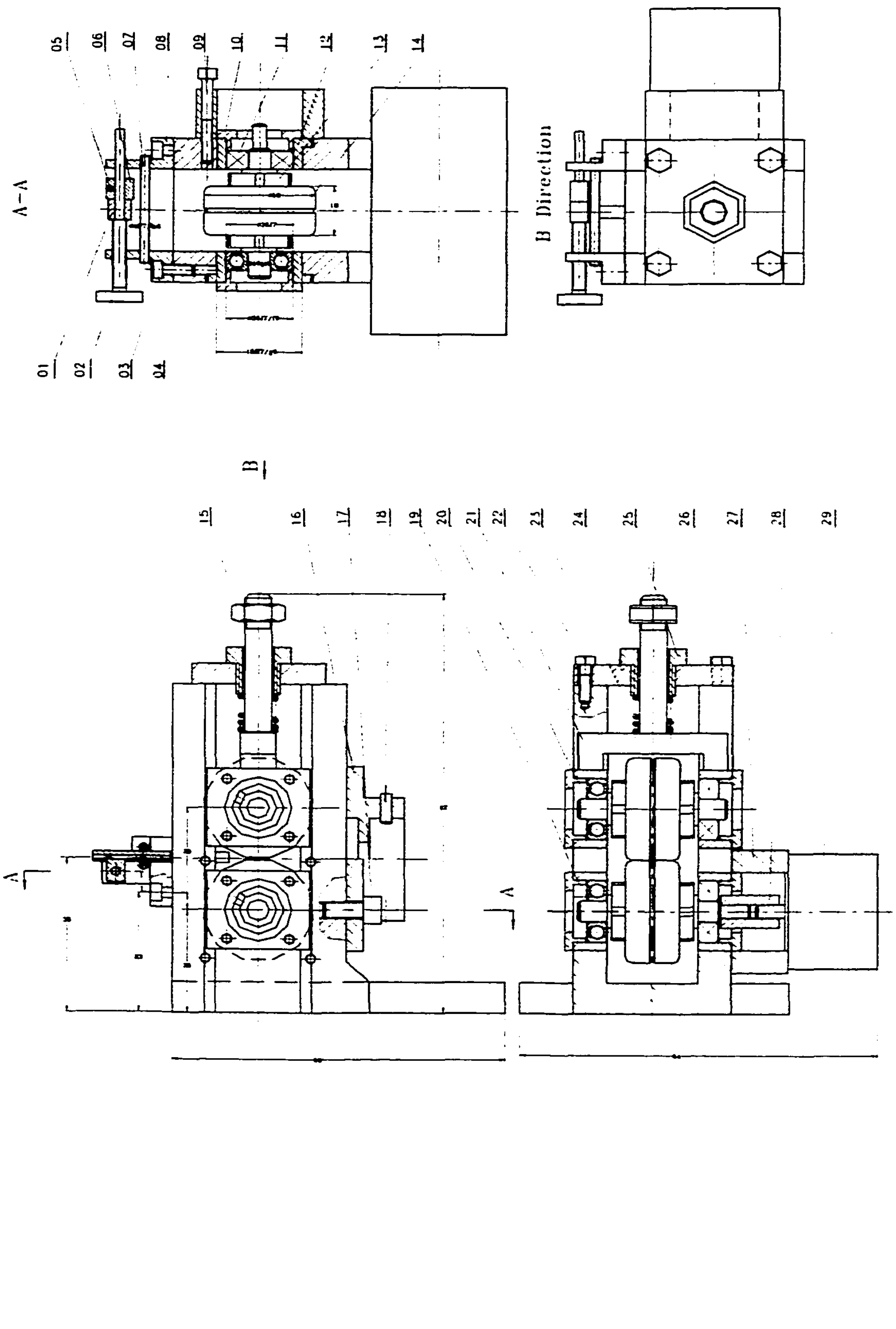

Fig. 5-16 The towpreg deposition device.

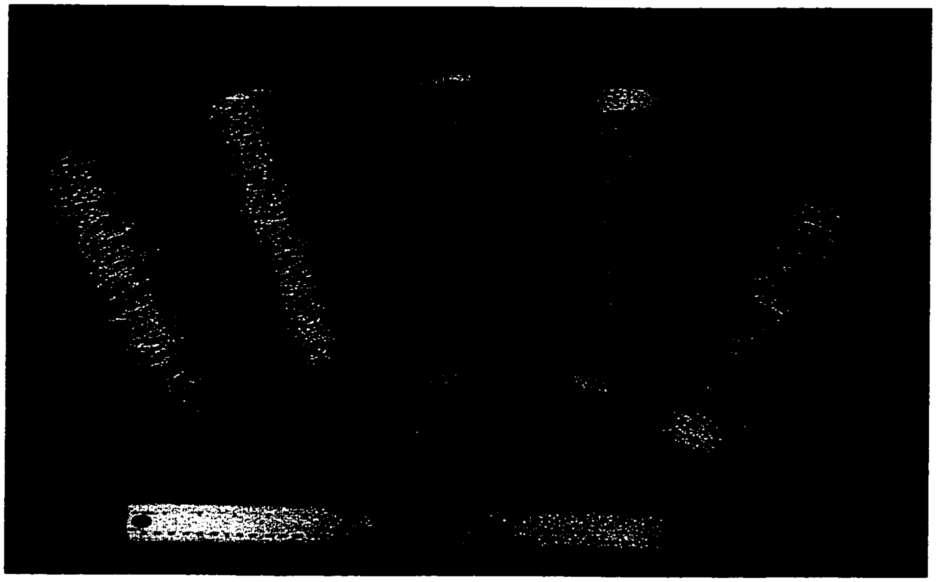

Picture 5-1 Formed towpregs.

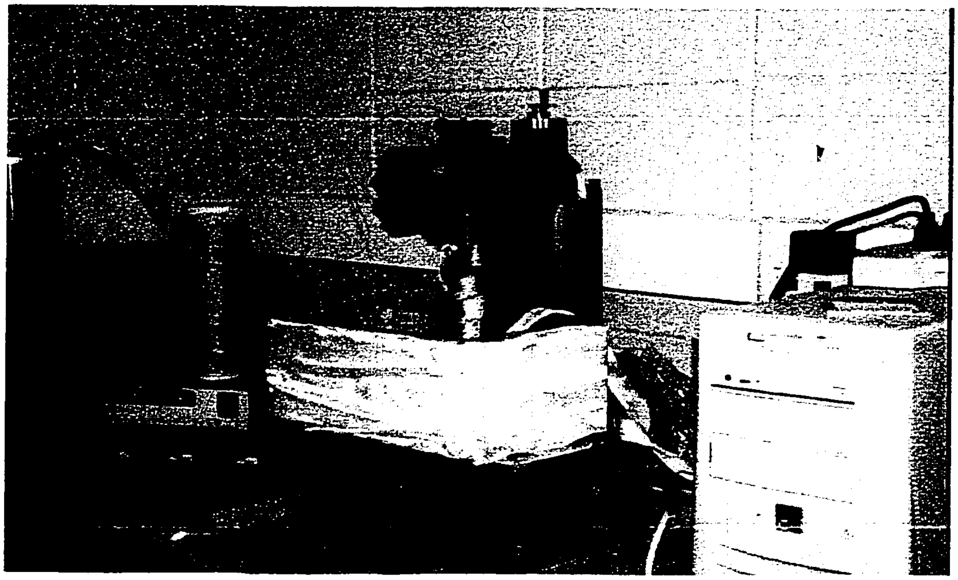

Picture 5-2 One of the CLM system.

Picture 5-3 Parts made by the CLM system.

Picture 5-1 shows the towpreg produced by this system. The towpreg was found to satisfactorily meet the subsequent deposition requirements.

5-5-2 Depositing Systems

A depositing system is shown in Picture 5-2. The deposition former, a main unit of the system, is shown in Figure 5-16. The list of parts table is given in Appendix D. The structures produced by this system are shown in Picture 5-3.

§5-6 EVALUATION OF MECHANICAL PROPERTIES

The mechanical properties of selected parts produced by the CLM method were measured and compared with those of corresponding parts produced by a traditional composite fabrication method, compression-molding.

5-6-1 Three Point Bending Test

To measure the elastic modulus of a composite material, on may choose to conduct the three-point bending test as recommended by ASTM. The test was done with a universal testing machine. The three-point bending set up is shown in Figure 5-17. Delamination strength is a very important index for a part or structure that is made of a composite material. So, the delamination strength was tested with a three-point bending mode. This test is also referred to as a "transverse bending" method.

5-6-2 Specimens from the CLM

A structure like a box formed by the CLM process is shown in Figure 5-18. The structure was built line by line and layer by layer with the self-anchoring method. The towpreg was deposited continuously, so each layer of this structure was unidirectional. The specimen was cut off from the structure. Where these specimens were cut from and the orientations of the specimens are shown in Figure 5-18B and 5-18C.

5-6-3 The Specimens from Compression-Molding (Hot Press)

In order to evaluate the mechanical properties of a part made from the CLM, a baseline structure should be made with a common composite method. The flow chart for this process is pictured in Figure 5-19. In this forming process, a slab was made from the same fiber and matrix, which was used in CLM, and a fiber volume fraction was almost maintained at the same percentage. Shown in Figure 5-22 A, B and C, this process is called FWPM (Filaments Winding and Press Molding). This process begins with the formation of laminar layers or " prepregs" by a filament winding type procedure, which is followed by prepreg cutting and lay-up.

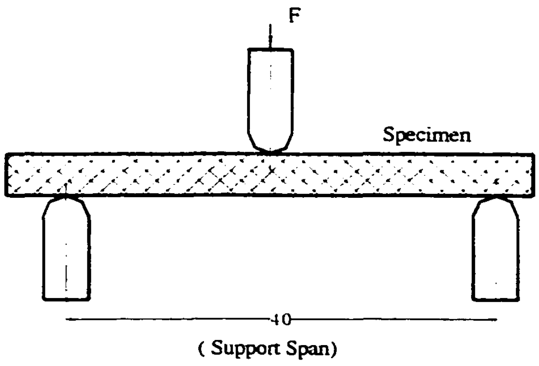

Fig 5-17A Three Point Bending.

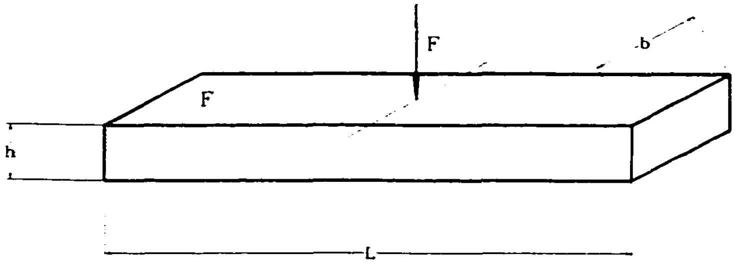

For flexural modulus and strength:

L=60 mm

h=6 mm

b=10 mm

For delamination testing:

L=50 mm

h=10 mm

b=12 mm

Fig 5-17B Specimen dimension.

Fig 5-17 The three point bending set up.

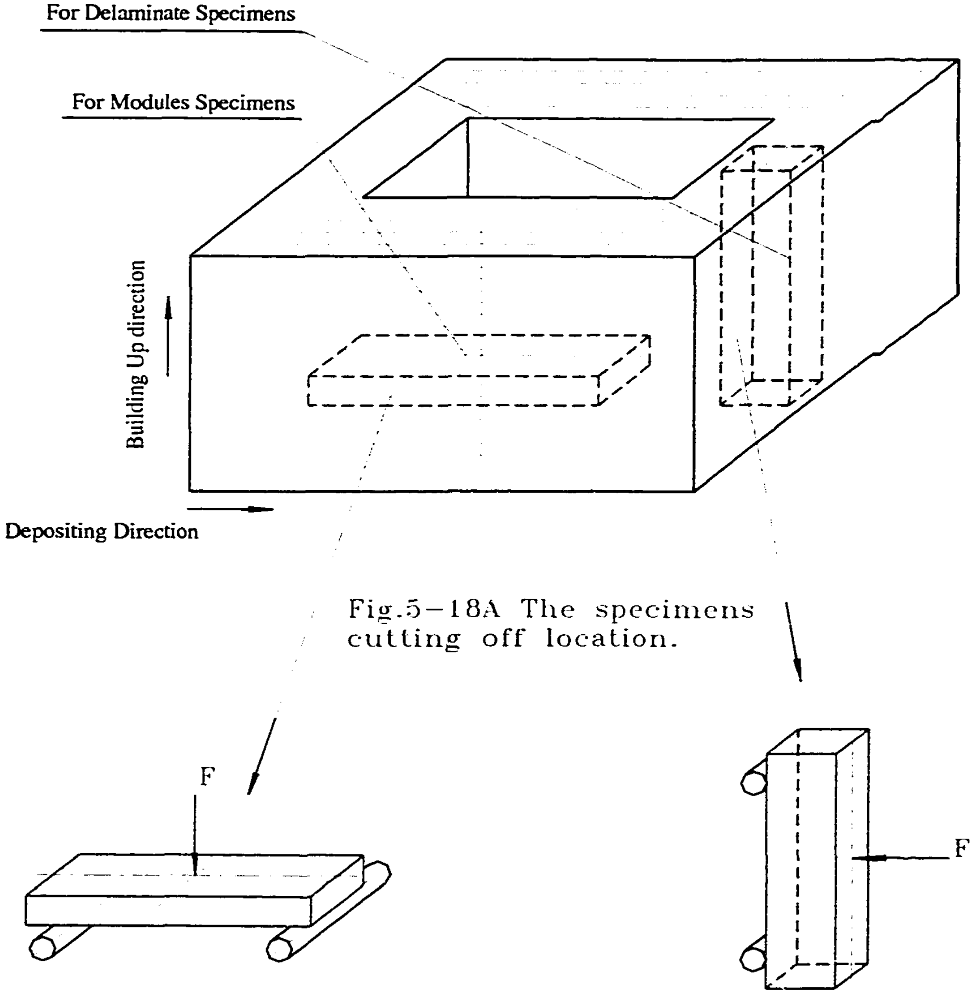

Fig.5−18A The specimens cutting off location.

Fig.5-18B Modules test.

Fig.5-18C Delamination test.

Fig.5-18 The orientations of the specimens

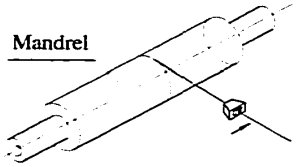

Fig.5-19A Laminar layers made by Filament Winding.

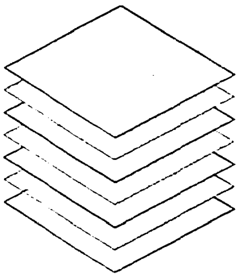

Fig.5-19B Layer-up with unidirection.

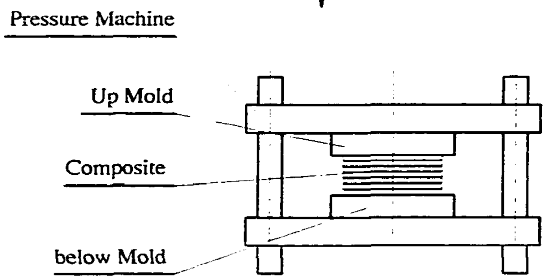

Fig.5-19C The hot press.

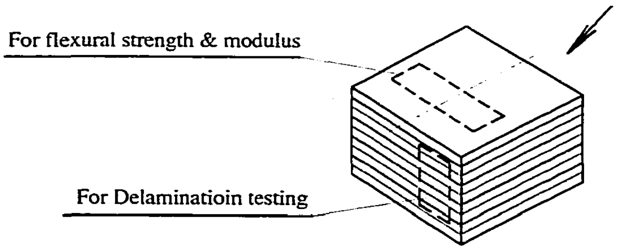

Fig.5-19D Specimen cut off.

Fig.5-19 The Specimen made by compression molding.

The laid-up prepreg assembly, placed in a mold, was then heated to a temperature above the melting point of the thermoplastic matrix, compressed under a pressure, and then allowed to solidify to form a slab. Then, specimens with proper fiber orientations and rectangular dimensions were cut off this slab.

5-6-4 Three-Point Bending Test for Flexural Strength and Modulus

Flexural properties and delamination strength of both CLM and FWPM samples were measured by using the three-point bending and transverse bending test, respectively. Five specimens were tested for each sample to get an average value.

The calculations for elastic modulus and flexural strength are given by Equation 5-2A and 5-2B:

$$E_B = \frac{\sigma}{\varepsilon} = \frac{W^3 F}{4\, d\, b\, h^3} = \frac{W^3}{4\, b\, h^3}\left(\frac{F}{d}\right) = \frac{W^3}{4\, b\, h^3}(m) \qquad (5\text{–}2A)$$

$$\sigma_{fl} = \frac{3\, W\, F_{max}}{2\, b\, h^2} \qquad (5\text{–}2B)$$

where: E_B = modulus of elasticity in bending, P_a,

m = slop of the load-deflection curve,

W = support span,

b = width of beam,

h = depth of beam,

d = deflection of the beam,

F = Force, N.

A record of the 3-point bending test is shown in Figure 5-20. According to the strain-stress curves, the modulus can be solved by Equation 5-2. As shown in Figure 5-20A and 5-20B, five specimens were tested for each of the CLM and FWPM samples, respectively. The modulus was an average value of the five specimens.

According to the data and a simple calculation, the modulus is:

For CLM: $E_{CLM} = (E_2 + E_3 + E_4 + E_5 + E_6)/5$

$= (1594.3+1151+1460+1815+1675)/5=1539$ MPa

For FWPM: $E_{FWPM} = (E_7 + E_8 + E_9 + E_{10} + E_{11})/5$

$= (1611+1276+1506+1171+1130)/5=1249$ MPa

Where E_{CLM} = modulus for the CLM sample,

E_{FWPM} = modulus for the FWPM sample,

E_2, E_3, ⋯⋯ modulus for each specimen.

This result could be normalized with respect to the fiber volume fraction. The modulus of a composite is a function of the fiber volume fraction:

$$Ec = E_f \times V_f + E_m \times (1 - V_f) \quad (5\text{–}3)$$

where Ec = modulus of composite

E_f = modulus of fiber, for Kevlar–49, 125GPa,

E_m = modulus of matrix, the range being around 1~6 GPa for most thermoplastic materials,

V_f = fiber volume fraction.

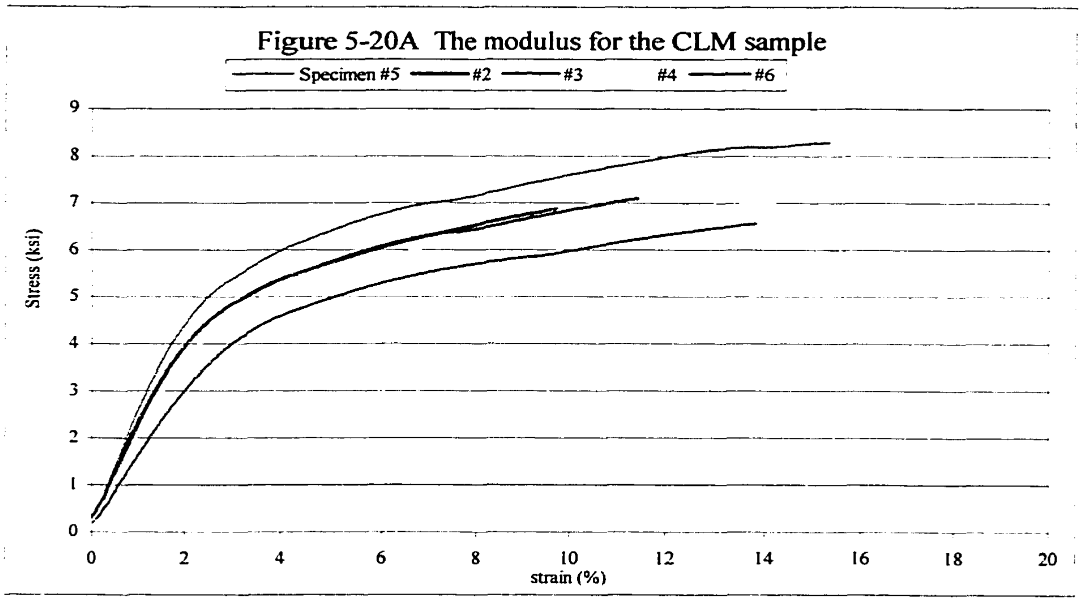

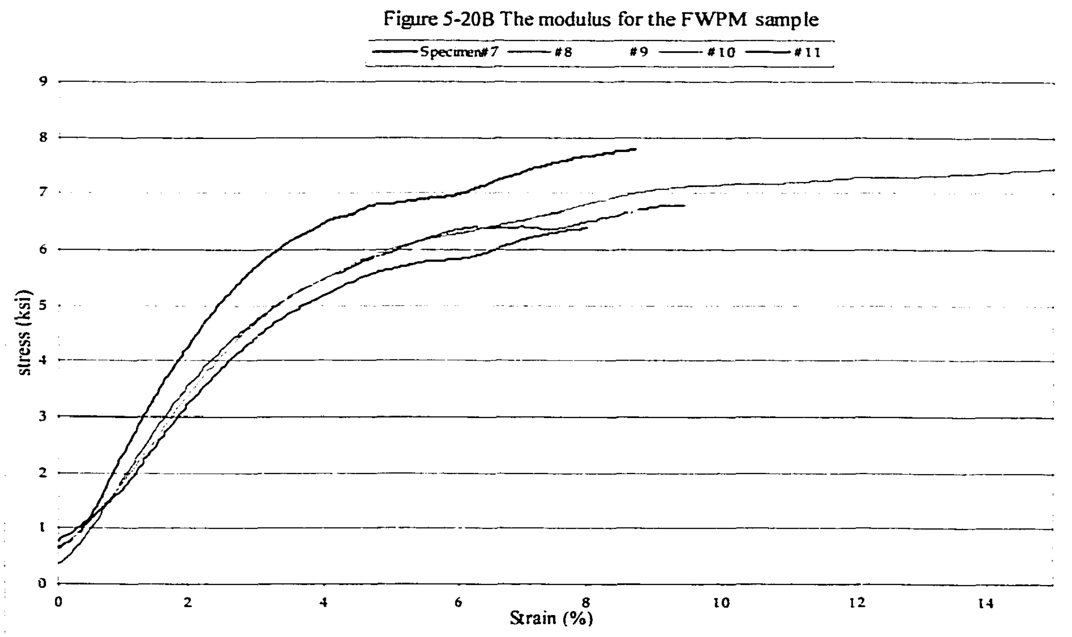

Figure 5-20 Flexural test results.

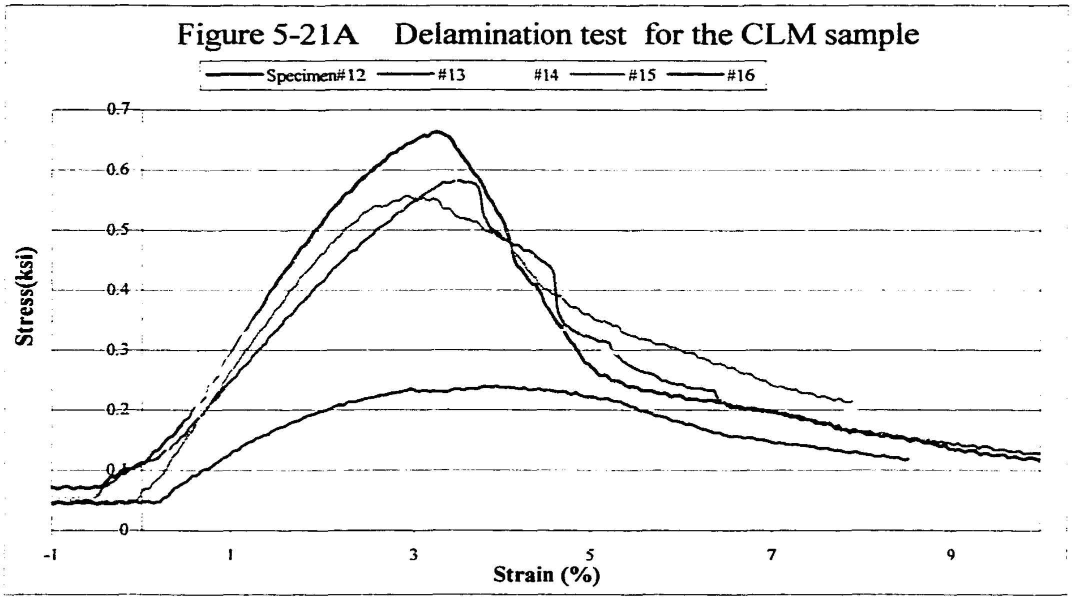

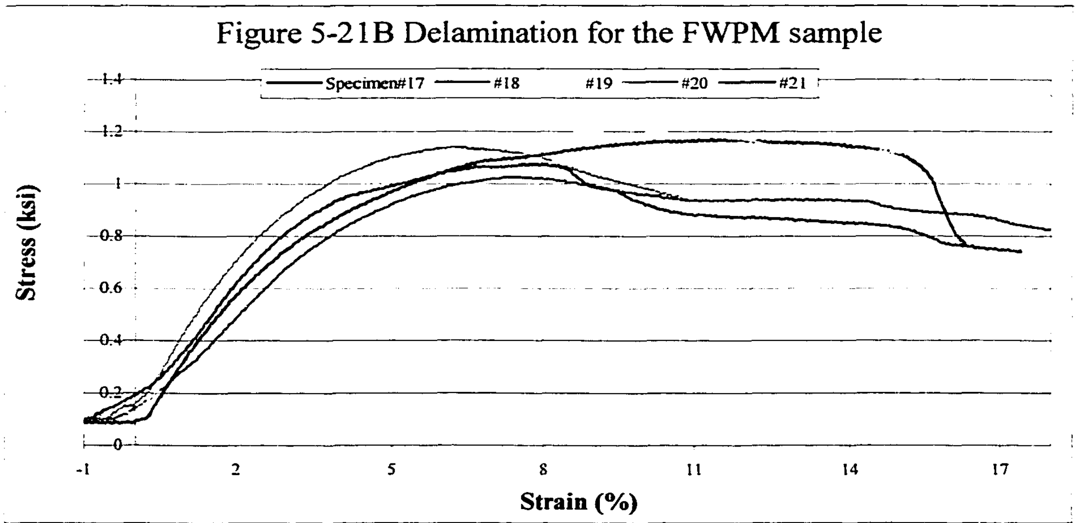

Figure 5-21 Delamination test results.

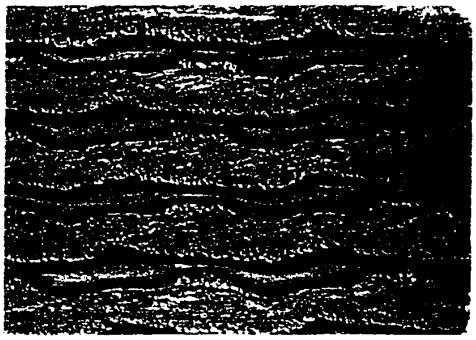

Picture 5-4 A CLM sample, *40X*
"fiber phase" was *65%* .

Picture 5-4 B FWPM sample *40X*
"fiber phase" was *78%*.

Picture 5-4 C CLM sample *400X*
Inside the "fiber phase", the fiber was *94%*.

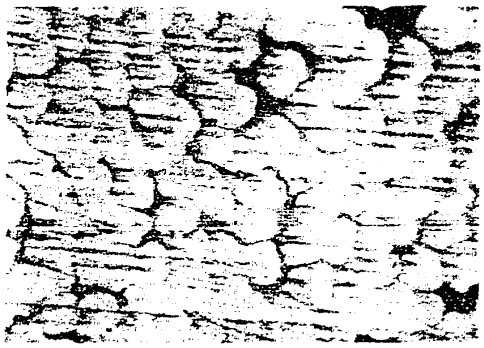

Picture 5-4d FWPM sample *400X*
Inside the "fiber phase", the fiber was *94%*.

Overall fiber volume fraction in the CLM sample: 60%,
Fiber volume fraction in the FWPM sample: 80%.

Picture 5-4 Pictures made by a metalloscope to analyze the matrix volume.

Equation 5-3 can be rewritten as:

$$Ec \approx E_f \times V_f \qquad (5\text{–}4)$$

According to a microscopic analysis, the fiber volume fraction is $V_{f.} = 78\%$ in the FWPM specimens and 59% in the CLM specimens (Picture 5-4). From Equation (5-4), we realize that the fiber fraction of the FWPM specimen is higher than that of the CLM specimen by *20%*. So, if the fiber fraction in CLM process is the same in FWPM process, the modulus would have been increased by *20%*. After the revision, the modulus based on a 78% fiber volume fraction basis could be:

$E_{CLM} = 1847$ Mpa

$E_{FWPM} = 1249$ Mpa

The modulus of the CLM process is larger than that of FWPM by almost 30%.

5-6-5 Transverse Bending Test for Delaminatoin Strength

The ability against delamination is defined as:

$$\sigma_{flex} = \frac{3\,L\,F_{max}}{2\,b\,h^2} \qquad (5\text{–}5)$$

where: σ_{flex} = the max stress,

L = support span

b = width of beam,

h = depth of beam,

F_{max} = Maximum Force.

A record of the delamination testing is shown in Figure 5-21. An average value for the CLM sample is:

$\sigma_{flex} = 3.66$ Mpa

For a transverse test, the composite modulus

$$\begin{aligned} F_c &= F_m = F_f \\ \sigma_c &= \sigma_m V_m = \sigma_f V_f \\ \sigma_{c\,Max} &\approx \sigma_m V_m \end{aligned} \tag{5-6}$$

where V_m = matrix volume fraction,

V_f = fiber volume fraction,

σ_m = matrix stress,

σ_f = fiber stress,

σ_{cMax} = max composite stress.

Revising the value with the fiber volume fraction yield an answer of:

$\sigma_{flex} = 3.66 \times (1+20\%) = 4.39$ (Mpa)

For FWPM process:

$\sigma_{flex} = 7.76$ (Mpa)

The ability against delamination of the FWPM sample is larger than that of the CLM sample by *43%*.

5-6-6 Result and Discussions

1. Elastic modulus of the part that is made from the CLM process is higher then that of the part made by the FWPM process.

2. The ability against the delamination is much lower for the CLM sample. From Picture 5-4A, we can see that a pure matrix interface is placed in each layer, and the mechanical properties of the interface are lower. During the CLM deposition procedure, very little pressure was exerted on the towpreg layers resulting in poorer contacts between the fiber and the matrix.

§5-7 PROPOSED FUTURE WORK

1. To optimize the existing system and method.

2. To develop a forming method to deposit the towpreg not only in the X-Y plan but also in the Z direction.

§5-8 CHAPTER SUMMARY

1. Experimental data have further validated the viability of the proposed CLM process.

2. The two primary forming methods in CLM have been tested and proven very effective in forming a part layer by layer.

3. The self-anchoring method and the required system have been developed. Composite parts have been successfully made using this method.

4. The mechanical properties of the part, were tested and analyzed.

CHAPTER 6 CONCLUSIONS

A novel solid freeform fabrication (SFF) technology, Composite Layer Manufacturing (CLM), has been developed. The CLM process is capable of building a continuous fiber reinforced composite part on a point-by-point and layer-by-layer basis. This computer-automated process converts a computer-aided design file of a part directly into a 3-D physical object of a complex shape and good mechanical integrity. Most of the conventional SFF technologies are limited to the fabrication of a concept model, a prototype, or a master pattern for casting and, therefore, are at best considered to be for "rapid prototyping". In contrast, the present dissertation study has laid down a solid foundation for a new SFF technology that provides "rapid tooling" as well as "rapid manufacturing" capabilities. Although the present study, due to time constraints, has been limited to the fabrication of polymer matrix composites, the same process can be readily adapted for the fabrication of other types of continuous fiber reinforced composites.

Specifically, in the present dissertation study, the technical feasibility of the CLM process has been demonstrated with a bench-top CLM machine constructed that is capable of fabricating both thermoplastic and thermoset resin matrix composites. This CLM machine rapidly dispenses, deposits and consolidates pre-impregnated fiber tows or towpregs to form a 3-D advanced composite component of a complex shape without using a mold or process tooling. Two CLM forming methods, the "self-anchoring" and the "automatic-extrusion", have been designed and developed based on the selection and evaluation of various forming theories.

Related part forming theories and material selection issues for the CLM have been studied during the earliest development stage of the CLM. Several innovative process strategies have been proposed and tested, including "active and passive material supplying", "one step forming method", and "multiple step forming method". These strategies were introduced to help categorize and create a deposition method for different matrix materials. Over ten CLM forming methods have been designed and analyzed. Based on comparison comparisons of their advantages, shortcomings and feasibility, two designs were considered as part of the best forming plans for CLM and were further investigated.

The sources, values, and governing factors of process errors in the CLM technology have been analyzed and evaluated. A series of equations have been derived to evaluate the magnitude of errors in different forming situations. When the parameters of the towpreg, nozzle and toolpath are inputted to these equations, the error could be calculated and the error diagrams could be drawn. The method for *a priori* design of mechanical properties of a composite made by CLM and the method for reducing the towpreg-cutting time during the towpreg deposition process were proposed and studied. These results of these studies could be used in the development of the required software for future commercialization of the CLM technology.

Self-anchoring and automatic extrusion methods have been analyzed in detail. Some analytical solutions were obtained to describe the mass and heat transfer processes involved. According to the studies, the self-anchoring forming speed has an effect on the towpreg bending strength. The bending strength is correlatable with the towpreg solidification, but the degree of solidification depends on its surrounding temperature. The initial and boundary conditions of the temperature fields for the self-anchoring process were considered and a modeling study was carried out by using ANSYS. The results could be used in the future for optimizing the whole process.

Numerical simulations were also obtained for the automatic extrusion process. Again, the results could be used to optimize the process directly. The simulation results were consistent with the experimental data, which further validated the viability of the proposed CLM process.

The two primary forming methods in CLM have been tested and proven very effective in forming a part layer by layer. The self-anchoring method and the required system have been developed. Composite parts have been successfully made by using this method.

The mechanical properties of the part were tested and analyzed. The modulus of the samples, which were cut from the CLM formed samples are greater than that of the part made by the FWPM process by almost 30%. But the ability against delamination of the FWPM sample is better than that of the CLM by 43%.

REFERENCES

1. Paul F. Jacobs. *Rapid Prototyping & Manufacturing*, 1992, pp 2-23.

2. W. L. Wang, C. M. Cheah, J. Y. H. Fuh and L. Lu. *Influence of process parameters on Stereolithography part shrinkage*, Materials & Design, Volume 17, Issue 4, 1996, pp 205-213.

3. R. E. Williams, S. N. Komaragiri, V. L. Melton and R. R. Bishu. *Investigation of the effect of various build methods on the performance of rapid prototyping (stereolithography)*, Journal of Materials Processing Technology, Volume 61, Issues 1-2, August 1996, pp 173-178.

4. D. T. Pham and R. S. Gault. *A comparison of rapid prototyping technologies*, International Journal of Machine Tools and Manufacture, Volume 38, Issues 10-11, October 1998, pp 1257-1287.

5. Lindsay, Karen F. *Rapid prototyping shapes up as low-cost modeling alternative.* Modern Plastics. Volume 67, n 8, Aug 1990, pp 40-41, 43.

6. Kai, Chua Chee. Three-dimensional rapid prototyping technologies and key development areas. Computing & Control Engineering Journal. Volume 5, n 4, Aug 1994. pp 200-206.

7. Ashley, Steve. *Rapid prototyping is coming of age*. Mechanical Engineering. v 117 n 7 Jul 1995, pp 62-68.

8. Ying-Chien Tsai and Wern-Kueir Jehng. *Rapid prototyping and manufacturing technology applied to the forming of spherical gear sets with skew axes*, Journal of Materials Processing Technology, Volume 95, Issues 1-3, 15 October 1999, pp 169-179.

9. James D. Cawley. *Solid freeform fabrication of ceramics*, Current Opinion in Solid State and Materials Science, Volume 4, Issue 5, October 1999, pp 483-489.

10. K. J. Jakubenas, J. M. Sanchez and H. L. Marcus. *Multiple material solid free-form fabrication by selective area laser deposition*, Materials & Design, Volume 19, Issues 1-2, 1 February 1998, pp 11-18.

11. U. Lakshminarayan and K. McAlea. *Manufacture of metal objects by selective laser sintering,* Metal Powder Report, Volume 53, Issues 7-8, 8 July 1997, pp 43.

12. N. K. Vail, L. D. Swain, W. C. Fox, T. B. Aufdlemorte, G. Lee and J. W. Barlow. *Materials for biomedical applications,* Materials & Design, Volume 20, Issues 2-3, 1 June 1999, pp 123-132.

13. Bor Z. Jang. *Advanced Polymer Composites.* ASM International, 1994, pp 61.

14. S.T. Peters. *Handbook of Composites.* Second edition 1998, pp 456~487.

15. Sabit Adanur, Ph.D. Wellington Sears *Handbook of Industrial Textiles* 1995, pp 31-268.

16. Bor Z. Jang. Advanced Polymer Composites: Principles And Applications. ASM International, 1994, pp 9-163.

17. Thompson, Michael P. *How vacuum bags really work: The myth of volatiles and breathers.* International SAMPE Technical Conference. Volume 30, 1998. SAMPE, Covina, CA, USA. pp 201-212.

18. Kim, J S. Lee, D G. *Development of an autoclave cure cycle with cooling and reheating steps for thick thermoset composite laminates*, Journal of Composite Materials. v 31 n 22 1997, pp 2264-2282.

19. Lossie, M. Van Brussel, H. *Design principles in filament winding*, Composites Manufacturing. v 5 n 1 Mar 1994, pp 5-13.

20. Sun, L. Mantell, S C. Banerjee, A. Cohen, D. *Thermoset filament winding process model and parametric study*, ASME Materials Division American Society of Mechanical Engineers, Materials Division (Publication) MD. v 69-1 1995. ASME, New York, NY, USA, pp 11-23.

21. Kim, Dae-Hwan. Han, Poong-Gyu. Jin, Geun-Ha. Lee, Woo Il. *Model for thermosetting composite pultrusion process,* Journal of Composite Materials. v 31 n 20 1997, pp 2105-2122.

22. Astrom, B Tomas. Pipes, R Byron. *Modeling approach to thermoplastic pultrusion. 1: formulation of models*, Polymer Composites. v14 n 3 Jun 1993, pp 173-183.

23. Eduljee, R F. Gillespie, J W Jr. *Weld line studies on transfer-molded thermosetting composite materials,* Polymer Composites. v 10 n 3 Jun 1989, pp 184-193.

24. Han, Kerang. Ni, Jun. Toth, James. Lee, L James. Greene, Joseph P. *Analysis of an injection/compression liquid composite molding process*, Polymer Composites. v 19 n 4 Aug 1998, pp 487-496.

25. Ngo, N D. Mohan, R V. Chung, P W. Tamma, K K. *Recent developments encompassing non-isothermal/isothermal liquid composite molding process modeling/analysis: Physically accurate, computationally effective, and affordable simulations and validations,* Journal of Thermoplastic Composite Materials. v 11 n 6 Nov 1998, pp 493-532.

26. Werner, Eran. *Powder-based prepreg fabric: What, how, why?* Evolving Technologies for the Competitive Edge International SAMPE Symposium and Exhibition. v 42 n 1 1997. SAMPE, Covina, CA, USA, pp 706-719.

27. Lacroix, Fv. Lu, H -Q. Schulte, K. *Wet powder impregnation for polyethylene composites: Preparation and mechanical properties*, Composites - Part A: Applied Science & Manufacturing. v 30 n 3 1999, pp 369-373.

28. Ghasemi Nejhad, Mehrdad N. Ikeda, Karen M. Design, manufacture, and characterization of composites using on-line recycled thermoplastic powder impregnation of fibers and in-situ filament winding, Journal of Thermoplastic Composite Materials. v 11 n 6 Nov 1998, pp 533-572.

29. Connor, M. Toll, S. Manson, J -A E. Gibson, and A. G. *Model for the consolidation of aligned thermoplastic powder impregnated composites,* Journal of Thermoplastic Composite Materials. v 8 n 2 Apr 1995, pp 138-162.

30. Shonaike, G O. Matsuda, M. Hamada, H. Maekawa, Z. Matsuo, T. *Effect of impregnation technique on bending properties of glass fiber reinforced polyethylene terephthalate composites*, Composite Interfaces. v 2 n 2 1994, pp 157-170.

31. Djumaev, A. Takahashi, K. *Effect of moisture absorption on damping performance and dynamic stiffness of NY-6/CF commingled yarn composite,* Journal of Materials Science. v 29 n 18 Sept 15 1994, pp 4736-4741.

32. Rapid Prototyping & Tooling State of the Industry: 1998 Worldwide Progress Report, pp 25-68.

33. Crump, S Scott. *Fast, precise, safe prototypes with FDM,* Intelligent Design and Manufacturing for Prototyping American Society of Mechanical Engineers,

Production Engineering Division (Publication) PED. Publ by ASME, New York, NY, USA. v 50. pp 53-60.

34. Lavoie, Francis. *Is 'desktop manufacturing' for you?* American Machinist & Automated Manufacturing. v 133 n 3 Mar 1989, pp 61-63.

35. Peters, Dean M. *Rapid prototyping update*, Foundry Management & Technology. v 124 n 6 Jun 1996, pp 5.

36. Uziel, Yehoram. *Beyond rapid prototyping - a seamless transition from CAD to manufacturing of functional metal parts with complex geometry,* Automotive Concurrent/Simultaneous Engineering SAE Special Publications. v 1233 1997. SAE, Warrendale, PA, USA. pp 59-64.

37. Wohler and associates *Rapid Prototyping & Tooling State Of The Industry, 1998 Worldwide Progress Report*, pp 9-204.

38. Capus, Joseph M. *Advances in powder metallurgy processing*, Advanced Materials & Processes. v 156 n 3 Sep 1999, pp 33-36.

39. Froes, Sam. *Laser forming titanium components from powder*, Materials Technology. v 15 n 1 2000, pp 8-12.

40. Anonymous. Beyond rapid prototyping to direct fabrication: *Forming metallic hardware directly from a CAD solid model*, Materials Technology. v 13 n 1 Mar 1998, pp 5-7.

41. Keicher, D M. Miller, W D. Smugeresky, J E. Romero, J A. *Laser Engineered Net Shaping (LENSTM)*: Beyond rapid prototyping to direct fabrication, Hard Coatings Based on Borides, Carbides & Nitrides: Synthesis, Characterization & Application TMS Annual Meeting 1998. Minerals, Metals & Materials Soc (TMS), Warrendale, PA, USA, pp 369-377.

42. Lewis, Gary K. Lyons, Peter. *Direct laser metal deposition process fabricates near-net-shape components rapidly*, Materials Technology. v 10 n 3-4 Mar-Apr 1995, pp 51-54.

43. Langdon, Ray. *Focus on rapid prototyping*, Automotive Engineer (London). v 24 n 3 1999, pp 44-46, 51, 52, 55-56.

44. Bryden, B G. Pashby, I R. Wimpenny, D I. Adams, C. *Laminated steel tooling in the aerospace industry*, Materials & Design. v 21 n 4 2000, pp 403-408.

45. Zhang, Wei. Leu, Ming C. Ji, Zhiming. Yan, Yongnian. *Rapid freezing prototyping with water*, Materials & Design. v 20 n 2 1999, pp 139-145.

46. Danforth; Stephen C; Agarwala; Mukesh; Bandyopadghyay; Amit; Langrana; Noshir; Jamalabad; Vikram R; Safari; Ahmad; van Weeren; Remco; Danforth. *Solid freeform fabrication methods*, U.S. Pat. No. 5,738,817. April 1998.

47. Valavaara; Viljo. *Topology fabrication apparatus,* U.S. Pat. 4,749,347, June 1988.

48. Masters; William E. and Batchelder, et al. *System and method for computer automated manufacturing using fluent material*, U.S. Pat.5,134,569, July 1992.

49. Batchelder; John S.; Curtis and, et al. *Model generation system having closed-loop extrusion nozzle positioning,* U.S. Pat. No. 5,402,351, 1995 and U.S. Pat. No.5, 303,141, 1994.

50. Sachs; Emanuel M, Haggerty; John S. and, et al. Three-dimensional printing techniques, U.S. Pat. No. 5,204,055, April 1993.

51. Deckard; Carl R. *Method and apparatus for producing parts by selective sintering*. U.S. Pat. 4,863,538, Sept. 5, 1989.

52. D. Klosterman, et al, in Proceedings of The 7th International Conference on Rapid Prototyping - 1997, March 31-April 3, 1997, San Francisco, CA, USA, ed. By R. P. Chartoff, et al.; pp.43-50 and pp. 283-292.

53. Jack A. Adams *Human factor engineering*, 1989, pp 149-231.

54. Richard G. Griskey Ph.D., P. E. Polymer Process Engineering pp. 109~129 & pp 141- pp 221.

55. J. Philip Mason, Ph.D. and Joseph F. Manning, Ph.D. *The Technology Of Plastics And Resins* 1945, pp 63-19.

56. G. Haim, *Manual For Plastic Welding* 1960, pp 101-107.

57. J. Alex Neumann and Frank J. Bockhoff, *Welding Of Plastics*, 1959, pp 9-109.

58. T. T. Loo and C. T. Sun, *Proceeding of International Symposium on Composite Materials and Structures* June 10-13, Beijing, China 1986, pp 143-438.

59. W. P. de Wilde and W. R. Blain editors, *Composite materials design and analysis* 1990, pp 55-170.

60. H.J. BOHM and F. G. Rammerstorfer, *Fiber Arrangement Effects On The Microscale Stresses Of Continuously Reinforced MMCS*, MicroStructure-Property Interactions In Composite Materials, 1994, pp 51-62.

61. Naim Afgan, Maria da Graca Carvalho, A. Bar-Cohen, D. Butterworth and W. Roetzel Edited *New Developments in Heat Exchangers* 1996 pp1-28.

62. Frank P. Incropera and David P. Dewitt, Fundamentals of heat and mass transfer, 1985, pp 243-297.

63. Warren M. Rohsenow, James P. Hartenttt and Ejup N. Ganic, *Handbook Of Heat Transfer Fundamentals*, second edition, 1985, pp 1-2, pp 42.

64. N. L. Hancox *the thermal conductivity of Composite materials* edited by C.A. Brebbia, W. P. de Wilde And W.R. Blain *Computer Aided Design in Composite Material Technology* proceeding of the International Conference, Southampton, and 1988 pp 189-207.

65. A. Brent Strong Brigham Young University *Plastics Materials and Processing* pp 125-131.

66. Rita Meter-Spasche, *Pattern Formation In Viscous Flows*, 1999, pp 1-19.

67. Nicholas P. Cheremisinoff, Paul N. Cheremisinoff " *Handbook of applied Polymer processing Technology*" 1996, pp 12-83.

68. Arnold G. Fredrickson and R. Byron Bird *Non-Newtonian Flow in Annuli*, Ind. Eng. Chem. 50(3): 1958, pp 347-352.

69. N. P. Cheremisinoff, Editor Polymer Flow Engineering Encyclopedia of Fluid Mechanics Volume 9 , 1986, pp 651-704.

70. N. P. Cheremisinoff, Editor Encyclopedia of fluid mechanics volume 7 Rheology and Non-Newtonian flows 1986, pp 174-119.

71. R. Byron Bird, R. C. Armstrong and Ole Hassager *Dynamics of Polymeric Liquids Volume 1 Fluid Mechanics*, 1987 pp 510-539.

72. R. Byron Bird, R. C. Armstrong and Ole Hassager *Dynamics of Polymeric Liquids Volume 2 Kinetic theory* 1987 pp 3-22.

73. Richard W. Hanks and K. M. Larsen, *The flow of power-low non-Newtonian fluids in concentric annuli*, Ind. Eng. Chem. Fundam. 18(1): 1979, pp 33-35.

74. Dominick V. Rosato, P.E. and Donald V. Rosato, Ph.D. *Injection Molding Handbook* 1986 pp 127-273.

75. A. Brent Strong, Second Edition, *Plastics Materials And Processing* 2000, pp 393-394.

76. Douglas M. Bryce, *plastic injection molding mold design and construction fundamentals*, 1998, pp 15-41.

APPENDIX A

Table 4-1 Parameters for the temperature field simulation.

	Polyethylene matrix	Kevlar fiber
Thermal Conductivity, k	*0.26 N/s k*	*0.04 N/s k*
Density, ρ	*976 kg/m³* → $976\ kg/m^3$	$1450\ kg/m^3$
Specific Heat, c	*2260 J/kg k*	*670 J/kg k*
Convection Exchange coefficient, α	$5\ N/m^2\ s\ k$	

APPENDIX B

The dimension table for the nozzles (see Figure 5-7 and 5-8).

Table 5-1

Dimensions	Symbol									Qty
	ØA	ØB	ØC	ØD	L1	L2	L3	L4	L5	
Dimension1	Ø3±0.01	Ø1.6±0.01	Ø2±0.01	Ø4±0.01	4.8	5	3.2	3.2	30	2
Dimension2	Ø2±0.01	Ø1.0±0.01	Ø1±0.01	Ø2±0.01	3	6	2	2	25	2
Dimension3	Ø1±0.01	Ø0.6±0.01	Ø1±0.01	Ø2±0.01	3	6	2	3	20	2

Table 5-2

Dimensions	Symbol										Qty
	ØA	ØB	ØC	ØD	L1	L2	L3	L4	L5	L6	
Dimension1	Ø3±0.01	Ø1.6±0.01	Ø2±0.01	Ø4±0.01	4.8	5	3.2	3.2	25	22	2
Dimension2	Ø2±0.01	Ø1.0±0.01	Ø1±0.01	Ø2±0.01	3	6	2	2	20	15	2
Dimension3	Ø1.6±0.01	Ø0.6±0.01	Ø1±0.01	Ø2±0.01	3	6	2	3	15	10	2

APPENDIX C

The results of the automatic extrusion experiment.

Results G: Good F: Failed Blank: None			Nozzle Diameter ØD															
			Length of Orifice L=9.9289				Length of Orifice L=1.9289				Length of Orifice L=0.4298				Length of Orifice L=0.1716			
			Ø1	Ø2	Ø2.5	Ø4	Ø1	Ø2	Ø2.5	Ø4	Ø1	Ø2	Ø2.5	Ø4	Ø1	Ø2	Ø2.5	Ø4
Number of Fiber Tows	Flat Head	1	F		F		F	F	G	G	F	G						G
		2							G	G								
		3										G	G	G				
		6					F			G				G				
	Taper Head	1			F			F	G	F								
		2										G	G	G				
		3								G								
		6								G				G				

Table 5-3 The result of automotive extrusion experiment.

APPENDIX D

The Parts list for the deposition device (see Figure 5-16).

	Name	Material	Quantity	
01	Alignment Tube	A3	1	
02	Regulator shaft	45	1	
03	Nut M5X15	45	4	GB70-85
04	Regulator lift Stand	A3	1	
05	Locking Bolt M2 X 6	45	1	GB77-85
06	Tube Locking Nut	45	1	
07	Balance Shaft	A3	2	
08	Regulator Right Stand	A3	1	
09	Bolt M5 X 40	45	4	GB70-85
10	Bearing Cover	A3	4	
11	Bearing 200		4	GB276-89
12	Bearing Support	A3	4	
13	Locking Nut M16X1.5	45	4	GB812-88
14	Roller	A3	2	
15	Nut M12	45	1	GB41-86
16	Depositing Holder	45	1	
17	Bolt M8X 25	45	4	GB70-85

18	Locking Bolt M5X12	45	3	GB77-85
19	Driving Shaft	45	1	
20	Driven Shaft	45	1	
21	Pushing Rod	A3	1	
22	Bolt M5X20	45	4	GB70-85
23	Compression Spring	50CrVA	1	
24	Front Cover	A3	1	
25	Compression Nut	45	1	
26	Main Support	A3	1	
27	Motor Support	A3	1	
28	Shaft Clipper			Existing
29	Stepping Motor			Existing

* GB China Standard